Catarina de Oliveira Rodrigues

Licenciatura em Ciências da Engenharia Química e Bioquímica

Optimization of 3D porous structures for controlled drug delivery using quality by design method.

Dissertação para obtenção do Grau de Mestre em
Engenharia Química e Bioquímica

Orientador: Telma Godinho Barroso, Doutora, GEO-Ground Engineering Operations

Co-orientador: Ana Isabel Nobre Martins Aguiar de Oliveira Ricardo, Professora Catedrática, FCT-UNL

Júri:

Presidente: Prof. Doutor Mário Fernando José Eusébio
Arguente: Prof. Doutora Ana Sofia Leonardo Vilela de Matos
Vogal: Doutora Telma Godinho Barroso

FACULDADE DE CIÊNCIAS E TECNOLOGIA
UNIVERSIDADE NOVA DE LISBOA

Setembro, 2017

Catarina de Oliveira Rodrigues

Licenciatura em Ciências da Engenharia Química e Bioquímica

Optimization of 3D porous structures for controlled drug delivery using quality by design method.

Dissertação para obtenção do Grau de Mestre em
Engenharia Química e Bioquímica

Orientador: Telma Godinho Barroso, Doutora, GEO-Ground Engineering Operations

Co-orientador: Ana Isabel Nobre Martins Aguiar de Oliveira Ricardo, Professora Catedrática, FCT-UNL

Júri:

Presidente: Prof. Doutor Mário Fernando José Eusébio
Arguente: Prof. Doutora Ana Sofia Leonardo Vilela de Matos
Vogal: Doutora Telma Godinho Barroso

FACULDADE DE CIÊNCIAS E TECNOLOGIA
UNIVERSIDADE NOVA DE LISBOA

Setembro, 2017

Optimization of 3D porous structures for controlled drug delivery using quality by design method

“Tell me and I forget,
Teach me and I remember,
Involve me and I learn.”

Benjamin Franklin

Agradecimentos

A realização desta tese e, também dos últimos 5 anos como estudante, contaram com a presença de pessoas que para além de terem sido importantes apoios foram a minha motivação para nunca desistir, pessoas essas que estarão comigo para sempre.

Quero começar por agradecer à Doutora Telma Barroso, pela sua orientação, paciência, apoio e disponibilidade total, por toda a sabedoria transmitida, pela ajuda, pela confiança que depositou em mim para este projeto e, principalmente, por todas as vezes que me mostrou que eu conseguia fazer mais e melhor. Não podia deixar de agradecer também à Professora Ana Aguiar-Ricardo, pela ajuda que me deu, por toda a disponibilidade e acima de tudo, por também confiar em mim para este projeto.

Às pessoas que me acompanharam todos os dias, os meus colegas da GEO, Jorge Capitão-mor, Stéphanie Leal, Leandro Parada, André Praça e António Cunha, pela ajuda que me deram ao longo destes últimos meses, pela boa disposição, por todo o apoio e por tornarem esta experiência uma das melhores que alguma vez tive.

Aos colegas de tese, António Tavares e Sara Leonardo por perceberem os meus dramas e por me apoiarem incondicionalmente. À Daniela Pequito, que foi, sem dúvida, uma das pessoas mais importantes nestes últimos meses, um muitissimo obrigada por tudo, de coração.

Quero também agradecer à minha família. Mãe e pai, um obrigada não chega para compensar todos os esforços que sempre fizeram por mim. Vocês são os melhores pais do mundo! Espero ter-vos deixado orgulhosos. Ao meu namorado, Jorge Matos, pela paciência de aturar o meu mau feitio e por me ter apoiado incondicionalmente. Que nada nos separe, nunca. Aos meus irmãos, cunhado e avó, Ana Caetano, Rui Caetano, Pedro Rodrigues e avó Teresa por me fazerem acreditar que tudo é possível. Aos meus sobrinhos, Pedrocas e Mariana, por me fazerem sonhar e por me fazerem sentir a pessoa mais especial do mundo. Amo-vos a todos.

Por último, mas não menos importante. Quero agradecer aos meus colegas de curso, principalmente, à Jessica Lea Mesquita, à Catarina Pires, à Catarina Nunes e à Mafalda Duarte e a todos os outros que de alguma forma fizeram parte da minha vida. Todo o apoio ao longo dos 5 anos, toda ajuda, todo o carinho, foram indispensáveis. Obrigada por nunca me deixarem desistir e por me levantarem quando estava mais em baixo.

Muito obrigada a todos, vou levar-vos no coração, para sempre!

Abstract

The objective of this work was to apply Quality by Design approach to obtain the best conditions to produce 3D polymeric structures for two distinct applications: oral and vaginal route of administration. The first should release 50 mg drug/g scaffold, in 5 hours and the second one 800 mg drug/g scaffold, during 8 h.

Initially, the data from previous studies was collected and inserted in MODDE software, and then the Design Space was built and according to those plots, the conditions to start the experimental validation were chosen. The model chosen to perform these studies was Partial Least Square Regression. Both green (probability of failure lower than 5 %) and yellow (probability of failure lower than 10%) zones from Design Space were taken into account and explored.

For experimental validation, through the data obtained from QbD studies, scaffolds of chitosan (CHT), xanthan gum (XG) and mixture of CHT and XG were prepared, with N-N'-methylene-bis-acrylamide (MBA) as a crosslinker and tetramethylenediamine (TEMED) and ammonium persulfate (APS) as catalyst and initiator. For the characterization of the produced structures, scanning electron microscopy (SEM), Fourier transform infrared spectroscopy – attenuated total reflectance (FTIR-ATR), mechanical analysis and swelling tests were performed and the ones that achieved the objective regarding morphological and swelling characteristics were chosen for drug impregnation and drug release studies. Additionally, mathematical models were adjusted to the experimental release profiles in order to describe the drug release mechanisms.

The studies showed that the porous scaffold that showed better performance for oral route of administration, considering the defined goals, was CHT_6, with 3% chitosan, 2% crosslinker and freezing temperature of -20ºC, that presented drug release of 63,6 mg IBU/g scaffold, in 5 hours. CHT_7, with 3% chitosan, 2% crosslinker and freezing temperature of -80ºC achieved the objective in the second hour, releasing approximately 70 mg IBU/g scaffold. Regarding vaginal route of administration, the scaffold that showed better performance was CHTXG_1 which released 1200 mg IBU/g scaffold, in 8 hours, however, CHT_7 was also very close to the objective, releasing 720,1 mg IBU/g scaffold.

Quality by Design approach was an essential and important tool during the development of these structures, once it allowed achieving the objectives set for this thesis, and also reducing the experimental shots (in more and less 60%) needed to achieve the desired goals, what reinforces the power of this tool in processes optimization.

Keywords: Quality by Design, design space, drug delivery, chitosan, xanthan gum

Resumo

Os objetivos desta dissertação consistem na aplicação do método "*Quality by Design*" para obtenção das melhores condições na produção de estruturas poliméricas 3D, para serem utilizadas em duas aplicações distintas: tratamentos via oral e via vaginal. A primeira estrutura, referente à via oral, deve libertar 50 mg fármaco/g estrutura, em 5 horas e a segunda, referente à via vaginal, 800 mg fármaco/g estrutura, durante 8 horas.

O primeiro passo consistiu em obter conhecimento de estudos já realizados e introduzir os dados no *software* MODDE. O modelo utilizado para realizar estes estudos foi a regressão dos mínimos quadrados parciais. Posteriormente, foram desenhados os gráficos de *Design Space*, e de acordo com a informação dada pelos gráficos, as condições de processamento foram escolhidas e assim foi iniciada a validação experimental. Tanto a zona verde (probabilidade de insucesso inferior a 5%) como a zona amarela (probabilidade de insucesso inferior a 10%) foram consideradas.

Durante a validação experimental foram preparadas estruturas de quitosano (CHT), goma xantana (XG) e mistura de CHT e XG. O reticulante utilizado foi N-N'-metileno-bis-acrilamida (MBA) e o catalisador e iniciador utilizados foram tetrametilenodiamina (TEMED) e persulfato de amónia (APS), respetivamente. Para a caracterização das estruturas produzidas, as técnicas utilizadas foram microscopia de varrimento eletrónico (SEM), espectroscopia de infravermelho por transformada de Fourier – refletância total atenuada por diamante (FTIR-ATR), análises mecânicas e testes de inchamento. As estruturas que atingiram os objetivos referentes às características morfológicas e de inchamento foram escolhidas para posterior impregnação e estudos de libertação. Foram também utilizados modelos matemáticos para o ajuste experimental dos perfis de libertação, para que fosse possível descrever os mecanismos de libertação.

Estes estudos demonstraram que a estrutura porosa que se mostrou mais adequada para ser utilizada na via oral, tendo em conta os objetivos definidos, foi CHT_6, com 3% quitosano, 2% reticulante e temperatura de congelamento de -20ºC, que apresentou uma libertação de 63,6 mg IBU/g suporte, em 5 horas. A estrutura CHT_7, com 3% quitosano, 2% reticulante e temperatura de congelamento de -80ºC, atingiu o objetivo durante a segunda hora dos testes, libertando 70 mg IBU/g suporte. No caso da aplicação vaginal, a estrutura que se mostrou mais adequada para ser utilizada na via vaginal foi CHTXG_1 que libertou 1200 mg IBU/g suporte em 8 horas. Contudo, a estrutura CHT_7 apresentou uma libertação de 720,1 mg IBU/g suporte, o que se encontra muito próximo do objetivo definido.

A utilização do *Quality by Design*, durante o desenvolvimento destas estruturas, foi indispensável e muito importante, uma vez que permitiu chegar aos objetivos definidos para esta

dissertação e, ainda, permitiu reduzir o número de ensaios experimentais (em aproximadamente 60%) necessários para atingir o objetivo, o que reforça o poder desta ferramenta em otimização de processos.

Palavras-chave: *Quality by Design*, *design space*, libertação de fármacos, quitosano, goma xantana

List of Contents

List of Figures

List of Tables

Abbreviations

3D	Three-Dimensional
ALG	Sodium Alginate
API	Active Pharmaceutical Ingredients
APS	Ammonium Persulfate
BSA	Bovine Serum Albumin
CHT	Chitosan
CMA	Critical Material Attributes
CO_2	Carbon Dioxide
CPP	Critical Process Parameters
CQA	Critical Quality Attributes
DoE	Design of Experiments
FDA	Food and Drug Administration
FTIR-ATR	Fourier Transform Infrared-Attenuated Total Reflectance
GL	Gelatin
HSV	Herpes Simplex Virus
IBU	Ibuprofen
ICH	International Conference Harmonization
IN	Isoconazole Nitrate
IV	Independent Variables
MBA	N,N-methylene bis(acrylamide)
MLR	Multiple Linear Regression
NSAID	Non-steroidal Anti-inflammatory Drug
PG	PolyGeo
PLS	Partial Least Square Regression
QbD	Quality by Design
QTPP	Quality Target Product Profile
$scCO_2$	Supercritical Carbon Dioxide
SCF	Supercritical fluid
SEM	Scanning Electron Microscopy
TEMED	N,N,N,N-tetramethylethylenediamine
XG	Xanthan Gum

1. Introduction

Nowadays, the number of mucosal and cutaneous fungal infection cases is growing worldwide [1]. Approximately 2.5 million cases of oral thrush appear every year [2]. Also, fungal infection of the vulva and the vagina is estimated to be the second most common cause of vulvovaginal inflammations [3], and it is estimated that approximately 1.4 million cases are reported every year [2].

The best way to administer the appropriate drugs to treat these kind of infections is exactly where these problems appear (mouth or vagina). These routes present a dense network of blood vessel [4], and in the case of the oral mucosa, it is considered permeable [5], which represents an important and significant advantage considering drug absorption. However, the drugs may lose efficiency, due to the active physiological removal mechanisms (physiological secretions as saliva and vaginal fluids) [6]. To circumvent this negative aspect, many efforts are being done to increase the drug efficiency when treating these infections.

However, one unsolved problem in pharmaceutical research is the development of methodologies to evaluate the drug product or device efficacy, biocompatibility and side effects. The necessary studies are performed in several stages. Firstly, the drugs or medical devices are tested using *in vitro* cell models, followed by *in vivo* animal models and finally in humans, upon approval of competent authorities. The overall studies are very expensive and take a lot of time. Quality by Design method, which represents a modern systematic approach that ensures the quality by developing a full understanding of the compatibility between the finished product and all of the components and processes involved in manufacturing, besides saving time, enables to save resources and money, since it is possible to achieve objectives with less experiments and with a high probability of success [7] [8].

1.1 Quality by Design

In pharmaceutical industry, it is well recognized that quality of a drug cannot be tested directly into the finished product, but in the manufacturing process, so that quality, safety and effectiveness of the pharmaceuticals are not compromised. So*, International Conference on Harmonisation of Technical Requirements for Registration of Pharmaceuticals for Human Used* (ICH) proposed the Quality by Design concept (QbD) in order to promote new initiatives and with the aim of guiding the developers with the pharmaceutical processes [9] [10].

The concept, firstly proposed by Dr. Joseph M. Juran, with the launch of the book: "*Juran on Quality by Design: The New Steps for Planning Quality into Goods and Services*", in 1992, that translates quality in pharmaceutical industry [11]. However the first thought of operation windows were taken in 1950s [12]. The application of this approach is rising. In 2005, the first QbD approved product appeared, and since then this number is increasing, leading to a total of approximately 70 products approved in 2012 [13].

In 2009, Food and Drug Administration (FDA) released ICH-Q8, defining "a systematic approach to development that begins with predefined objectives and emphasizes product and process understanding and process control, based on sound science and quality risk management" [14]. This approach uses a statistical tool, Design of Experiments (DoE), to develop a robust method "design space". This "design space" defines a region where changing process parameters will not affect, significantly, the results [15] [16]. This means that, working inside this space is not considered a change in the process [14].

This method allows the achievement of product quality specifications, which are based on clinical performance. Also, using this approach, the process capability is raised while product variability and defects decrease, by enhancing product and process design, understanding and control. Another purpose of this method is to increase product development and manufacturing efficiencies and to enhance root cause analysis and post-approval change management [11] [14].

QbD is no more than a set of steps systematically applied, during the process development. The strategy includes five steps, as shown in **Figure 1.1**. First, it is important to define and specify the method goals, which consist in defining the quality target product profile (QTPP) and the critical quality attributes (CQA) of the drug product. After, it is necessary to scout and evaluate the method, and this consists in truly understand the process and product performance so that it is possible to identify the critical material attributes (CMA) and the critical process parameters (CPP), and the relationship between CMA/CPP and CQA. Then, when all the specifications are known, the method selection and the risk assessment can be performed. This is possible using statistical tools, as DoE. Using the results obtained from the risk assessment, it is possible to determine the strategy to control the method performance and this consists in performing

suitability tests and elaborating a mitigation plan for controlling critical method variables. Lastly, there is a need to verify the built-in method performance, and this will determine if the method is valid or not (method validation) [11][17].

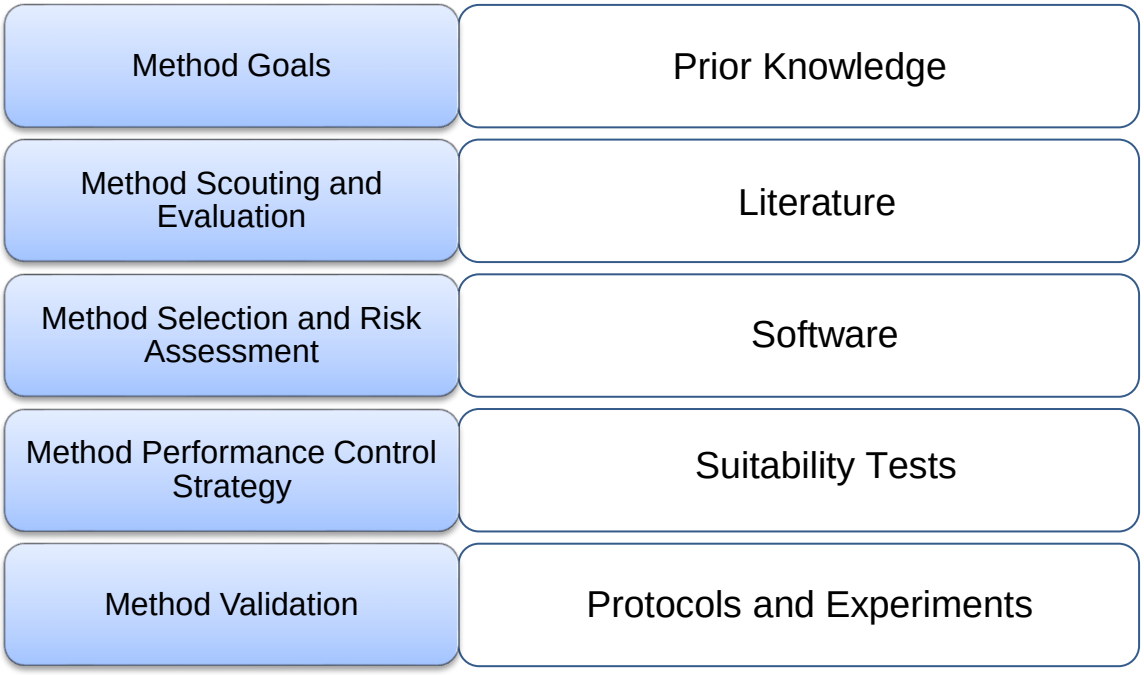

Figure 1.1 Method: strategy and tools, adapted from [17].

The quality target product profile (QTPP) is the combination of product characteristics that ensure the efficacy, and the safety promised in the label. In order to achieve this profile, there are some aspects that must be known such as, the intended use in clinical setting, the route of administration, the dosage form, the delivery systems, the dosage strength, the container closure system, among others. The CQA consist in the physical, chemical, biological and microbiological properties of the final drug product (output) that must be within an appropriate limit, to assure the required quality [18]. It is necessary to consider all the product qualities and characteristics, including the physical properties, such as appearance (color and shape), odor, size, score configuration or friability, content uniformity, dissolution profile and drug release, degradation products, residual solvents, moisture and microbial limits. The CMA consist in the physical, chemical, biological and microbiological properties of the input material that also must be within an appropriate limit, so that the product will have the desired quality. The CPP are selected process parameters that affect the CQA, so they must be monitored and properly controlled to assure that the drug product respects the quality standards [19].

The adoption of this kind of method has many advantages such as, higher development efficiency, in terms of time and cost, but, more important, it allows compliance with the guidelines and expectations from the competent authorities and the approval time is reduced. This approach also creates a quick response to any kind of deviation or change in the production process [7] [14] [20]. Therefore, QbD method guarantee the achievement of sufficient information with less number of experiments, and varying only the parameters that actually make some difference, which leads to a significant reduction of time needed to test and optimize the process parameters. [21].

It is possible to enumerate a few cases where QbD improved and was useful during the development and optimization in case studies. One of these examples is the use of QbD in the optimization of high-performance liquid chromatography (HPLC), what has been made by B. Debrus *et al.* [22], in 2011. HPLC method is used to separate the compound of a mixture, and this separation can be hampered by the similar chromatographic behavior, which can take a lot of time to the analyst to make sure that all the components are correctly separated in a reasonable time [23]. To improve this method, the authors used QbD method and the statistical tools were successfully applied and all the nine components were separated from an unknown sample mixture in less than 40 minutes, and for the latter analysis, time was shortened to less than 14 minutes. In 2012, A. Baldinger *et al.* [24], utilized QbD in the optimization of the spray-drying process. The purpose of using spray-drying was to build a structure with specific pore size, in the range 1-5 µm, for inhalation aerosols. This required specific conditions that might take a lot of time to optimize. With this study, they concluded that despite a full factorial design is not sufficient to describe the effects of the process parameters on the outcomes, DoE is useful in the rational choice of spray-drying conditions and it can also be used to predict the spray-dried product attributes, based on the process conditions. More recently, in 2015, E. Pallagi *et al.* [25], adapted QbD in the early pharmaceutical development of an intranasal nanosized formulation. The development of nanodrugs takes a lot of time and money, once Nano drugs are very complex and specific characteristics are required. The authors concluded that the QbD predictions could result in a shorter development time, lower costs and also fewer needs for human resources, once there is more effective target orientation. Therefore, this study demonstrates the applicability and relevance of QbD in the early stages of pharmaceutical development.

There are different statistical software to help performing DoE or other necessary statistical analysis. In 2008 CMC-IM Working Group developed, in association with Conformia™, the project named “Pharmaceutical Development Case Study:”ACE Tablets””, using the QbD approach, and to help during statistical studies the selected software was Design-Expert®[26]. Another case of QbD utilization appeared during the development of the design space for robust optimization in liquid chromatography, performed by B. Debrus *et al.* [22], they used another statistical tool, the ICA algorithm – fastICA R package -, giving DoE results that could be filtered, to obtain the best ones. In 2012, A. Baldinger *et al.* [24] used MODDE® and Simca-P+ softwares to setup and

evaluate DoE, in the optimization of a spray-drying process. In 2015, Pallagi E. *et al.* [25] choose software Lean QbD Software®, during the early development of an intranasal nanosized formulation. Also in 2015, BOSCH organized a seminar named “Statistical Design Space Development for Pharma”, and in the agenda, the software mentioned was MODDE®-software [27].

In 2012, Theodora Kourti and Bruce Davis [8], published an article where they demonstrate the answers of two unknown companies that adopted QbD methodology in their research. In total, 12 companies answered to their questioner, and only one of them claims that “they don’t apply QbD”. The name of this company was not revealed. However, it is possible to know the name of the other eleven: Abbott (USA), AstraZeneca (UK), Bristol Myers Squibb (UK and USA) [28], GlaxoSmithKline (USA) [29], Jazz Pharmaceuticals Inc. (USA), Eli Lilly and Company (USA) [30], Merck (USA and Ireland) [31]; Pfizer (USA), Centocor Biologics (J&J) (Ireland), Vertex Pharmaceutical (USA) [32] and United Therapeutics Inc. (USA).

1.1.1 Models in Quality by Design

During QbD risk assessment, it is necessary to predict values for the responses (dependent variables), in order to achieve the specifications of the product and consequently to optimize the production method [33]. Thus, in order to predict these values, it is necessary to explain the influence of independent variables (these variables represent the data collected from previous studies) in the dependent ones. Quality by Design software are able to do this through relationships explained by two different models: multiple linear regression (MLR) and partial least square (PLS) [34].

1.1.1.1 Multiple Linear Regression

In multiple linear regression (MLR), there is a linear relationship between a dependent variable Y and k independent variables, x_j (j=1,2,…,k) [35]. These independent variables can also be called explanatory or regressors once they are able to explain the variations in Y or they can be called predictable variables, once they can be used to predict values in Y [36]. An easy way to organize the data to apply this type of regression is a table similar to **Table 1.1**.

Table 1.1 Table representing the data organization to apply MLR, adapted from [36].

Y	X_1	X_2	...	X_k
Y_1	X_{11}	X_{12}	...	X_{1k}
Y_2	X_{21}	X_{22}	...	X_{2k}
...	...	...	...	...
Y_n	X_{n1}	X_{n2}	...	X_{nk}

As every model, MLR has a specific equation to create the relationship between the k independent variables, x_j, and the dependent variable, Y[37]. For this model, **equation (1.1)** represents this relationship.

$$Y = \beta_0 + \beta_1 x_1 + \beta_2 x_2 + \cdots + \beta_k x_k + \varepsilon \qquad (1.1)$$

Where Y represents the dependent variables, x the independent variables and ε the random error. The partial regression coefficients, β, also present in **equation (1.1)**, represent the expected variance in Y response, for each unit of variation in x_j, when all the other regressors, x_i ($i \neq j$) are considered constant in experimental terms [36].

To adjust this model, and due to the calculation difficulties and in handling with the large number of parameters, it is better to express the mathematical operations using matrix notation. An example of the matrix that can be built is the matrix above [36], [38].

$$Y = \beta x + \varepsilon \qquad (1.2)$$

$$Y=\begin{pmatrix} Y_1 \\ Y_2 \\ \dots \\ Y_n \end{pmatrix}, \quad X=\begin{pmatrix} 1 & X_{11} & X_{12} & \dots & X_{1k} \\ 1 & X_{21} & X_{22} & \dots & X_{2k} \\ 1 & \dots & \dots & \dots & \dots \\ 1 & X_{n1} & X_{n2} & \dots & X_{nk} \end{pmatrix}, \quad \beta=\begin{pmatrix} \beta_1 \\ B_2 \\ \dots \\ \beta_n \end{pmatrix} \quad e \quad \varepsilon=\begin{pmatrix} \varepsilon_1 \\ E_2 \\ \dots \\ \varepsilon_n \end{pmatrix}$$

Matrix **Y**, is a column vector (n x 1) constituted by the observations of the dependent variable. In matrix **X**, (n x p), the lines are constituted by the values of the independent variables, which means that contains the information about the levels of the independent variables at which the observations are obtained. In vector **β**, are present the values of the regression coefficients to each combination of the regressors. Finally, in vector **ε**, are represented the random errors [36], [38].

MLR can be used in different occasions: (i) when there is the need of adjusting data and to study the effect of an x variable, taking into account other independent variables; (ii) when the goal is to obtain an equation to predict Y values from the values of several independent variables x_1, x_2, …, x_k; (iii) when the objective is to explore the relationship between multiple variables (x_1, x_2…x_k) to determine which are the independent variables that actually influence Y [37].

As every statistical model, MLR also has its own assumptions. First of all, the observations in Y and the values in X are statistically independent from each other, which means they must not be correlated. Also, the errors must be identically distributed, normal distributed with null averaged and variance σ^2. The dependent and independent variables must have a linear relationship, which means that the mean of Y for each specific combination of X_1, X_2, …, X_k is a linear function of X_1, X_2,…, X_k. The non-linearity may result in the sub-estimation of the real relation. At last, homoscedasticity must be present. This means that the error variance is the same in all levels of independent variables. When this does not happen, it is called heteroscedasticity and it can lead to a serious distortion of the conclusions and, consequently, weaken the analysis [39], [37].

Although MLR can handle with many independent variables at the same time, it has some limitations in defining which ones are the most significant. This limitation may lead to inconsistencies and to incorrect predicted results. The utilization of alternative models might be useful to overcome this problem.

1.1.1.2 Partial Least Squares Regression

One example of an alternative to MLR is partial least squares regression (PLS). In many cases of a large number of independent variables, the models always try to explain the results through all of them, however, only a few are really significant and have impact in the results [40].

So, PLS purpose is exactly to reduce the independent variables (also called predictors) to a smaller group and then modeling the predicted responses in a correct way [41].

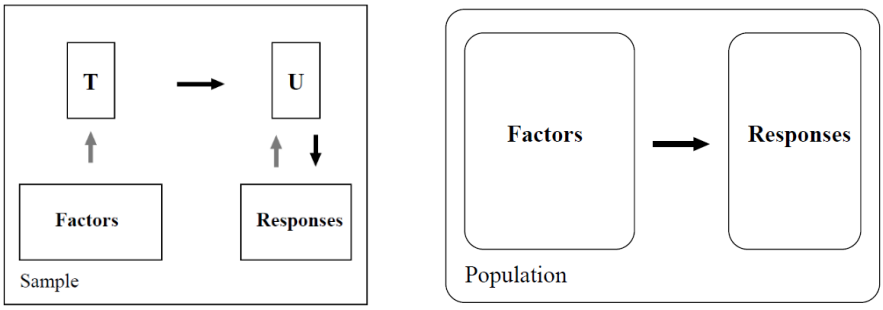

Figure 1.2 Schematic outline of PLS modeling, adapted from [42].

In **Figure 1.2**, it is a schematic outline of PLS modeling, representing precisely, the idea of the selection of latent variables [42]. Latent variables are those whom have impact or are significant in the responses variation [43]. So, the overall goal of a statistical model is to analyze the factor of the population to predict the responses, however, PLS analyzes

the factors, extracts the latent variables, T, and then uses T to predict U and then U is used to build the predicted responses [42].

The statistical-mathematical basis of PLS is an algorithm that in each iteration tries to maximize the variance of dependent variables explained by the independent one, reducing the independent variables to a minimum of optimized vectors, redistributing the weights to the original variables. The following equations represent this algorithm [41].

Step 1 $W \propto E^T u$ (estimates X weights)

Step 2 $t \propto E\,W$ (estimates X scores)

Step 3 $C \propto F^T t$ (estimates Y weights)

Step 4 $u = Fc$ (estimates Y scores)

Initially, it is important to create two matrices, E = X and F = Y. The iteration process begins by arbitrating values for *u* vector. To simplify the calculations, this *u* vector might begin as a unit vector (u= (1,1,…,1)) or, in the case of more than one Y variable, it might begin with the values of one column of Y matrix. Then, step 1 begins, with the aim of estimating X weights. In this step, the transpose matrix of E is calculated in order to normalize the data. When X values have different order of magnitude, PLS might be induced in error and estimate the weight based on order of magnitude, and by normalizing the data, they will always be in the interval from -3 to 3. After estimating X weights, PLS scores each variable depending on the weight. Thus, a *t* matrix is created and then used in step 3 to estimate the Y weights. In this step, just like in step 1, the matrix used is the transpose with the aim of normalizing the data. Finally, in step 4, the Y scores are calculated and vector *u* gains new values to restart the iteration process [41], [44], [45].

The assumptions of PLS model are the same of MLR described in **1.1.1.1**. However, this model has another assumption related with the existence of latent variables. It is assumed that the system under investigations is influenced by only a few variables, the latent. The number of these variables is unknown, and one of the objectives might be estimate this number [43], [44].

The models MRL and PLS are useful while using QbD, which is an approach that is becoming an obliged procedure in pharmaceutical industry for the optimization of processes for production of pharmaceutical products and for the improvement of the quality and characteristics of products. In this work, QbD will be implemented for the development of 3D porous structures for drug delivery in the treatment of oral and *in situ* vaginal infections.

1.2 Buccal and vaginal diseases

1.2.1 Buccal diseases

It is known that oral health is more than a healthy dental care [46]. There are several types of superficial oral lesions that may include candidiasis, herpes labialis, recurrent aphthous stomatitis, erythema migrans, hairy tongue and lichen planus [46], or they can turn up as masses (that can be associated to carcinomas) [47].

Until 1940s the treatment of oral mucosa diseases was almost nonexistent, since they were mostly caused by fungus [48]. Between 1960 and 1986, it was estimated that about 62% of healthy people presented signs of *Candida Albicans* existence. This microorganism is responsible for oral thrush (oral candidiasis), which is a disease known for almost 2000 years [49]. This type of infection is very usual in infants, but also adults may be affected, especially when suffering from (i) any immune deficiency caused by viruses like human immunodeficiency virus (HIV) or some therapies that might lower the immune system, or (ii) other illnesses (as leukemia, malnutrition) [46].

Herpes simplex virus (HSV) can cause a primary oral infection at young age, and it is asymptomatic in 80% of the cases [50]. When there is any kind of symptom, it is with an acute outbreak of oral vesicles that collapse to form erythema and ulceration. In some cases, the virus might not disappear, being present in a latent way, and leading to recurrent infections. Some probable causes for these recurrent infections might be ultra violet light exposure, trauma, fatigue, stress and menstruation [46].

Another case of oral disease is recurrent aphthous stomatitis, or mostly common, “canker sores”. The effective cause or predisposing factors for this type of lesions is unknown, however, some variety of host and environmental conditions are associated with this illness [46]. Curiously, these ulcers affect mostly nonsmokers, women, people under 40, Caucasian patients and people of high socioeconomic status [51].

Erythema migrans is often confused with lyme disease because it is the first symptom of this disease [52]. The symptoms, in most cases, are tongue lesions that appear as erythema caused by atrophy of the filiform papillae. It affects children and adults, but women are most likely to suffer from this kind of condition. In general, patients are asymptomatic, but when the symptoms come up they can be painful and burning [46].

Hairy tongue is another example of oral disease which is caused by improperly desquamation or increased keratinization of the papillae, and the papillae’s length may rise from 1 mm to 12-15 mm. It affects mainly men, smokers, coffee and tea “addicts”, or drug addicts [46][53].

Oral lichen planus is a chronic inflammatory disease that may affect any lining mucosa, and it can emerge in several different patterns. Generally, it affects the buccal mucosa, tongue, and the gingiva and it appears as reticular, popular, plaque-like, erosive, atrophic or bullous type. It is very difficult to understand the causes of this disease, however, and once more, it is related with immune deficiency [46] [54] [55].

Another type of manifestation of oral diseases is the appearance of masses, that may lead to a concern about oral cancer [47]. Palatal and mandibular tori consist in the existence of a mass that is due to an extra bone covered by a layer of cortical bone [56].

The treatments for the different diseases described above are synthetized in **Table 1.2**. For oral candidiasis, there are mainly three drugs that might be used. The most common is miconazole and in alternative to that it could be used Nystatin. However, for more severe cases, Fluconazole is the best option [57]. To treat herpes simplex virus infections [58], the most used drug is Acyclovir [59], but Famciclovir [60] and Valacyclovir [61] are also options to be considered. The treatment for recurrent aphthous stomatitis has a lot of options that might be useful such as antiseptics, anti-inflammatory, analgesics, antibiotics, corticosteroids and anesthetics [62]. In the case of erythema migrans, hairy tongue and oral linchen planus, there are no specific treatments. The only thing that can be done to help people suffering from these conditions is to encourage them to have a healthy and proper dental care [63] [64] [65].

Drug delivery through oral mucosa cavity has many advantages. One example of that is the fact that this route of administration allows to contour the hepatic “first-pass” elimination that follows gastrointestinal absorption [66] . In addition, the gastric acid or digestive enzyme-mediated degradation occurring in the gastrointestinal tract is avoided. When the drug is metabolized in the organism, between its site of administration and the site of sampling for measurement of the drug concentration, it stands before “first-pass” elimination. The liver is usually assumed to be the major site, however gastrointestinal tract can also be considered a potential site of first-pass metabolism [67]. Another advantage of using oral route of administration is the fact that after oral mucosal administration, the potential variation in the gastric-emptying rate or the presence of food do not influence the absorption of the drugs [66].

Table 1.2 Medication used to treat the different oral diseases, adapted from various sources [59-67]

Disease	Drug	Form
Oral Candidiasis	Miconazole	Gel
	Nystatin	Drops
	Fluconazole	Tablets
Herpes Simplex Virus	Acyclovir	Liquid suspension
		Capsules
		Tablets
	Famciclovir	Tablets
	Valacyclovir	Tablets
Recurrent Aphthous Stomatitis	Chlorhexidine	Gel
	Triclosan	Gel
	Diclofenac	Topical
	Amlexanox	Ointment
	Doxycycline	Gel
	Corticosteroids	Topical
	Hyaluronic acid	Topical
	Anesthetics	Topical
Erythema Migrans	No specific treatment	-
Hairy Tongue	No specific treatment	-
Oral lichen planus	No specific treatment	-

The first steps to develop alternative devices for oral drug administration have already been taken. Although gums are not a very common device for oral route of administration, they were developed for the first time in 1928. Despite this kind of device didn't receive many acceptance, Aspergum, the gum, is still available in the market [68]. However, this non-acceptance for gums, as devices for oral route of administration changes when the nicotine chewing-gum, Nicorette, was distributed, in Britain, in 1980 [69]. In 1991, Pedersen M. and Rassing M., developed a chewing gum as a drug delivery system to release Miconazole. Each gum had 55 mg of the

antifungal drug, miconazole (6,25%), and the amount released range was between 2.6 mg to 5.0 mg, corresponding to 30 minutes of mastication [70]. Later, in 2005, Maggi, L. et al prepared the 3TabGum, another gum-type device. The results showed that after 10 minutes chewing, the drug was almost all released and the amount of drug still present in the residual gum was 5-10% of the initial quantity. It was also possible to conclude that, increasing the chewing time, no significant differences would be evidenced among the quantity released [71]. More recently, in 2012, A. Aslani *et al*., developed a caffeine gum prepared by softening of gum bases and then mixed with other formulation ingredients. Two different types of gums were developed, one with 20 mg of caffeine and another one with 50 mg. After the tests, it was observed that with 30 minutes chewing, the gums released about 90% of their own drug content [72].

Other alternative device are candy matrices. In 1985, T. Stanley and B. Haque claimed a patent about the development of a candy matrix device to incorporate sedatives, analgesics and anesthetics, to be absorbed through mucosal tissues. In the examples given, the drug release was evaluated for 8 hours, and the maximum quantity for drug release was 10 ng per mL plasma. [73]. In 1992, R. Acharya *et al.* claimed a patent to the method and composition of calcium polycarbophil controlled release. The matrices of this invention can be applied for candy structures, so, one of the examples given is precisely about that. Unfortunately, there is no available data or results regarding the time and amount of drug release [74].

Recently, GEO company has been developing alternative devices. A. Batuca started the development of 3D porous scaffolds for controlled drug release through oral route of administration, as gum and candy devices. There were several polymers used during this work and the best candidates for candy structure were native PolyGeo and the combination between Xanthan Gum with PolyGeo resulting on a medium pore size of 50 μm, a swelling rate higher than 30%, high degradation rate (till 9 days), and the drug release after 5 hours was 80 mg per gram of scaffold. Regarding the gum format, the best options were Chitosan mixed with TEMED and Chitosan mixed with Xanthan Gum and TEMED, which presented a medium pore size of 100 μm, a swelling rate lower than 30%, low degradation rate (more than 120 days) and the drug release in 2.5 hours was 60 mg per gram of scaffold [75].

1.2.2 Vulvovaginal Infections

During reproductive age, women may suffer from vaginal infections [76]. It is estimated that fungal infection is the second most common cause of vulva and vagina inflammation, being bacterial vaginosis the first [77] [78]. This infection is caused by overgrowth of the yeast *Candida* [79]. Between 85% to 90% of the cases, the most common pathogen is *Candida albicans* [77].

In 1849, Wilkinson first described vaginal candidiasis [80], but it was only in 1875 that Haussmann demonstrated that the microorganism causing both vulvovaginal and oral candidiasis is the same [81].

The most common symptoms of this kind of infections are external dysuria, vulval pruritus, swelling or redness [82]. Other signs may be vulva oedema, fissures, excoriation or thick curdy discharge [83].

Episodic vulvovaginal candidiasis can be divided in two types: uncomplicated or complicated [83]. The first, uncomplicated cases are the cases caused by *C. albicans*. The complicated cases are caused by other species rather than *C. albicans*. These cases may occur by severe infections, during pregnancy or being associated with another medical condition such as immunosuppression or diabetes. Another form of uncomplicated cases is recurrent vulvovaginal candidiasis, and this is considered when a woman suffers for four or more episodes per year [3].

The treatment for vaginal candidiasis depends in the type of infection: complicated or uncomplicated cases. In 90% of the uncomplicated cases, a short-term local therapy or a single-dose oral treatment is effective. In this case, the local agent easily available are azoles. An alternative of local therapy may be the oral treatment with, for example, fluconazole. For complicated cases, the treatment must be prolonged. Fluconazole is also used for this therapy [3].

It is important to increase the residence time of drugs in the vaginal cavity, to improve the treatment efficiency. Amongst drug delivery systems, the vaginal offers a very good route to release different antifungal, antibacterial and contraceptive drugs. The conventional vaginal dosage formulation, vaginal tablets, vaginal foam, vaginal gel, vaginal cream and vaginal suppositories have some advantages, such as (i) the avoidance of the “first-pass” metabolism, (ii) they are easy to formulate, (iii) it is possible to self-administrate them and (iv) they have low cost. However, they have some disadvantages associated to their use. They may produce itching, irritation of vagina, discomfort and low residence time. Novel systems of drug release may enhance the delivery of many drugs offering better therapeutic outcomes [84] [85].

GEO company in collaboration with LAQV-REQUIMTE at FCT-NOVA has already started the development of a device with tampon structure for controlled drug delivery, through vaginal route. In 2016, D. Lopes [86], started the development of this device to treat vulvovaginal candidiasis. Among the polymers selected for this study and the possible combinations between them, the results suggested that native chitosan (3% w/v) and chitosan mixed with xanthan gum (2% w/v) were the most suitable options. Native chitosan based structure swelling capacity was 30%, the compression modulus was 6.7 kPa, the pore size was 700 μm and in 8 hours, the amount of drug released was 99.1 mg per gram of scaffold. For the second option, the swelling capacity was

25%, a compression modulus of 6.2 kPa, a pore size of 150 μm and the amount of drug release in 8 hours was 104.8 mg per gram of scaffold. The most common devices for vaginal drug delivery are gelatin capsules [87] or gels [88], and it was not found any other study using tampons as the device for vaginal drug delivery.

1.3 3D Porous Structures as Treatment Vehicles

One of the most complicated issues on buccal and vaginal drug delivery is the active physiological removal mechanisms (physiological secretions as saliva and vaginal fluids) [6]. Therefore, there is a need to improve the routes for controlled release of the drug product and to assure that the drug product maintains the characteristics and efficiency needed. Due to this, the interest on drug delivery in a three-dimensional (3D) form is growing rapidly [89] [90].

Scaffolds, 3D porous structures, are commonly used for several applications in biomedical area, such as drug delivery or tissue engineering [28] [29]. Typically, scaffolds are porous networks, composed by biocompatible and biodegradable materials, **Figure 1.3**, and they appear as (i) typical 3D porous matrix, (ii) nanofibrous network, (iii) thermosensitive sol-gel transition hydrogel and (iv) porous and permeable microspheres impregnated in a polymeric matrix [92] [93] [94]. Scaffold matrices are used as controlled drug release systems, and are composed by natural or synthetic polymers [92] [95]. The aim of this structures is to yield adequate microenvironments, which means, mechanical support, physical and biochemical stimuli for optimal cell or tissues function [91] [93].

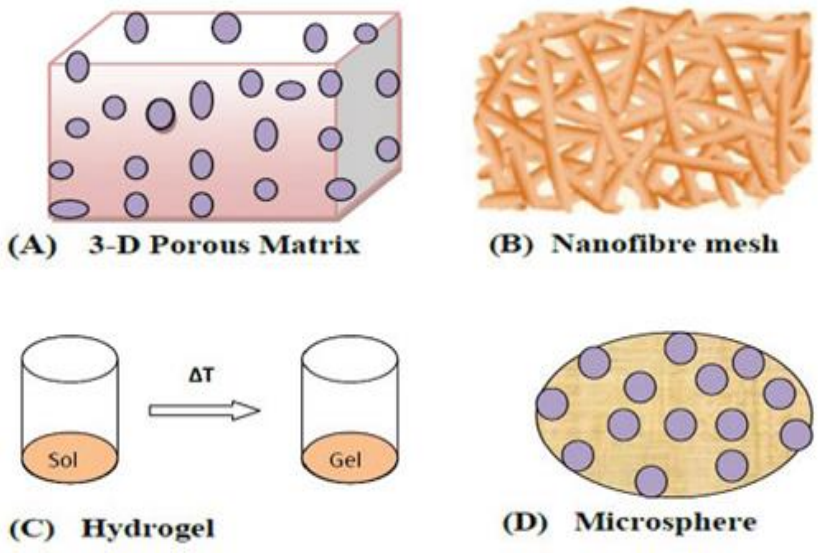

Figure 1.3 Examples of scaffold structures [92]

The chemical and structural properties of scaffold are (i) a 3D structure with appropriated volume, shape and mechanical strength, (ii) a highly porous structure, (iii) and chemical properties that don't compromised biocompatibility of the drug product in human organism [95] [96]. Thus, 3D porous scaffolds allow effective release profiles by controlling the morphology, porosity and composition of the polymeric structure. If these properties are not properly controlled, according to the requirements of their applicability, the structural stability and efficiency of the drug product may be compromised [91] [97].

1.3.1 Polymers

One of the first polymers used in drug delivery systems was lactic acid, and it was introduced in 1970s [98]. Since then, many efforts are being performed to introduce and optimize polymers in drug delivery systems.

The active pharmaceutical ingredients (API) are rarely administered alone, so excipients are used, and they are the substances where the API are incorporated. One of the reasons that excipients are used is to help rising not only the bioavailability but also the acceptance of the drug in the organism [99]. When excipients were firstly used, they were recognized as inert since they do not exert any therapeutic action or any influence in biological action of the drug [100]. However, with the advances in science, it is known that these substances may influence the velocity and extent of drug absorption and that the pharmaceutical form of these substances affect drug bioavailability [96].

The use of polymers as support for structures in drug delivery systems has many advantages, since the availability of the drug product can be higher and the bio distribution can be altered, favorably. Also, these compounds allow hydrophobic drug administration which allows the transport of the drug product to sites of action that may be inaccessible. Another great advantage is the fact that polymers (smart polymers) can turn the drugs available to certain stimulus [101] [102]. So, it is possible to group polymer devices in several categories, such as (i) diffusion-controlled devices [103], (ii) solvent-activated [104], (iii) chemically controlled (biodegradable) [105] and (iv) externally-triggered systems [106]. In diffusion-controlled systems the therapeutic substance is dissolved in a non swellable or fully swollen matrix, that prevents the degradation of the therapeutic life [107]. The solvent-activated systems are characterized as result of packing the drugs in dehydrated hydrophilic polymers and they can be swelling- or osmotically-controlled [108]. To promote dissolution in chemical or biodegradable systems, both the absorbance of the surrounding aqueous solvent by the polymer and an interaction with the water through charge interactions or hydrogen bonding mechanisms are necessary [107]. Finally, in externally-triggered systems it is possible to have as an example the polymers responsive to pH, temperature and photo or redox responsive systems [106].

One of the critical characteristics of polymeric excipients is their removal mechanism, in other words, how they are expelled from human organism. There are two options. The first is through renal clearance, where they are expelled directly via the kidneys after degradation in the liver, and the second is through metabolic clearance, and this happens when the polymer biodegrades into small molecules and then is expelled from the body. [96]

Both synthetic and natural polymers can be used in drug delivery systems [92][95] but all present advantages and disadvantages. It is easier to control the polymeric structures of synthetic polymers, since it is possible to tailor-made the material suitable to the envisaged biological application. Another advantage is the control of 3D structures, so it is possible to adapt the properties and orientation of specific functional groups that may interact with the drug product. All these characteristics turn the synthetic polymers a good bet, however, it is very important to consider a uniform molecular weight distribution of these kind of polymers, because they don't biodegrade easily, which indicates that they must be expelled through renal excretions [109] [101].

Biodegradable polymers also attract a lot of attention once they allow the release of the drug in a controlled manner and because after their functionality they can be degraded into non-toxic monomers [101]. Despite that, the degradation products can be considered desirable or not. They must be tested since there are innumerous variables that might affect the biodegradation of the original polymer [110]. For example considering the chemical structure of the polymer it allows to control the speed and degradation conditions [96].

1.3.1.1 Chitosan

Chitosan (CHT), **Figure 1.6**, is the result of chitin N-deacetylation, and it was firstly identified in 1884. It is a linear polysaccharide composed by glucosamine and N-acetyl glucosamine that can be placed in blocks or randomly, which result from the preparation method [111] [112]. When in solid state, chitosan is a semicrystalline polymer. Considering chitosan applications, their most important features are the variation of molecular weight and the degree of deacetylation from chitin, and consequently the dependence of its solution properties [111].

Being the only pseudo natural cationic polymer and due to its unique characteristics, such as non-toxicity, biocompatibility and biodegradability, chitosan can have innumerous applications, as well as, drug delivery and tissue engineering [111] [113] [114]. In systemic absorption of hydrophilic polymers, which is the case of chitosan, it is advisable that their molecular weight is suitable for renal clearance. The degradation can be through chemical or enzymatic way, and the chemical one refers to acidic catalyzed degradation, in stomach. If the degradation is enzymatic, it must be done by enzymes that hydrolyze glucosamine–glucosamine, glucosamine–N-acetyl-glucosamine and N-acetyl-glucosamine–N–acetyl-glucosamine linkages. [113].

There are some unique and suitable characteristics provided by chitosan-based scaffolds. They can become hydrated which is useful for cell adhesion, and can generate porous structures with open interconnected channels created by the fiber network, which makes them an interesting host system [115].

In 2004, J. Lee *et al.* [116] developed a three-dimensional chitosan based scaffold, with collagen and glycosaminoglycan to the controlled release of TGF-β1. The physical-chemical characteristics were revealed, and the pore size of the structure was approximately 195.7 µm and a compressive modulus of 145.5 kPa. Three years later, in 2007, M. Prabaharan *et al.* prepared and characterized a hybrid scaffold mixing chitosan with poly(L-lactic acid). The pore size obtained was identical to the pore size of native poly(L-lactic acid) scaffolds, which may vary between 300 to 800 µm. The highest drug loading was 141.2 mg/g scaffold [117]. More recently, in 2016, U. Adhikari *et al.* studied the characteristics of a chitosan based scaffold mixed with carboxymethyl chitosan (CMC) and magnesium gluconate, also to be used in biomedical applications. Depending on the concentration of chitosan and carboxymethyl chitosan, the pore size range were different. For 4-5% CHT/CMC scaffolds the pore size range was 50-150 µm and for 2% CHT/CMC scaffolds was 150-250 µm. The compressive strength of the scaffolds increased from 0.04 MPa to 0.25 MPa as the concentration of CHT/CMC was increased from 2 wt% to 5 wt% [118].

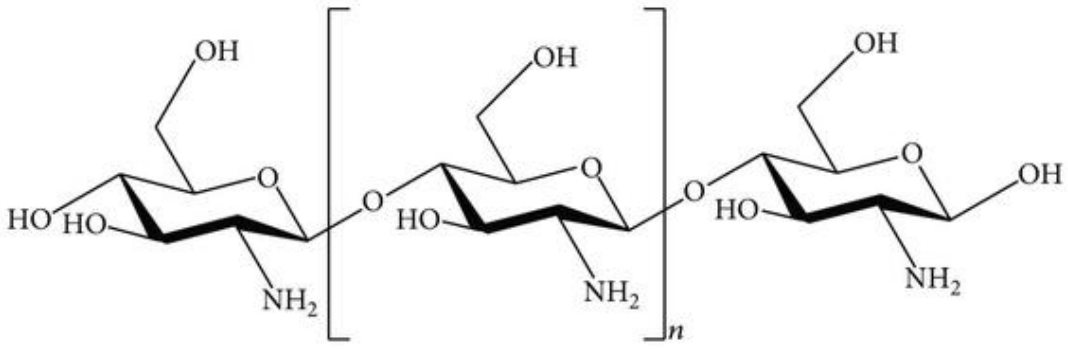

Figure 1.4 Chitosan molecule [214]

1.3.1.2 Xanthan Gum

Xanthan Gum (XG), **Figure 1.5**, is a natural polysaccharide produced by the gram-negative bacteria *Xanthomonas campestris*. Its primary structure consists on repeated pentasaccharide units. The main chain is composed by β-D-glucose units and the chemical structure counts on two glucose units, two mannose units, and one glucuronic acid unit [119] [120].

There are only a few microbial exopolysaccharides available in the market, however xanthan gum is one of them, and it represents a well-established product. The success of xanthan gum is due to its characteristics and properties. Over time, there was a lot of research on the properties and characteristics of xanthan gum and it was found that it is non-toxic and it does not inhibit growth. It was already proved that xanthan gum does not cause skin or eye irritation. For all these reasons, xanthan gum has, nowadays, various applications not only in the food industry but also in pharmaceutics, as emulsion stabilizer or uniformity in dosage formulation [119] [121].

In 1995, M. Talukdar and R. Kinget studied the swelling and drug release behavior of Xanthan Gum matrix tablets. The swelling of the gum was fast and within 45 minutes the maximum was reached, and it was about 90% above of the initial value [122]. In 2003, O. D'Cruz *et al.,* evaluated in vivo a gel formulation, to be administrated through vaginal route. The gel was composed by microcrystalline cellulose and xanthan gum. They proved that favorable toxicity profile of administered intravaginal gel may provide the foundation for its clinical development as a safe and effective broad-spectrum anti-HIV microbicide [123]. In 2007, T. Phaechamud and G. Ritthidej performed a study to evaluate the sustained-release of propranolol HCl from a matrix composed by chitosan and xanthan gum, and the results showed that almost 100% of the drug product was released in approximately 13 hours. All the matrix had the same amount of propranolol HCl, 80 mg/tablet. They concluded that the releasing from the tablets containing chitosan and xanthan gum was slower than the ones containing native chitosan [124]. This clearly demonstrates that the polymer nature it is an important factor to design different porous structures with different practical behaviors.

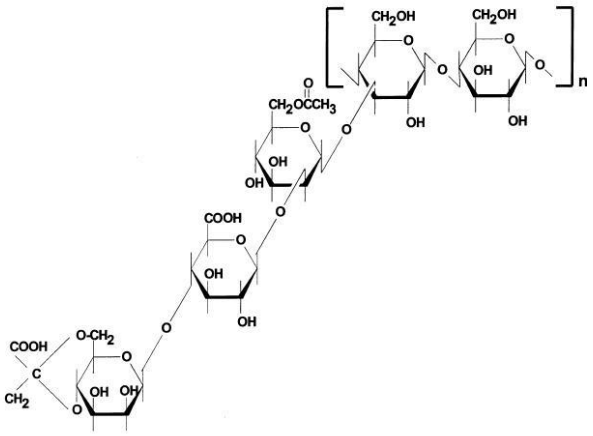

Figure 1.5 Xanthan gum structure [125]

1.3.1.3 PolyGeo

PolyGeo (PG) is a synthetic polymer, of GEO company, water-soluble, and it is based on an anionic polyacrylamide.

Although acrylamide monomer, **Figure 1.6**, has been shown to be toxic, it is generally accepted that polyacrylamide is not, and there are a lot of efforts being done to produce super porous hydrogels based on polyacrylamide [126] [127]. Actually, PolyGeo was already submitted to biocompatibility tests and none toxicity for cells was registered.

One of the most important applications of polyacrylamide based polymers is as hydrogel scaffolds for cartilage in tissue engineering [128]. Also, polyacrylamide can be used in plastic operations [129], drug treatment [130], contact lenses [131] and wound dressing [132].

The scaffolds formation is dependent on the crosslinking degree and it happens through covalent, ionic or hydrogen bonds. The synthesis and characterization of pH- and temperature-sensitive hydrogels by copolymerization and crosslinking are not well stablished, but a lot of studies are being done in this area [133] [134] [135] [136].

In 2016, two studies were performed in order to develop 3D porous structures for controlled drug delivery through different routes of administration, buccal and vaginal. In these works, several polymers were used and PolyGeo was one of them. To the oral route of administration, two devices were developed: a gum and a candy. The best scaffolds for the candy structure were native PG and PG mixed with Xanthan Gum scaffolds, having a medium pore size of 50 µm, a swelling rate higher than 30%, a high degradation rate (till 9 days) and the drug release after 2.5 h was 60 mg per g of scaffold [75]. For gum structure, it was supposed to develop a structure with low and slow swelling rate compared with the candy matrices, and once PG did not fit those conditions, it was not the best option [75]. So, for this structure, the best polymer combinations were chitosan with TEMED and chitosan mixed with xanthan gum and TEMED, which presented a medium pore size of 100 µm, a swelling rate lower than 30%, a low degradation rate (more than 120 days) and the drug released after 5 h was 80 mg per g of scaffold. In the second work, related to vaginal route of administration, native PG was not a success, since it was impossible to perform swelling tests due to the instable behavior of the structures. However, when mixed with other polymers or crosslinked, its integrity improved, but unfortunately, the swelling rate did not surpass 20% and due to that, no more studies were performed [86].

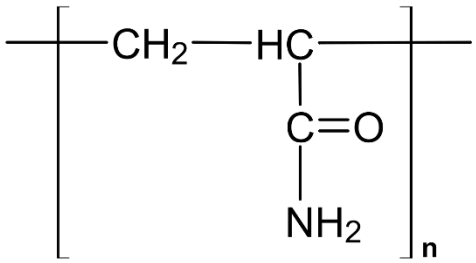

Figure 1.6 Polyacrylamide structure

1.3.1.4 Sodium Alginate

Sodium alginate (ALG), **Figure 1.7**, is a natural polymer presented in brown algae [137]. Alginates are a family of natural polysaccharides which contain different amounts of 1,4'-linked β-D-mannuronic acid and α-L-guluronic acid residues. The preparation of alginate beads is made by extruding a solution of sodium alginate into a divalent crosslinking solution [138]. The biosynthesis of alginate consists of four steps: (i) synthesis of precursor substrate, (ii) polymerization and cytoplasmic membrane transfer, (iii) periplasmic transfer and modification, and (iv) export through the outer membrane [139].

Alginate biocompatibility has been extensively studied in vitro and in vivo, despite this the impact of alginate composition is not yet well stablished. Alginate hydrogels are prepared by different cross-linking methods. Structurally alginates have similarities to extracellular matrices of living tissue and because of that it is possible to use this compound in several biomedical applications, such as wound healing [140], delivery of bioactive agents [141] and cell transplantation [142] [143]. Some properties also enable alginate to be used as a matrix for drug delivery. One example is relatively inert aqueous environment within the matrix that they have and a mild room temperature encapsulation process free of organic solvents associated with their production. A high gel porosity which allows for high diffusion rates of macromolecules and the ability to control this porosity with simple coating procedures are other two positive properties of alginate, as well as dissolution and biodegradation of the system under normal physiological conditions [138].

In 2006, G. Sharma *et al* developed a bioadhesive dosage form of clotrimazole, mixing Carbopol 934P with sodium carboxymethyl cellulose and sodium alginate. In vitro release studies showed that the structure with 2:1 ratio of Carbopol 934P / sodium alginate containing 986.1 mg of clotrimazole, which represent 99% of tablet weight (approximately 995 mg), release 976.2 mg of clotrimazole over 24 h [144]. In 2007, Y. Xu *et al*., prepared a dual crosslinked matrix made of sodium alginate and chitosan, for controlled and site-specific drug delivery. They concluded that the total protein released from the sodium alginate and chitosan structures, for a mass ratio of 9:1

was 81,24%, a higher value than for those with a mass ratio of 7:3 and 5:5 that showed to be less than 60%. However in terms of retarding drug release, there was no significant advantage in using the mixture of the two polymers [145]. In 2011, G. Lee *et al.*, produced a scaffold for biomedical applications made of calcium phosphate cement with sodium alginate. The pore size obtained were in the range from 200 to 600 µm, and, within 12 h, up to 20-30% of the drug was released for all loading conditions [146].

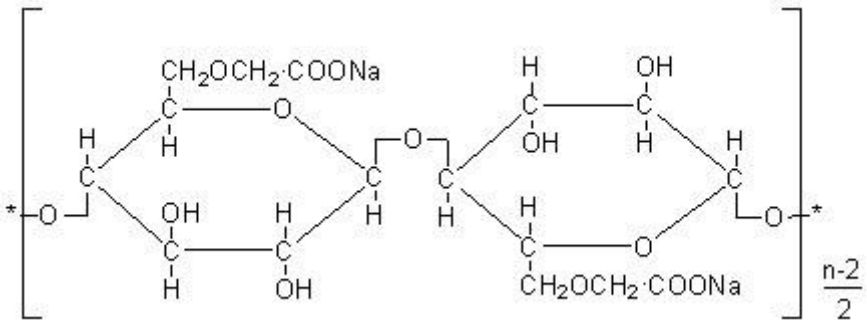

Figure 1.7 Sodium alginate structure [147]

1.3.1.5 Gelatin

Gelatin (GL), **Figure 1.8**, is a protein fragment obtained by partial degradation of water insoluble collagen fiber. Structurally, gelatin is constituted by large and complex polypeptide molecules of the same amino acid composition as the parent collagen, covering a broad molecular weight distribution range. Despite the similarities to collagen, gelatin exhibits essentially the same common properties of typical polymeric substances, which is not the case of native collagen. It is non-toxic and it is compatible in living body, and due to that gelatin has been widely used in biomaterials, food and cosmetic fields [148] [149].

Gelatin is a good candidate to imitate the chemical composition of natural collagen, once it derives from collagen through acidic or basic hydrolysis. Another good characteristic of gelatin is the fact that potential pathogens are eliminated once gelatin is a denatured protein, and the denaturing process prevents pathogens. As biopolymer, gelatin is often used in tissue engineering and as a carrier in drug delivery [150][151].

In 2010, X. Wu *et al*., developed a 3D structure using unidirectional freeze-drying method. The mean pore size of the scaffolds was between 50 to 100 µm. It was also performed degradation tests and it was concluded that the scaffolds degradation depends on the gelatin concentration. The scaffolds produced from 1% gelatin solution, presented a weight loss percentage of

approximately 95% after 18 days, meaning that it was almost completely degraded. In the case of scaffolds produced from 5% gelatin solution, the percentage of weight loss was 59% [152].

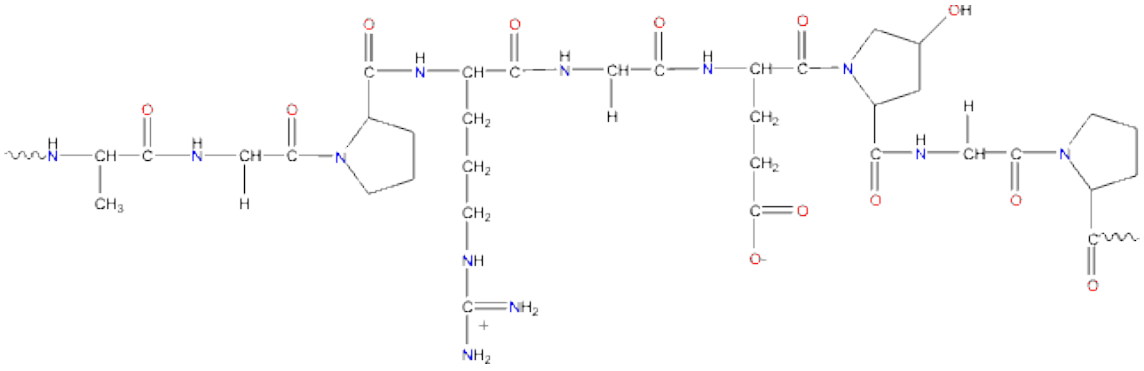

Figure 1.8 Gelatin structure [153]

1.3.2 Polymers Processing

There are different methods for polymer processing to produce scaffolds for pharmaceutical applications. Some examples are freeze-drying, scCo2, electrospinning [154], 3D printing [155], particulate leaching methods [156], gas foaming methods [157], sol-gel technique [158], thermally induced phase separation [159], fiber mesh [160], rapid prototyping [161], emulsion templating [162] and textile technologies [163].

1.3.2.1 Freeze-drying

Freeze-drying process, also known as lyophilization, is widely used in the production of porous materials namely for tissue engineering among other biological applications [164] [165], but also, in pharmaceutical industry to provide stability to drug products [166].

The freeze-drying method, despite its complexity, is considered a unit operation, and is well accepted and it is widely used in pharmaceutical industry [167]. This is due to the process temperature, because it is known that working with negative temperatures (in this case between -70ºC to -10ºC, or , when working with liquid nitrogen, around -196ºC) does not affect significantly unstable bioproducts, comparing to drying at ambient temperature or higher temperatures [168].

This method consists in three steps: (i) freezing, (ii) primary drying and (iii) secondary drying. It is during the first step, that the material is hardened by freezing process and all fluids present

become solid bodies. As freezing progresses, the solute phase becomes highly concentrated and might finally crystallize. This leads to a volumetric expansion of the system [169] [170]. The second step, primary drying, also known as ice sublimation, starts as the pressure in chamber is reduced, and placed under vacuum. The porous structures are formed from the voids left by the removed solvent [166] [169] [170]. Lastly, the third step of freeze-drying method is secondary drying. The beginning of this step happens once the ice is distilled away, and a higher vacuum allows the progressive extraction of bound water at above-zero temperatures [169] [170].

There are some substances such as peptides, proteins and complex synthetic organic molecules that must be monitored, because they are susceptible from suffering chemical reactions in aqueous solutions [171]. Many of the reactions may jeopardize the safety and efficiency of the drugs. Some of these are hydrolysis [172], cross-linking, oxidations [173], aggregation [174] and disulfide rearrangements [168]. Over time, it was possible to understand that this kind of reactions may be retarded, when in dry state.

The “freeze concentrate” is when the solute phase becomes highly concentrated, and this happens as freezing progresses. This kind of process may induce some stress in the system, mainly when proteins or drug products are impregnated. This stress has some consequences in their characteristics. An example is the change in products concentration that is raised or the interaction between them that is also raised which may lead to aggregation. The appearance of crystals or buffer salts may reduce hydrophobic interactions, may change the pH of the system and, also, can improve the formation of large ice-aqueous interfaces and a huge increase in ionic strength [166] [169].

Controlling some freeze-drying variables such as freeze temperature, solution concentration, nature of the solvent and solute and the freeze direction, it is possible to obtain specifics pore sizes, pore volumes and morphologies [175]. If the freezing process occurs at low temperatures (-80ºC) and this means that the sample freezing time is very short, the formation of ice crystals is rapid and it is possible to obtain a very small pore size (approximately 85 µm). If the temperature of the process is higher (-20ºC) it is possible to obtain a larger pore size (approximately 250 µm). Another choice is liquid nitrogen, and in this case the temperature is even lower (-196ºC) and this results in a pore size of approximately 45 µm [167] [176].

In 2008, N. Sultana, and M. Wang, fabricated scaffolds based on hydroxyapatite and poly(hydroxybutyrate-co-valerate) using freeze-drying as polymer processing method. The temperature of freeze-drying vessel was set at -35ºC, the samples were freeze dried for 72 hours and at vacuum. The resulting pore size reached 300 µm [177]. In 2012, T. Garg, *et al.* developed a chitosan based scaffold using this technology. The freezing occurred for 5 days at -70ºC and then the lyophilization lasted another 3 days. The preparation before the lyophilization contemplated three steps. In the first step, freezing phase, the temperature was -40ºC at vacuum

(6.4mbar), and the duration was 10 minutes. During the second step, the sample was exposed to -15ºC and vacuum (1.4mbar) for 20 minutes. The last step took 5 days, and the drying was performed at 30ºC and 0.98 mbar. The mean diameter of the pores obtained was between 10-20 µm [178]. In 2016, A. Abdal-hay, *et al.* developed 3D porous structures to be used in biomedical applications. The chitosan based scaffolds were produced by lyophilization at -20ºC during 20 hours. The pore size was about 33 µm and the swelling rate very high, varying between 150% to 720% in 15 minutes [179].

1.3.2.2 Supercritical CO_2

Supercritical fluid technology is considered to have a huge potential in biomedical and pharmaceutical applications namely, considering the development of materials and formulations, especially when morphology control and high purity are required [180]. Supercritical fluids can be defined as a substance for which both temperature and pressure are above the critical value [181], as shown in **Figure 1.9**, that represents a schematic pressure-temperature phase diagram for a pure component, showing also the supercritical fluid region.

In biomedical applications, the absence of any kind of undesirable residual solvent is required, once they may contaminate the device and cause toxicity problems. To avoid this kind of contamination, new approaches are being developed and the most commonly used is carbon dioxide (CO_2) in supercritical state [182].

Carbon dioxide (CO_2) is a clean, non-toxic, non-flammable and versatile solvent used in synthesis and processing of different materials. The use of supercritical CO_2 ($scCO_2$) can have several chemical, environmental and financial benefits. Among the environmental advantages and the possibility to control parameters that may control the morphology, such as pressure, temperature and depressurization rate, $scCO_2$ has liquid-like densities and gas-like viscosities and diffusivities, which helps penetrating porous structures. In addition, CO_2 can be easily removed from the materials without leaving any residues, because CO_2 reverts to the gaseous state upon depressurization. Also, due to the high pressure of this technology, it allows the production of sterile, ready-to-use devices. However, this kind of process requires high pressures and relatively specialized equipment, and it might be a negative aspect that need to be considered according to the given application [182] [183].

$ScCO_2$ can be used to form foamed scaffolds and with this method the escape of CO_2 from a plasticized polymer melt generates gas bubbles that shape the developing pores [184]. In the preparation of devices for controlled-release drugs, $scCO_2$ can be an alternative to the liquid solvent that is used to swell the polymer matrix and that serve as a carrier for the drug component [185].

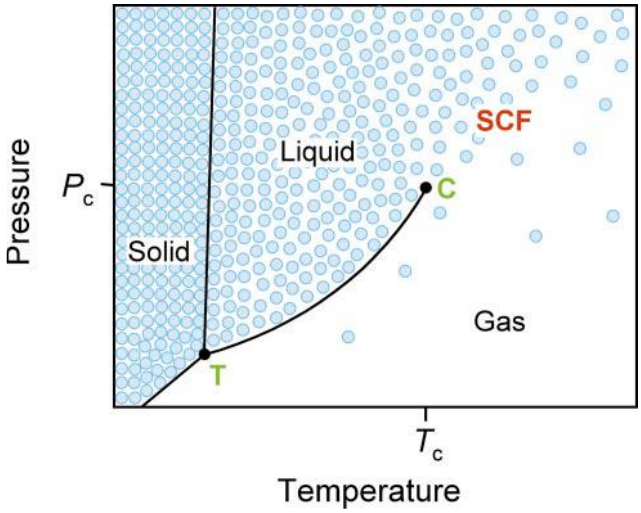

Figure 1.9 Schematic pressure-temperature phase diagram for a pure component showing the supercritical fluid (SCF) region [183]

In 2007, H. Tai *et al.* produced porous scaffolds to be used in biomedical application, using $scCO_2$ technology. This study was performed with poly(lactic acid-co-glycolic acid) with different ratios of lactic acid and glycolic acid, and depending on this proportion the pore sizes varied between 38.8 µm to 580.1 µm [186]. In 2015, B. Chen *et al*. also used $scCO_2$ to produce a porous structure for biomedical applications, using polylactic acid and polyethylene glycol. The average size of polylactic acid pores was about 77 µm, in the presence of 10% of polyethylene glycol [187]. In 2016, A. Batuca when developing the scaffolds for the gum devices, used this technique to obtain large pores, as intended. The average pore size obtained was around 160 µm [75].

1.4 Strategy: QbD implementation in two case studies

This Master thesis purposes the implementation of Quality by Design method as an optimization tool to guide in a conception of a medical route solution for two case studies, one applied to buccal route of administration and the other applied to vaginal route of administration. Therefore, this work will be divided in two phases: QbD studies and practical validation in laboratory.

During the application of Quality by Design approach, it is necessary to go through several steps.

The first step consists in defining the objectives or method goals and, also defining the quality target product profile (QTPP) and the critical quality attributes (CQA) of the drug product. This step will be accomplished using data already acquired by GEO Company in previous projects.

Secondly, it is necessary the scouting and evaluation of the method. Once this work is applied to two cases that have already been studied, the best results of those works are the inputs of this thesis. So, in this step the CMA and the CPP are defined. This step will be accomplished using previous data already acquired by GEO Company in previous projects.

The third step incorporates the method selection and the risk assessment, being possible to also identify the “design space”. Is in this stage of the project that Design of Experiments is used, and consequently the software SIMCA. The reason why this software was chosen is due to the fact that FCT-NOVA host research group has already used it in previous studies and this makes it easier to learn how to use the software. Once the results from risk assessment are known, it is possible to perform suitability tests to identify the critical method variables. Herein, it might be possible to understand what are the suitable conditions to achieve the purposed objectives, not only in terms of polymers processing method, but also, in terms of polymer choice and every single process conditions.

The last step of QbD approach consists in method validation. This means performing, testing and characterizing the 3D porous structures with and without drug, as well as, to perform releasing studies to understand if the goals are reached.

1.5 Thesis Organizational Outline

The objective of this thesis is the optimization of 3D porous structures for controlled drug delivery, through two types of routes of administration, oral and vaginal.

For the first route of administration, oral, the candy characteristics are (i) 150 μm of pore size, (ii) 5 kPa of compression modulus, (iii) a swelling capacity at pH values between 5 and 7 and (iv) the capacity to release 50 milligrams of drug per gram of support in 5 hours.

For the second one, vaginal route, the specifications are (i) a porous size between 2 and 15 μm, (ii) a compression modulus higher than 4.7 kPa, (iii) a swelling capacity at pH value 3,8 and (iv) the capacity to release 800 milligrams of drug per gram of support in 8 hours.

The Introduction chapter is divided in four main subchapters. The first one, *Quality by Design*, describes this method, including the elements and the steps, and identify the main advantages of QbD implementation. The second subchapter, *Buccal and Vaginal diseases*, focus on oral and vaginal diseases and infections and includes examples of three drugs associated with these routes of administration. The third subchapter, *Porous Structures as Treatment Vehicles*, was related to the utilization of 3D porous structures e controlled drug release, including the polymers used and the processing methods. Finally, the last subchapter, *Strategy: QbD implementation in two case studies*, shows the drive line of the implementation of the QbD approach to the cases in study.

The Materials and Methods chapter focus not only in the material and protocols used in the laboratory work, but also to the tools and protocols necessary during statistical analysis.

The Results and Discussion chapter is divided in three main section. In the first one, the results of QbD statistical analysis are presented and discussed. The second section is related with scaffolds characterization results, obtained through swelling tests, mechanical analysis, SEM and porosity and density measurements, FTIR-ATR analysis, degradation studies and biocompatibility tests. The last section focuses on the results obtained from swelling tests.

A Conclusion chapter is also included with the purpose of critically evaluate the work described, the strategy followed and the results obtained, and finally suggest possible future work.

An Appendix section incorporating any important additional information of this study that was not included in the main text, is provided at the end of the thesis.

2. Materials and Methods

2.1 Reagents

For the casting solutions: acetic acid (AA, CAS No 64-19-7, purity ≥ 99%, from ROTH), ammonium persulfate (APS, CAS No 7727-54-0, purity ≥ 98%, from Xilong Chemical Co., Ltd.), medium molecular weight chitosan (CHT, CAS No 9012-76-4, from Sigma Aldrich), *N*,*N*-methylenebis(acrylamide) (MBA, CAS No 110-26-9, purity ≥ 98%, from Xilong Chemical Co., Ltd.), tetramethylenediamine (TEMED, CAS No 110-18-9, purity ≥ 99%, from Merk) and xanthan gum (XG, CAS No 11138-66-2,purity ≥ 98%, from Solbetec). The active principle used were ibuprofen (IBU, CAS No 15687-27-1, purity ≥ 99%, from Alfa Aesar). For the swelling, degradation and release studies, citric acid (CA, CAS No 77-92-9, purity ≥ 99%, from Merk), sodium hydroxide (SH, CAS No 1310-73-2, purity ≥ 98%, from Xilong Chemical Co., Ltd.), sodium phosphate monobasic (SPM, CAS No 7558-80-7, purity ≥ 99%, from VWR Chemicals) and sodium phosphate dibasic (SPD, CAS No 7782-85-6, purity ≥ 99,9%, from VWR Chemicals) were used.

2.2 Equipment

For the casting solution, the materials used were: gobbles, heating and magnetic stirrer plates, pipettes, magnetic stirrer, tubes (1.3 cm diameter and 4 cm height), scales, steel containers (1.3 cm diameter and 4 cm height). For freeze-drying method, the materials used were: freezer, lyophilizer (from Biobase). For scanning electron microscopy Hitachi S-2400 equipment was used. For FTIR-ATR analysis an ATR accessory (from Bruker) containing a platinum crystal was used. For the mechanical tests, it was used a tensile equipment (MINIMAT firmware 3.1. For the drug impregnation, the materials needed are tubes with 1.5 cm diameter and 5 cm height, and for the drug release studies falcons and a Helius Alpha Double-Beam UV/VIS spectrophotometer were used.

2.3 QbD Protocols

2.3.1 Construction of QbD design space

The possible variables of the process for 3D porous scaffolds production were identified (as exemplified in **Table 2.1**).

Table 2.1 Example of possible variables of the process. In this example, the variables are concentration of casting solution ([casting]), concentration of the polymer in the casting solution (% polymer), the concentration of the crosslinker ([crosslinking]), the freezing temperature (Freezing Temp.), the freezing time (Freezing time), the concentration of solids, which includes polymer and crosslinkers (% solids), the ratio of polymers, when a mixture is considered (% mix) and finally the nature of the polymer (Polymer).

Possible Variables		
[casting]	% polymer	[crosslinking]
Freezing Temp.	Freezing time	% solids
% mix	Polymer	-

All the combinations between the variables were studied and **Table 2.2** was constructed to define the X, Y and Z variables.

Table 2.2 Example of the columns to construct the table of all possible combinations between variables.

Possible Cubes					
Cube number	**X variable**	**Y variable**	**Z variable**	**Pore Size**	**Swelling**

One of the combinations was selected to build another table with five columns: X variable, Y variable, Z variable, and Values obtained in previous studies for the characteristic in study. It is very important that all the variables are independent from each other. All the columns were filled with the respective data and then the information was copied to the cube. The cube was drawn and in each vertex the respective values of the variables were filled, according to **Figure 2.1.**

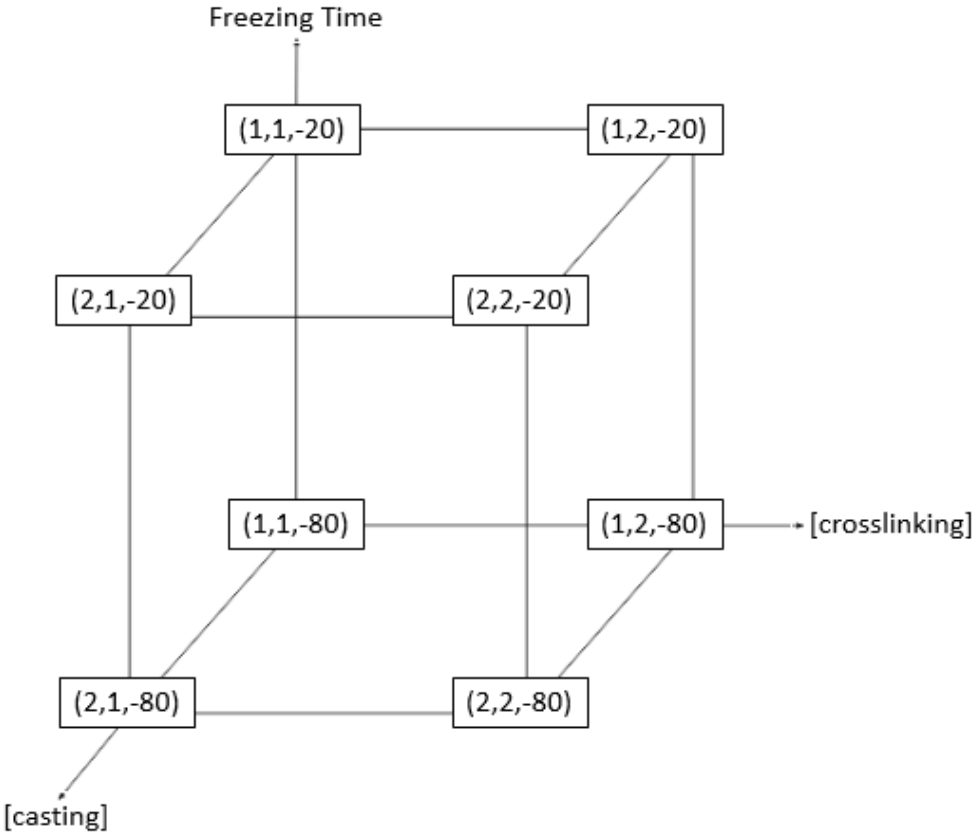

Figure 2.1 Example of a cube. In this example, the X variable is the concentration of the casting solution ([casting]), the Y variable is the concentration of the crosslinker in the casting solution ([crosslinking]), and the Z variable is the freezing temperature (Freezing Temp.). The maximum and minimum values that the variables can have are: 1 and 2% respectively, for X and Y variable, and -20ºC and -80ºC respectively, for Z variable.

2.3.2 Inserting the data in MODDE software

An Excel file was created, with a table with the same number of lines as the number of inputs. Define, in the first column, it was defined which are the variables of the process to be studied and, in the other column, the values that will be varied. The input column was filled with the different possible combinations and the output column with the values of the results obtained with previous studies.

Table 2.3 Example of the Excel table needed to introduce the data in the software.

Gelation Temperature (ºC)	Gelation time (h)	Polymer Concentration (%)	Pore Size (µm)	Swelling (%)

In the software, the commands were File -> New -> Import external design, and then the Excel file previously created was selected. It was necessary to define the last two columns as responses, selecting them and clicking the button “response”.

2.3.3 Model fitting

After inserting the data (according to **2.3.2**), it was selected the option “Fit Model” and the desired model was selected. Then “Summary if Fit” opened automatically, and the plot was analyzed. Also, the software suggests that if R^2 is higher than 0.7 and Q^2 higher than 0.5, this means that the results fit in the model. If those constants are out of the required value, try the other model and analyze again the “Summary of Fit”.

2.3.4 Wizard Analysis

After inserting the data (according to **2.3.2**) and fit them into the suitable model (according to **2.3.3**), it was selected the “Wizard Analysis” tool. All the graphics of this tool were analyzed.

2.3.5 Design Space

After inserting the data and fit the suitable model (according to **2.3.2** and **2.3.3**), the target of the respective response was defined and written in the proper place. In “Home” tab, the tool “Design Space” was selected. In “Plot Options”, the acceptance limit was defined as 10%. It is important to check if all the factor were considered.

2.4 Experimental Validation

2.4.1 Casting Solution Preparation

Chitosan was dissolved in 50 mL of the acidic water solution (1%v/v), at 80ºC, to reach the desired concentration. For xanthan gum, it was dissolved 50 mL of distilled water, at room temperature. Both dissolutions lasted about 24h. 5 mL of the solubilized polymer were placed in tubes, with 1.5 cm diameter and 5.5 cm height or in steel containers (with the same dimensions as the tubes).

Addition of crosslinker

After dissolution, MBA was added.

Addition of catalyst and initiator

After the dissolution of the crosslinker (around 3 h), TEMED and APS were added.

Drug impregnation

The solutions were pipetted into 5 mL tubes and then 90 mg of ibuprofen were added to each tube for further freezing and lyophilization.

2.4.2 Processing Casting Solutions

2.4.2.1 Scaffolds Preparation by Freeze-Drying

The casting solutions were frozen during 48 hours (freezing temperature is defined in **Table 2.4**). After that, the frozen casting solutions were freeze-dried during 48 h, at -50 ºC and 0.7 mPa.

Table 2.4 Freeze-Drying conditions.

Run	Freezing Temperature (ºC)
CHT_1/XG_1	-20
CHT_2/XG_2	-20
CHT_3/XG_3	-80
CHT_4/XG_4	-80
CHT_5/XG_5	-80
CHT_6	-20
CHT_7	-80
CHT_8	-80
CHT_9	-80
CHTXG_1	-80
CHTXG_2	-80

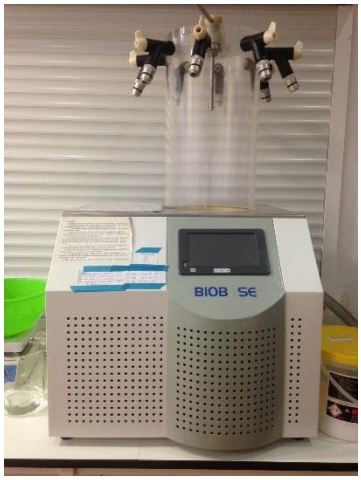

Figure 2.2 Lyophilizer

2.4.3 3D Porous Scaffolds Characterization

2.4.3.1 Scanning electron microscopy (SEM) analysis

The scaffold samples were frozen in liquid nitrogen (-196 ºC). This step allowed the fracture of the samples, for further cross-section analysis. All samples were gold coated before analysis and the accelerating voltage was set at 15 kV.

2.4.3.2 Fourier Transform Infrared Spectroscopy – Attenuated Total Reflection (FTIR-ATR) analysis

The ATR accessory contained a platinum crystal at a nominal incident angle of 45º, yielding about 12 internal reflections at the sample surface. All spectra (100 scans at 4.0 cm^{-1} resolution and rationed to the appropriate background spectra) were recorded at approximately 25 ºC. The average weight of samples was 0.02 g.

Figure 2.3 FTIR-ATR equipment and computer

2.4.3.3 Swelling Tests

The samples of the scaffolds (0.06 g) were immersed in the two different swelling solutions: citrate buffer solution (0.1 M) at pH 5.0 or 3.8 and phosphate buffer solution (0.1 M) at pH 7. The samples were placed in the swelling solution (about 100 mL for normal swelling tests and 2,5-5 mL for confined swelling tests) and the weight of the swollen samples was measured against time. Periodically, the samples were removed from the swelling medium, whipped to remove excessive water of the surface and weighted. The tests were performed on a shaker with a rotation of 100 rpm, during 24 hours. The equilibrium hydration or swelling degree (W (%)) of the samples was determined as defined in Equation (1):

$$W(\%) = \left(\frac{W_w - W_d}{W_W}\right) \times 100 \quad (2.1)$$

where W_w is the weight of the sample with water and W_d is the weight of dry sample.

2.4.3.4 Porosity and Density Measurement

The porosity and density were determined via liquid displacement method with ethanol as the displacement liquid because it can easily penetrate the pores of the scaffolds and does not induce shrinkage or swelling as a non-solvent of the polymers.

A sample of weight W was immersed in a graduated cylinder containing a known volume (V_1) of ethanol. The sample was kept in the ethanol for 15 minutes until the volume stays similar for a long time. The total volume of the ethanol and the structure was recorded as V_2. The volume difference (V_2-V_1) is the volume of the scaffold. The scaffolds were removed from the tube, and the residual volume was recorded as V_3. Thus, the total volume of the composite scaffolds was:

$$V = (V_2 - V_1) + (V_1 + V_3) = V_2 - V_3 \quad (2.2)$$

The density of the scaffold, ρ, was expressed as:

$$\rho = \frac{W}{V_2 - V_1} \quad (2.3)$$

The porosity of the open pores in the scaffold, ε_p, was obtained through:

$$\varepsilon_p = \frac{(V_1 - V_3)}{(V_2 - V_3)} \quad (2.4)$$

2.4.3.5 Mechanical Analysis

The samples were prepared cutting them into cylindrical shape. The tests were performed in a tensile equipment with uniaxial compression, at room temperature. The compression strength was measured using a mechanical tester, at a crosshead speed of 1 mm/min, a full-scale load of 20 N and a maximum extension of 40 mm. During compression test, the compression modulus was calculated from the slope of the linear portion of the stress-strain curve.

$$Stress = \sigma = \frac{F}{A} \quad (2.5)$$

$$Strain = \varepsilon_s = \frac{\Delta L}{L} \quad (2.6)$$

where F is the applied force, A is the cross-sectional area, ΔL is the change in length and L is the length between clamps.

2.4.3.6 Drug release studies

A sample from each scaffold (100-150 mg) was placed in a flask containing 45 mL of a buffer solution (pH 5-7 for gum device and 3.8 for tampon device), at 37ºC. A sample of 1 mL from each medium was taken passed 15 min, 30 min and 1 h, until 5 hours for candy structures and until 8 h for tampon device. Every time that a sample was taken from a flask, 1 mL of fresh buffer solution was replaced. The buffer solutions used were the same as the ones used for swelling tests.

For drug quantification, the samples taken from each medium (1 mL) was pipetted to a quartz cell and then the absorbance was read in a UV/VIS spectrophotometer.

3. Results and Discussion

The aim of this thesis was the optimization of the production method of two 3D porous structures, for different applications, such as oral (candy device) and vaginal (tampon) drug delivery, using an innovative method known as Quality by Design. Due to that, the characteristics of both structures are different. The pore size of the scaffold for the treatment of oral diseases must be bigger than the pore size of the scaffold for vaginal application, so the first should be around 150 µm and the second one 2-15 µm. Both structures should present around 30 % swelling capacity in acidic pH (for the vaginal application at pH 3,8 and for the oral at pH 4-7), once the normal vaginal pH is acidic and the existence of an oral infection leads to a decrease in the pH value. The mechanical properties of each scaffold are very similar once the ideal compression modulus is 5kPa for oral device and must be bigger than 4,7 kPa for the vaginal device. At last, the scaffold for the oral application must be able to release about 50 mg drug/ g scaffold in 5 h, and the scaffold for the vaginal application must release about 800 mg drug/ g scaffold. These set-points were defined according to two previous studies carried out in GEO company [75], [86].

3.1 Quality by Design studies (QbD)

The first step during the development of this project was the application of Quality by Design method to optimize the processing method of the two different structures described before. Once the objectives were defined (first step of QbD method) and all the previous information/data was collected (second step of Qbd), there were conditions to begin the third step Risk Assessment, that were defined. For this stage, MODDE software was chosen to perform the statistical analysis and to predict the best conditions to achieve the required characteristics of both structures.

MODDE software is equipped with two different statistical models and it was important to decide which one was suitable for this study. Although multiple linear regression (MLR) can deal with a lot of different independent variables (IV), it is not able to measure the significance of each IV, which might lead to false and non-trustable predicted results. However, partial least squares regression (PLS), is an example of a model that considers the weight and significant of each IV. Therefore, the chosen model was PLS.

As in any kind of investigation, it is important to define criteria to make decisions, since without this, it is impossible to make a conscious choice about the obtained results. When it comes to a statistical investigation, there are three parameters that are really important such as R^2, p-Value and Q^2. The first, R^2, shows the model fit, which means that it tells how much of the data is explained by the model. To be easier to understand, if R^2 is 0.5 this means that 50% of the data is well explained by the model. For this parameter, the acceptable range was above 0.7. P-value, the second parameter, is important to understand if the model is significant. This is something to

take into account because even if R^2 is lower than 0.7 it is possible and correct to accept the model, if p-value is smaller than 5%. At last, Q^2 shows an estimate of the future prediction precision. This is very important in QbD since the aim of this study is to predict the best conditions to produce the desired 3D porous structures. The difference between R^2 and Q^2 should be smaller than 0.3.

Therefore, it is possible to define the criteria to accept or reject a statistical study in risk assessment of QbD approach. So, the chosen criteria are:

$$R^2 \geq 0{,}7 \wedge P - value \leq 5\% \wedge Q^2 \geq R^2 - 0{,}3$$
$$0{,}5 \leq R^2 < 0{,}7 \wedge P - value \leq 5\% \wedge Q^2 \geq R^2 - 0{,}3$$

During this subsection, two responses were analyzed by MODDE Software, the pore size and the swelling capacity. After searching and reading studies about processing methods of 3D porous structures, the values of these two responses and also the values of the process parameters were collected and inserted in the software. In parallel to the theory, the process parameters correspond to independent variables and the values for pore size and swelling capacity correspond to dependent variables.

3.1.1 Cube 1: % polymer vs % crosslinker vs freezing temperature

In Cube 1, the three characteristics under study were the percentage of polymer, the percentage of crosslinker and the freezing temperature. The data were inserted in MODDE Software and the tool Summary of Fit was analyzed. In this plot, it is possible to obtain the values of R^2 and Q^2, from the three criteria parameters. Once the idea is to analyze two responses, pore size and swelling capacity, two plots were given by the software. The sample size for this cube is 12.

a)

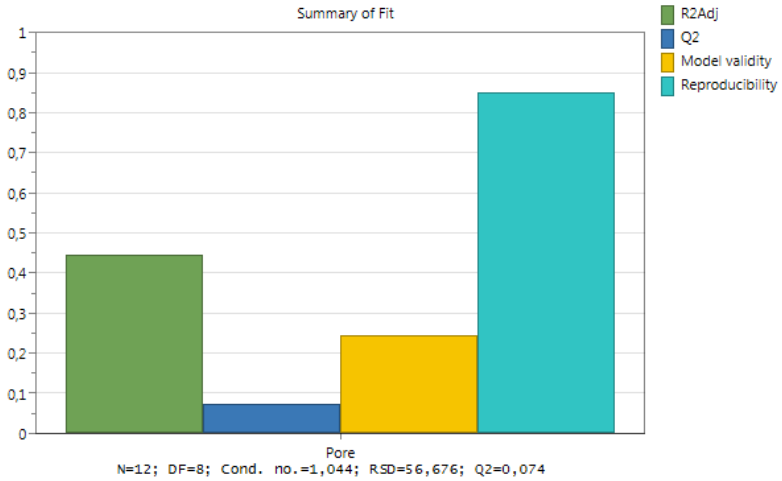

b)

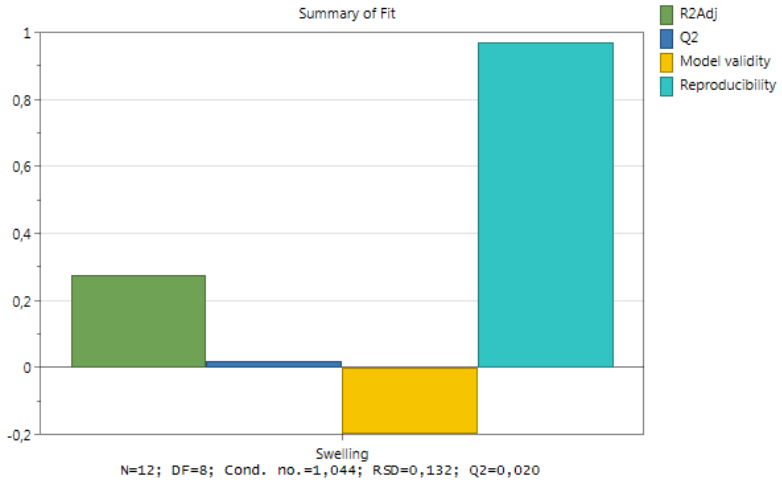

Figure 3.1 Summary of Fit for data of Cube 1: a) for pore size response, b) for swelling capacity response. Green column refers to R^2, dark blue column refers to Q^2, yellow column refers to model validity and light blue columns refers to reproductibility of the model.

In **Figure 3.1**, it is represented the Summary of Fit for the data corresponding to three different variables: % of polymer, % of crosslinker and freezing temperature.

In **Figure 3.1** (a), corresponding to pore size response, it is possible to observe that two of the three criteria defined before are graphically represented, R^2 and Q^2. The first, R^2 is around 0,45 (which is lower than 0,5) which is considered not acceptable, and Q^2 is approximately 0,074. Another parameter that is important to consider is p-value. For this case, p-value is 5,3%, which is higher than 5%. Due to this, the model does not explain correctly the data and consequently it will not be considered. In **Figure 3.1** (b), for swelling response, R^2 is also out of the gap defined in the criteria, once it is approximately 0,3. In contrast, the difference between R^2 and Q^2 is lower

than 0,3. Regarding to p-value for this experiment, it is 14,5%, which is far above 5%. Similar to the previous one, therefore this experiment was considered not acceptable.

These results suggest that in both cases, the model does not explain the data, and this is because the relationship between the independent variables (% polymer, % crosslinker and freezing temperature) and the dependent variables (pore size and swelling capacity) is not linear. There is a way to bring this relationship closer to a linear one, and it is through logarithmic and inverse transformation of the data [43].

3.1.2 Cube 2: Logarithmic and inverse transformation of the data collected for Cube 1.

In order to approximate the relationship of dependent and independent variables to a linear one, the data used in Cube 1 suffered two different transformations: logarithmic and inverse. After these transformations, the data were inserted again in MODDE Software and the Summary of Fit was, once again, analyzed. The sample size for this cube is 12.

a)

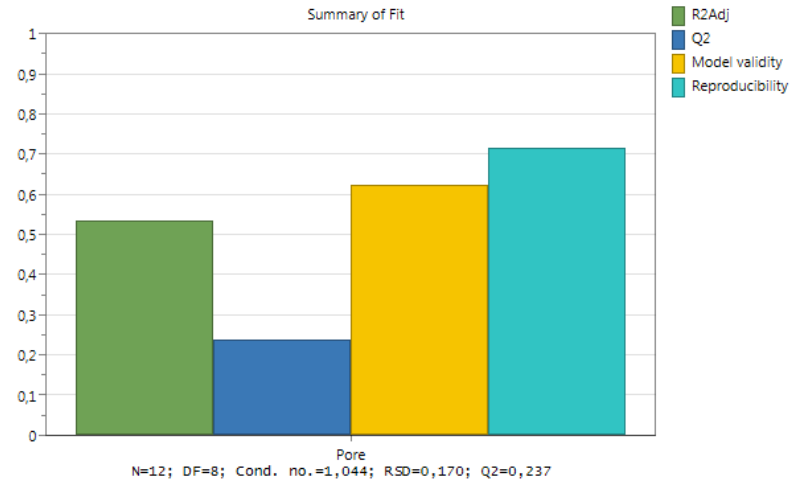

b)

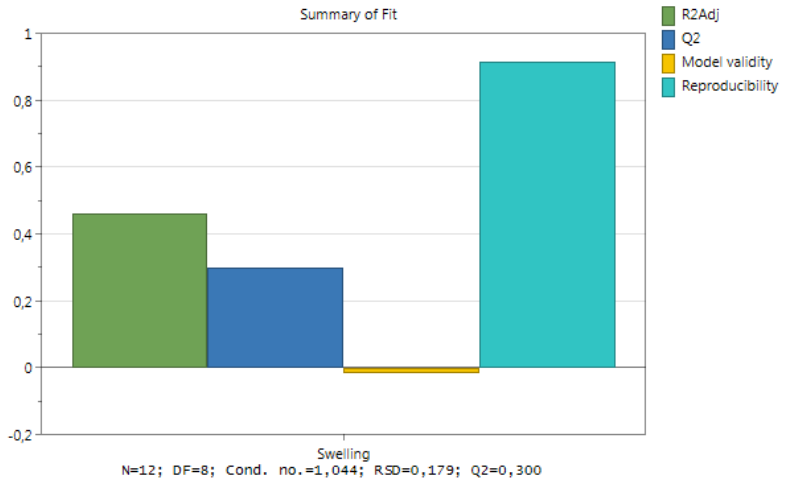

c)

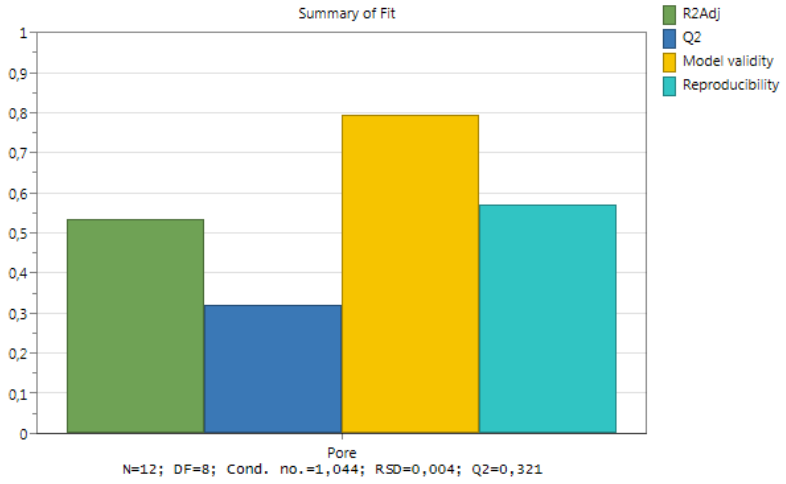

d)

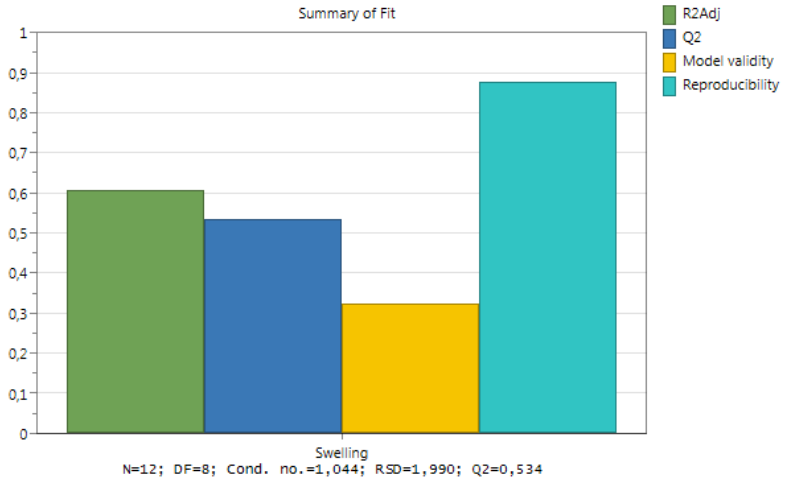

Figure 3.2 Summary of Fit for transformed data of Cube 1: a) for pore size response and inverse transformation, b) for swelling response and inverse transformation, c) for pore size response and logarithmic transformation, d) for swelling response and logarithmic transformation. Green column refers to R^2, dark blue column refers to Q^2, yellow column refers to model validity and light blue columns refers to reproducibility of the model.

Table 3.1 P-value for the tranformed data.

Transformation	Response	p-value (%)
Logarithmic	Pore size	2,8
	Swelling capacity	1,4
Inverse	Pore size	2,8
	Swelling capacity	4,8

It is represented, in **Figure 3.2**, the Summary of Fit for the transformed data of Cube 1. It is notorious the improvement of R^2 and Q^2 from the previous experiment.

Regarding logarithmic transformation, R^2 assumed values of 0,5 for pore size response and 0,6 for swelling capacity. Both of these values fit in the criteria defined. The huge improvement observed was for Q^2 that achieved 0,3 for pore size response and 0,5 for swelling capacity response, turning the difference between R^2 and Q^2 lower than 0,3. The p-value also fitted in the criteria. For pore size response, it was 3% and for swelling capacity response it was around 1%. Regarding inverse transformation, R^2 increased to 0,5 for both responses. Q^2 also increased to 0,2 for pore size response and to 0,3 for swelling capacity response. Thus, the difference between R^2 and Q^2 is lower than 0,3 for both responses. Also, p-value fitted the criteria, once it is 3% and 4,8% for pore size and swelling capacity responses, respectively.

Thus, it is possible to conclude that these transformations were useful in the approximation of the relationship between independent and dependent variables to a linear relation. This lead to results that fit perfectly in the criteria, and due to that, it is possible to proceed to Design Space Plot Analysis, which correspond to the last part of Risk Assessment step.

3.1.3 Design Space Plot Analysis

Design Space plot is an example of a graph that shows the probability of failure to achieve the target defined. For example, for the case of this study, the targets for pore size were set as 150 and 8,5 µm for oral and vaginal devices, respectively, and in the case of swelling capacity as 30 % for both structures.

a)

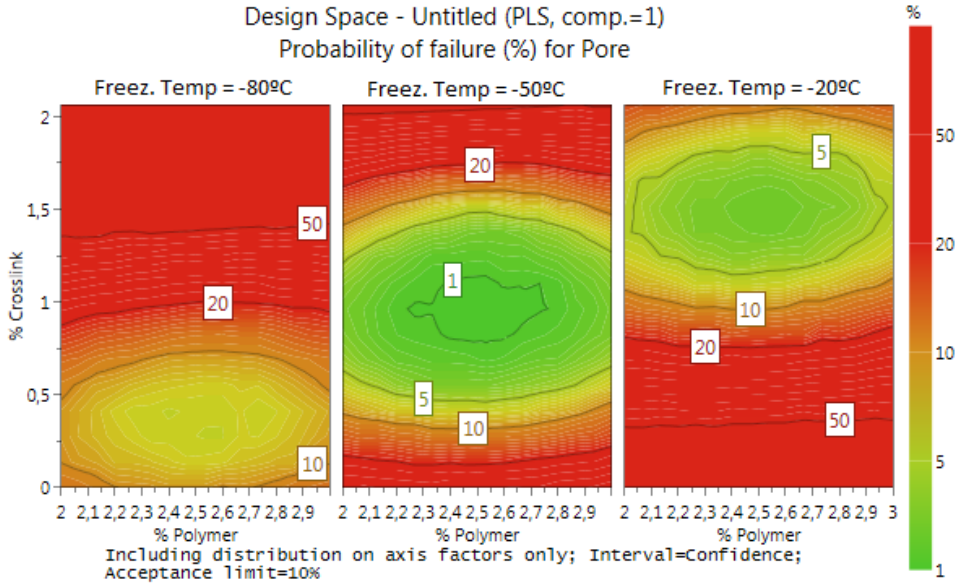

b)

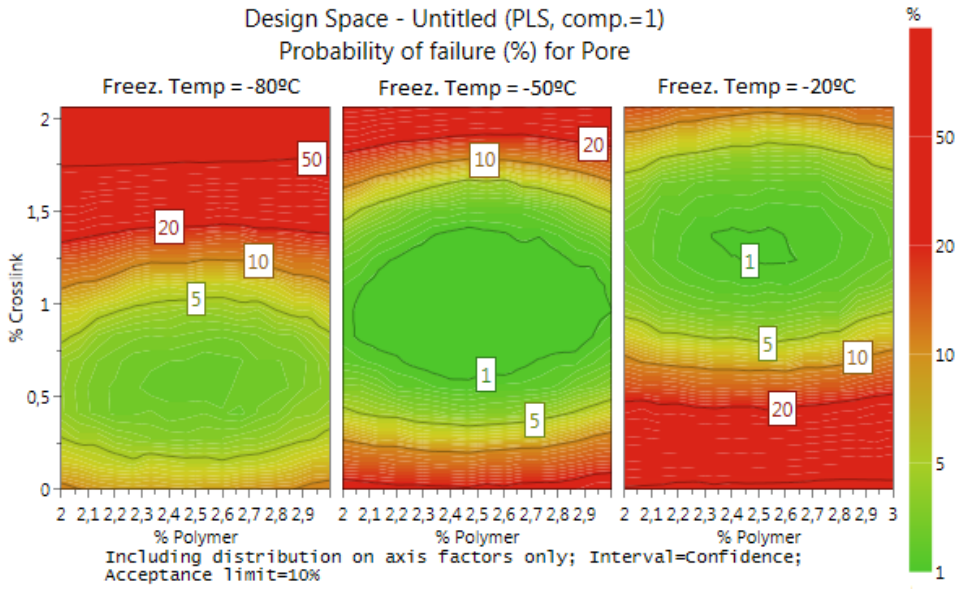

Figure 3.3 Design Space for pore size response of oral device: a) inverse transformation, b) logarithmic transformation. The green zone refers to a probability of failure lower than 5 %, the yellow zone lower than 10% and the red zone higher than 10%. The horizontal axis represents the polymer concentration and the vertical axis the crosslinker concentration.

Figure 3.3 represents the design space plot regarding pore size response, which the target was set as 150 µm, that is according to the objective of pore size for oral device. The green zone represents, in all cases, a probability of failure lower than 5%, the yellow zones a probability of failure lower than 10 % and the red one a probability of failure between 20 and 100%. Thus, based on this, it is recommended operate in green and yellow zones.

Both plots showed a green zone approximately according to the same conditions. If the freezing temperature chosen is -20ºC, in both plots, 3.3 a) and b), it is possible to observe that the suitable concentration of polymer and of the crosslinker are 2-3% and 1-1,75%, respectively. In the case of the freezing temperature chosen is -50ºC, the suitable concentration of polymer and of the crosslinker is 2-3% and 0,5-1,5%, respectively. At last, for -80ºC the suitable concentrations are 2-3% for polymer and 0,25-1% for crosslinker.

a)

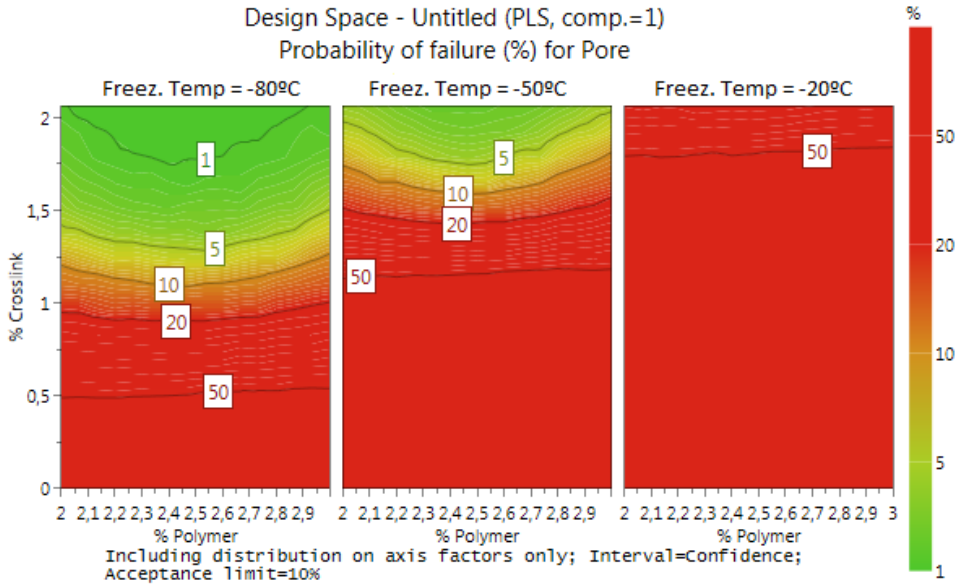

b)

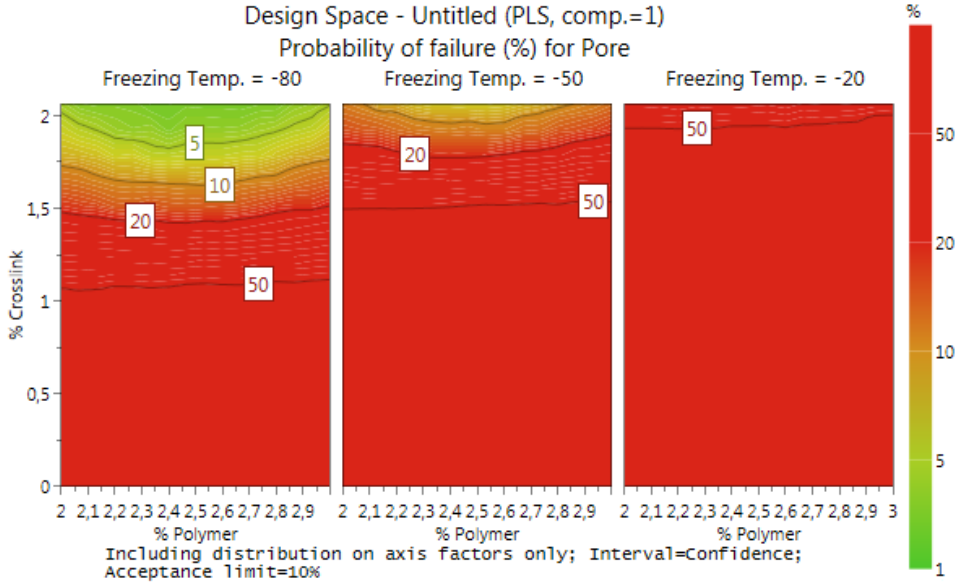

Figure 3.4 Design Space for pore size response of vaginal device: a) inverse transformation, b) logarithmic transformation. The green zone refers to a probability of failure lower than 5 %, the yellow zone lower than 10% and the red zone higher than 10%. The horizontal axis represents the polymer concentration and the vertical axis the crosslinker concentration.

Figure 3.4 also represents the design space plot for pore size response, but in this case the target was set as 8,5 µm because it is in the middle of the gap required to the vaginal device (2-15 µm). It is possible to observe that -20ºC is not an adequate temperature to obtain pores with this size. This information is in agreement with previous studies, once, for this temperature the range of pore size is 50-100 µm [75]. In this case, the discrepancy between the two transformations is more pronounced. However, it is possible to define conditions that fit the green zones of both plots. Considering both plots, -80ºC is the best option regarding freezing temperature combined with 2-3% polymer concentration and 1,7-2 % of crosslinker are the suitable conditions to achieve the target.

a)

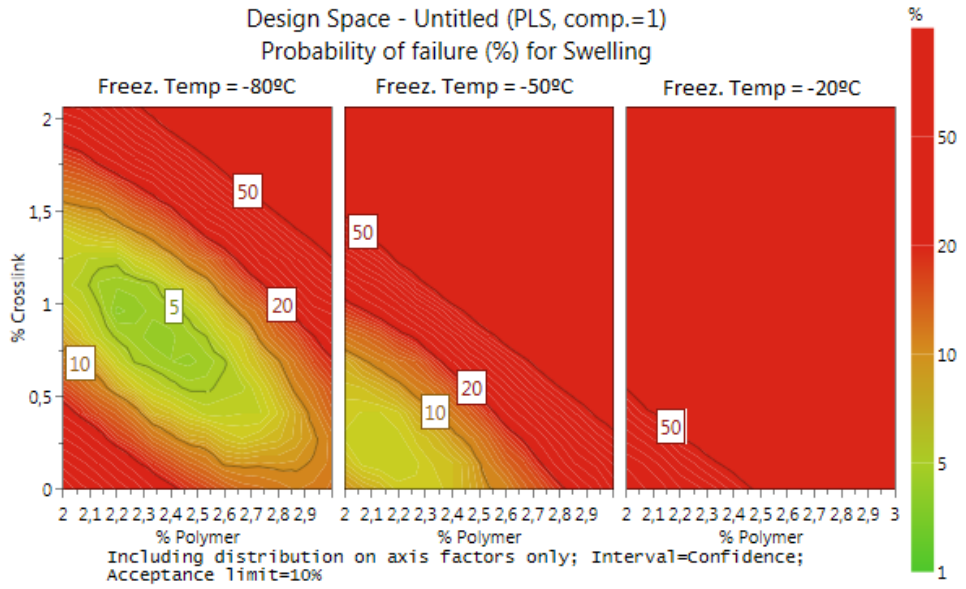

b)

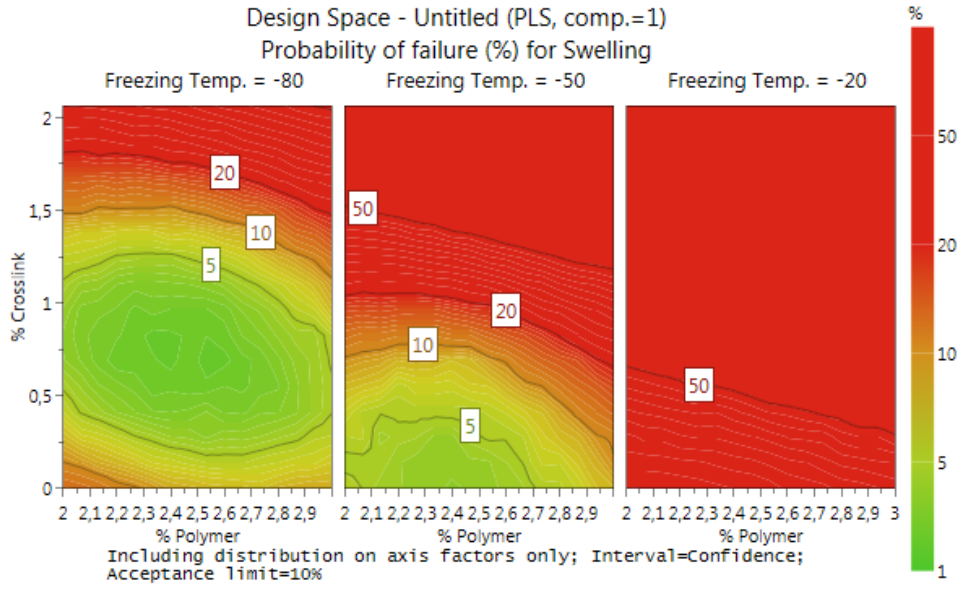

Figure 3.5 Design space for swelling capacity response of both devices (oral and vaginal): a) inverse transformation, b) logarithmic transformation. The green zone refers to a probability of failure lower than 5 %, the yellow zone lower than 10% and the red zone higher than 10%. The horizontal axis represents the polymer concentration and the vertical axis the crosslinker concentration.

Figure 3.5 represents the design space plot for swelling response. Herein, the plots are adequate for both structures once the target was set as 30% of swelling capacity.

Once again, the plots are very similar for both transformations. Thus, for all freezing temperature, the polymer concentration in the green zone is between 2 and 3% and the main difference is the crosslinker concentration that at -20ºC is in the range 0,75-1,75%, at -50ºC is in the range 0,3-1,6 and at -80ºC varies between 0,25-1%.

It is important to notice that independently of the response and the target defined, the plots studied before suggest that the suitable concentration of polymer always varied between 2 and 3%.

a)

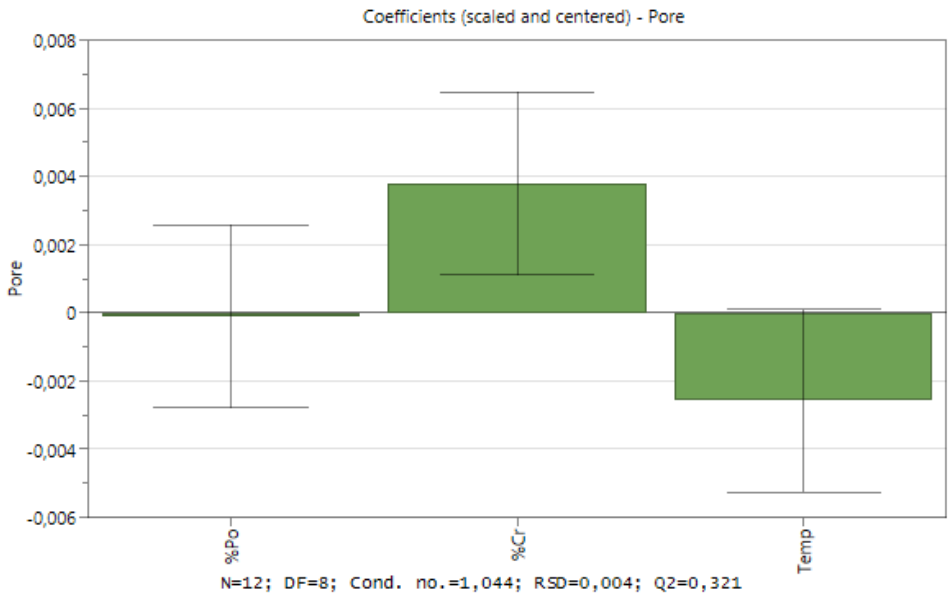

b)

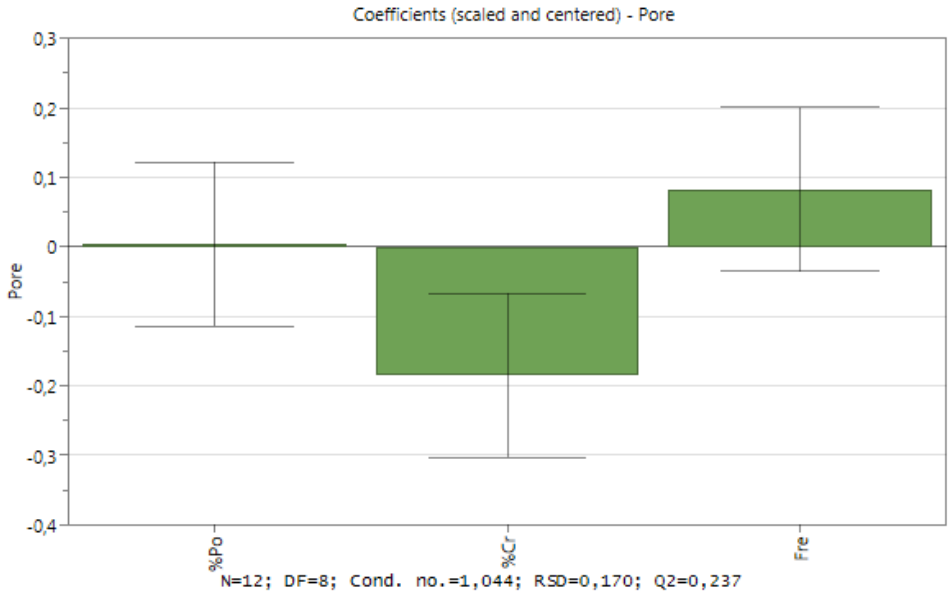

c)

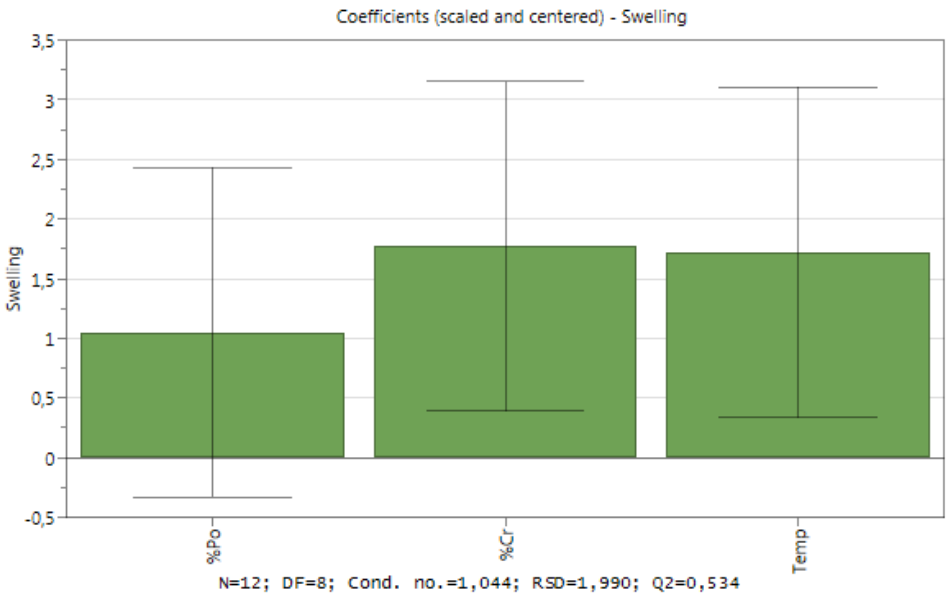

d)

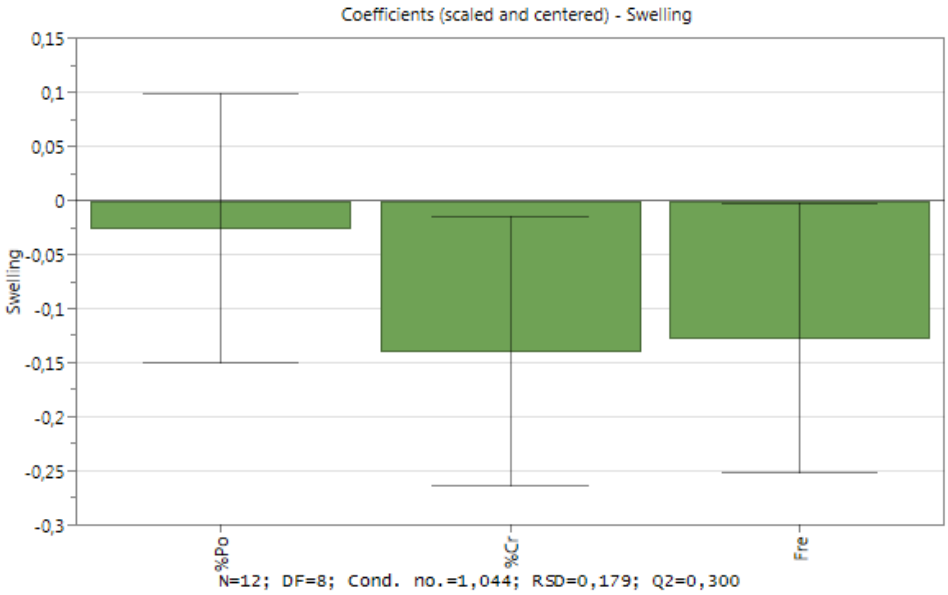

Figure 3.6 Coefficients plot (scaled and centered) for: (a) pore size responser and inverse transformation, b) pore size response and logarithmic transformation, c) for swelling response and inverse transformation, d) for swelling response and logarithmic transformation. %Po refers to polymer concentration, %Cr refers to crosslinker concentration and Fre referes to freezing temperature.

In **Figure 3.6**, it is represented a coefficients plot (scaled and centered) for both responses (pore size and swelling capacity) and for both transformations (inverse and logarithmic). In the horizontal axis, there are represented the three independent variables (polymer concentration, crosslinker concentration and freezing temperature) and in the vertical axis it is represented the coefficients of the model. The aim of this graphical representation is to understand which independent variables are significant and have impact in the model explanation. By analyzing the

plots, it is possible to conclude that the polymer concentration is the only variable that, in all cases (different responses and transformations) does not have impact or is significant in the model. This is possible to observe once the green bar is between the limits of the black line and not out of its limits. This is due to the fact that the data do not take into account the polymer nature, once that is a qualitative variable, and the model only works with quantitative variables. This fact explains why the polymer concentration range is always the same, independently of the transformation or the target set.

In the next chapter, experimental validation of the Qbd method will be described and also the results of the characterization methods.

3.2 Experimental Validation

3.2.1 Casting solution Preparation

The scaffolds in study were produced by freeze-drying method. The freeze-drying conditions were chosen according to the results of the design space plots from QbD studies, and in an attempt to obtain two different pore sizes depending on the application. For the structures to be used in oral drug delivery the pore size should be around 150 µm and for vaginal drug delivery should be within 2-15 µm. Therefore, different freezing conditions (-20 ºC and -80 ºC) and concentrations of casting solutions (2,35-3% of polymer) were studied.

In detail, the polymers used were chitosan and xanthan gum in different concentrations and with different freezing conditions. These two polymers were considered once they have been widely investigated to be used in biomedical application. Chitosan is pH sensitive with microbial properties and there are a lot of studies on vaginal and oral drug delivery systems using it [85], [188], [189]. Xanthan gum is a temperature responsive polymer that has been studied as food addictive and in several biomedical applications [120]. Moreover, both polymers are biocompatible and biodegradable [6], [190], [191], [192]. In the previous studies carried on GEO Company, both of these polymers presented the suitable results for the objective set for this thesis [75], [86].

Initially, the casting solutions were prepared only with chitosan or xanthan gum with concentrations of 2,35 and 2,5% of each polymer in the casting solution. For these concentrations, also the percentage of crosslinker was different varying between 1 and 1,7%, according to the QbD data. However, during these studies, there was a need to consider other concentrations such as 3% of polymer and 2% of crosslinker and also the blend between chitosan and xanthan gum. It is important to notice that all of these conditions respect the design space plots obtained in QbD studies. Finally, it has been considered two freezing temperatures: -20º C and -80º C.

Table 3.2 Composition of casting solutions and freezing conditions.

Application	Designation	Polymer	Polymer concentration	Crosslinker concentration	Freezing Temperature
Candy	CHT_1	Chitosan	2,5	1,3	-20
	XG_1	Xanthan Gum	2,5	1,3	-20
	CHT_2	Chitosan	2,35	1	-20
	XG_2	Xanthan Gum	2,35	1	-20
	CHT_3	Chitosan	2,5	1,3	-80
	XG_3	Xanthan Gum	2,5	1,3	-80
Tampon	CHT_4	Chitosan	2,5	1,7	-80
	XG_4	Xanthan Gum	2,5	1,7	-80
Candy and Tampon	CHT_5	Chitosan	2,35	1	-80
	XG_5	Xanthan Gum	2,35	1	-80
	CHT_7	Chitosan	3	2	-80
Candy	CHT_6	Chitosan	3	2	-20
Tampon	CHT_8	Chitosan	2	2,5	-80
	CHT_9	Chitosan	1,5	3	-80
	CHTXG_1	Chitosan	2	2	-80
		Xanthan Gum	1		
	CHTXG_2	Chitosan	1,5	2	-80
		Xanthan Gum	1,5		

It is important to refer that the combination between variables was decided considering the application of each structure. All of these conditions may influence the morphology of the resulting structures. Freeze-drying method is known for generate a high degree of interconnected pores which is highly important once it facilitates the drug diffusivity. The freezing temperature is one of the most important factors to consider when using this kind of method, once lower freezing temperatures (-80ºC) lead to smaller pores (20-100 µm) [193].

The conditions of production process of the first tenth structures (CHT_1, XG_1, CHT_2, XG_2, CHT_3, XG_3, CHT_4, XG_4, CHT_5, XG_5), were selected from the medium point in the green zone of Design Space plots. However, the results obtained regarding swelling capacity and mechanical analysis (results presented with more detail in further sections of this thesis) were not the expected, which means they did not fit in the objective of this thesis. Thus, the design space

plot was, once again, analyzed and the boundaries of the green zone were also considered. With this data revision, new analysis also new conditions were considered and the new scaffolds (CHT_6, CHT_7, CHT_8, CHT_9, CHTXG_1, CHTXG_2) were produced.

In the next subchapters, the characteristics of all structures will be carefully analyzed through several characterization methods.

3.2.2 Fourier Transform Infrared Spectroscopy – Attenuated Total Reflectance Analysis (FTIR-ATR)

FTIR-ATR was the first analysis taken into account, once it is useful to identify the most predominant chemical interaction in each structure. Due to that, this method becomes essential to evaluate the crosslinking effect, the interaction between polymers and also the interaction of the drug with the polymer.

a)

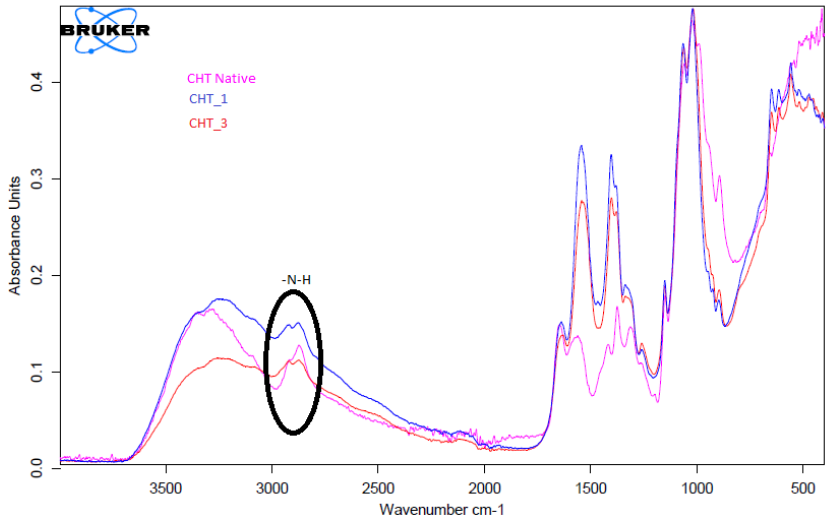

b)

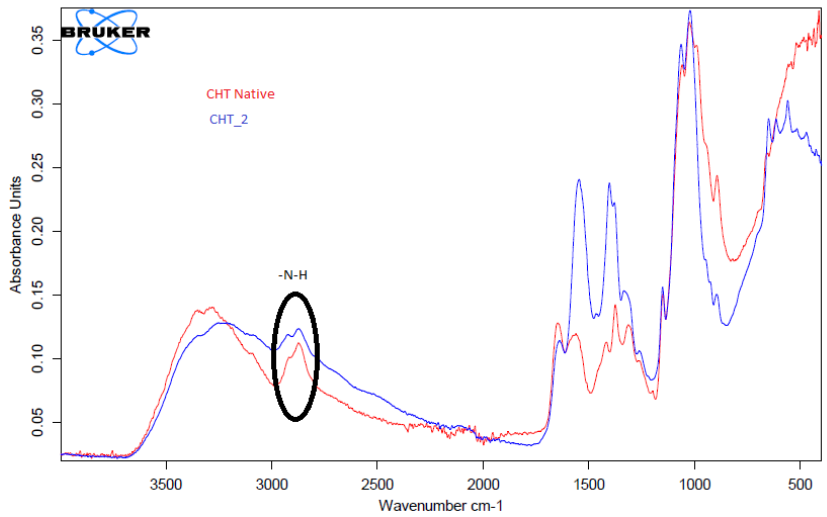

Figure 3.7 FTIR-ATR of: a) CHT Native vs CHT_1 vs CHT_3, b) CHT Native vs CHT_2. The horizontal axis refers to wavenumber (cm^{-1}) and the vertical refers to absorbance units.

a)

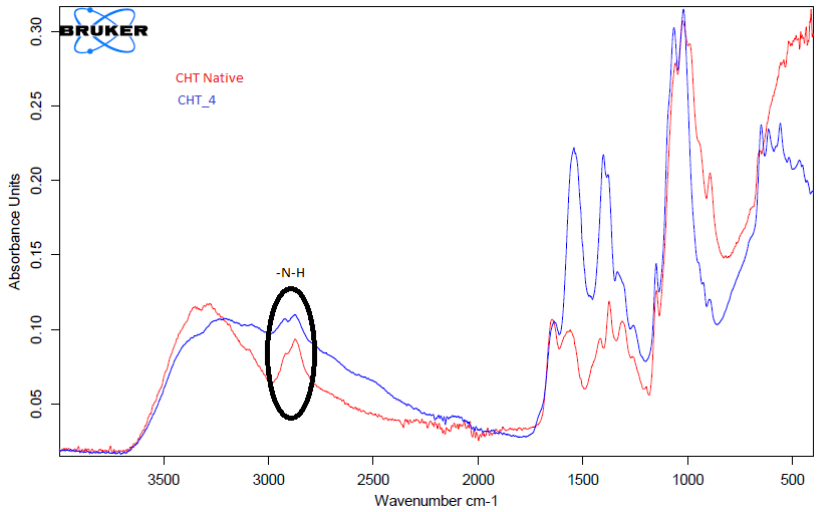

b)

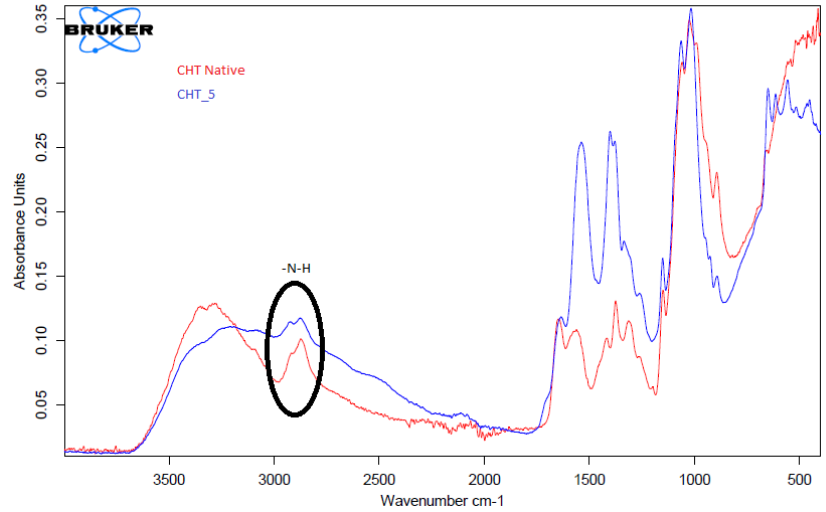

c)

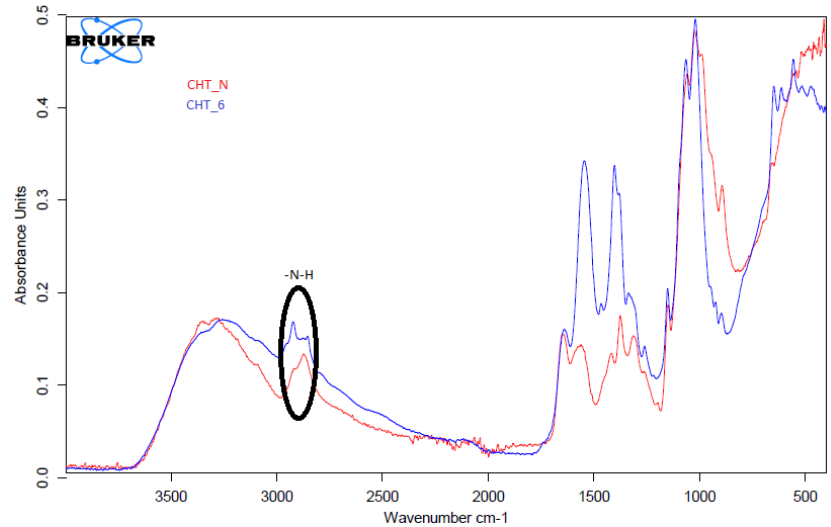

Figure 3.8 FTIR-ATR of: a) CHT Native vs CHT_4, b) CHT Native vs CHT_5, c) CHT Native vs CHT_6. The horizontal axis refers to wavenumber (cm^{-1}) and the vertical refers to absorbance units.

a)

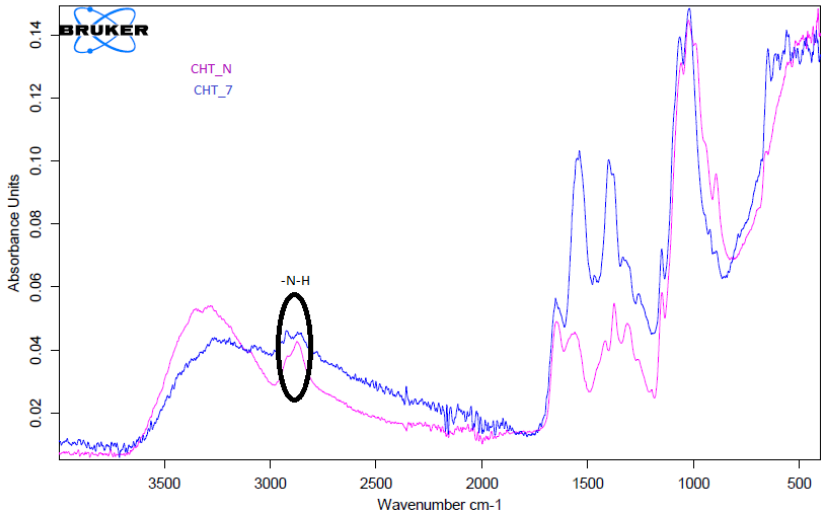

b)

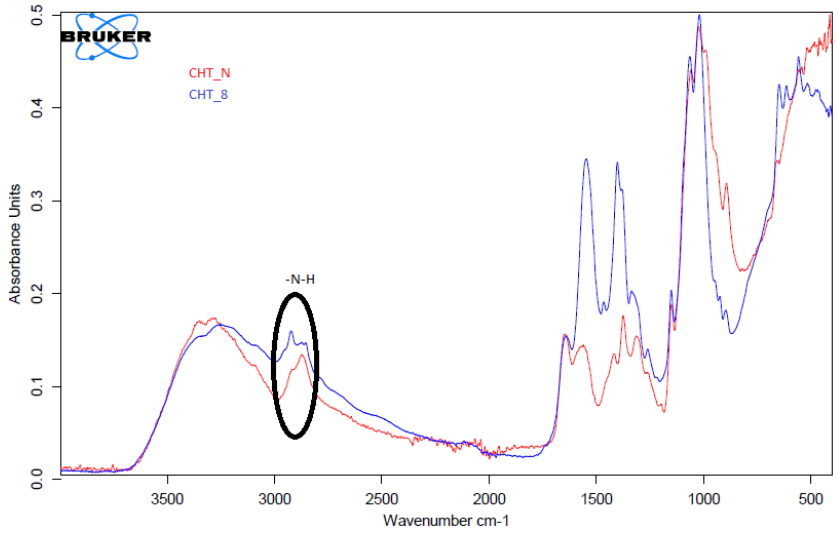

c)

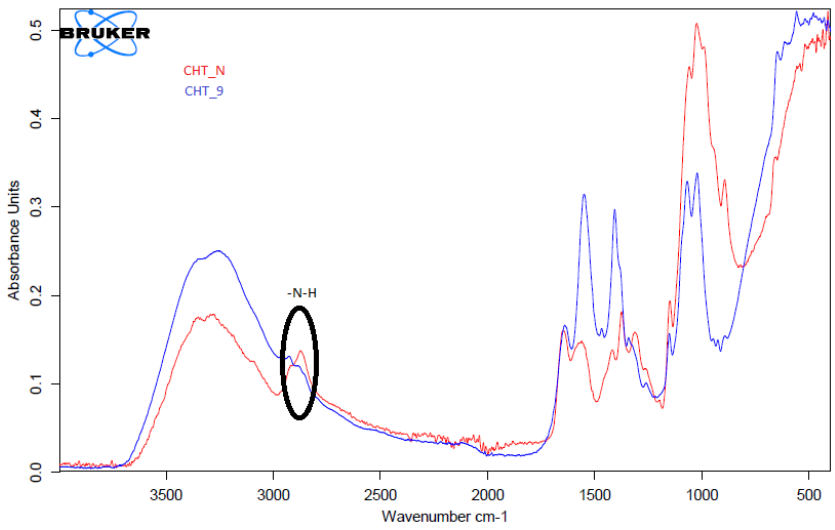

Figure 3.9 FTIR-ATR of: a) CHT Native vs CHT_7, b) CHT Native vs CHT_8 and c) CHT Native vs CHT_9. The horizontal axis refers to wavenumber (cm^{-1}) and the vertical refers to absorbance units.

In **Figure 3.7**, **Figure 3.8** and **Figure 3.9**, it is possible to see the FTIR-ATR spectrums comparing the spectrum of native chitosan with the crosslinked scaffolds. In all cases, it is notorious the deviation in the amino group (-N-H) of chitosan. It is also possible to notice some alterations in the vibrations of -H, -CH in the ring (1407.15 cm^{-1}) and -C-O-C- in glycoside linkage (1068.19 cm^{-1}).

All of these observations suggest the loss of the charge in the amino group. Thus, it is possible to conclude that the crosslinking effect between chitosan and MBA is established by convalent bonding to the -NH group of chitosan molecules [194], [195].

a)

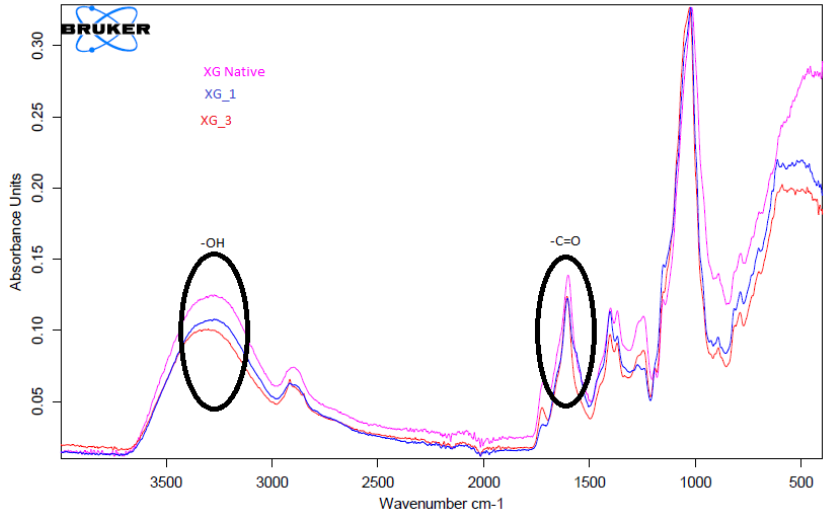

b)

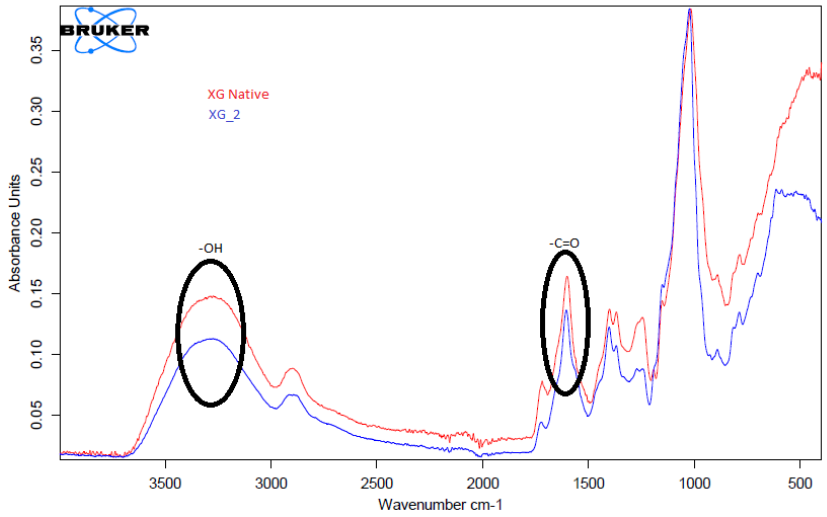

Figure 3.10 FTIR-ATR of: a) XG Native vs XG_1 vs XG_3, b) XG Native vs XG_2. The horizontal axis refers to wavenumber (cm^{-1}) and the vertical refers to absorbance units.

a)

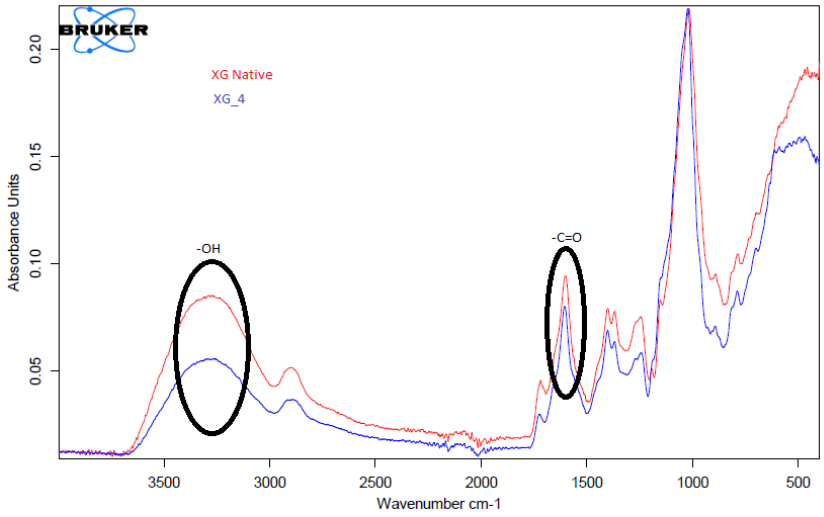

b)

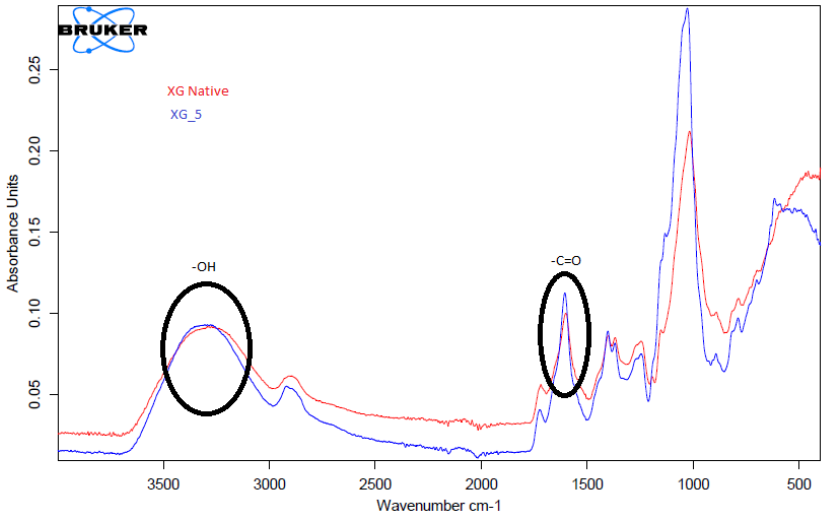

Figure 3.11 FTIR-ATR of: a) XG Native vs XG_4 and b) XG Native vs XG_5. The horizontal axis refers to wavenumber (cm^{-1}) and the vertical refers to absorbance units.

In **Figure 3.10** and **Figure 3.11**, it is possible to observe the FTIR-ATR spectrums comparing native xanthan gum and the other xanthan gum based scaffolds crosslinked with MBA.

For xanthan gum structures, the deviations are regarding -OH and -C=O bands. These deviations are more intense in the case of XG_1, XG_2, XG_3 and XG_4. This might be due to the fact that the concentration of MBA in XG_5 is only 1%.

The deviation on -C=O of pyruvate pick (1607.80 cm^{-1}) is affected by the charge change in the carboxyl group. This, allied to the deviation in -OH band suggest that the crosslinking effect between xanthan gum and MBA was successful and occurs in the carboxyl group [196].

a)

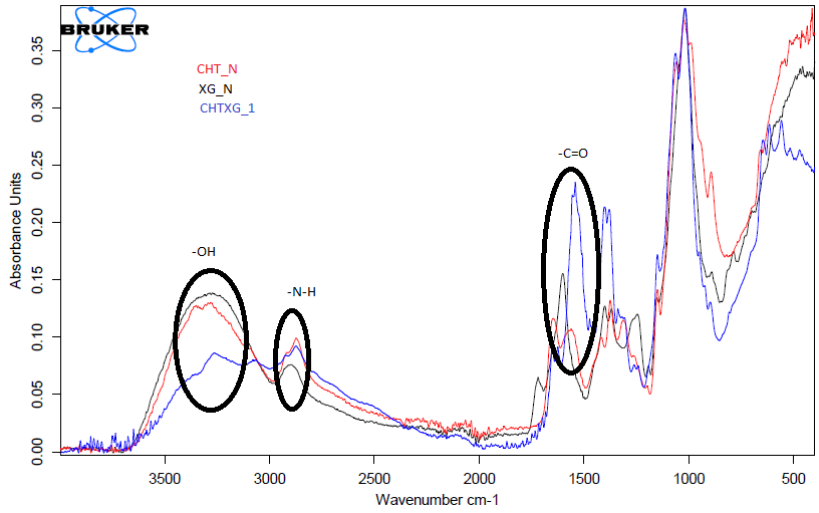

b)

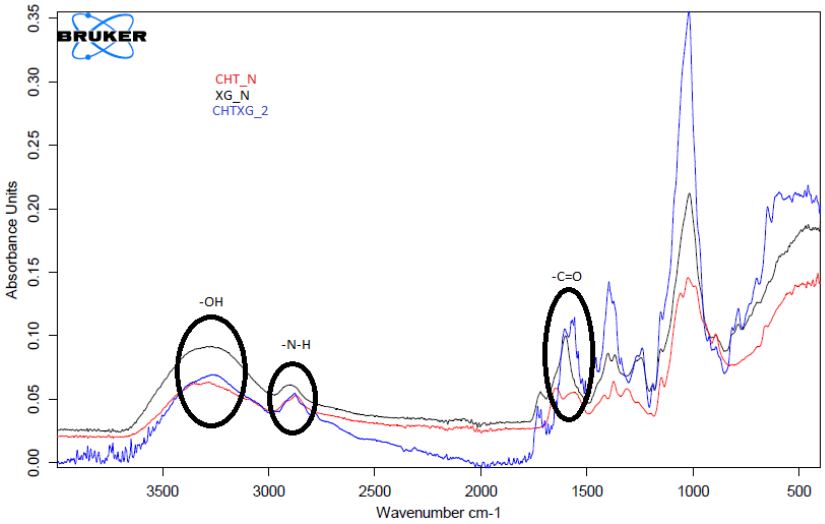

Figure 3.12 FTIR-ATR of: a) CHT Native vs XG Native vs CHTXG_1 and b) CHT Native vs XG Native vs CHTXG_2. The horizontal axis refers to wavenumber (cm^{-1}) and the vertical refers to absorbance units.

In **Figure 3.12**, it is possible to analyze the FTIR-ATR spectrums of native chitosan and native xanthan gum with the scaffolds produced by the mixture of these two polymers.

It is possible to see that due to the interaction between chitosan and xanthan gum, in the spectrums of CHTXG_1 and CHTXG_2, -N-H band and -C-N stretch present deviations from the native chitosan spectrum (1632.04 cm^{-1} and 1019.29 cm^{-1}, respectively) and regarding native xanthan gum spectrum, the most affected peak was -OH (3201.40 cm^{-1}). Both spectrums show a clearly interaction between the amino group from chitosan and the carboxylic group from xanthan gum. This kind of deviation might be explained by the effect of the crosslinker in the polymeric mixture, once it was seen before that chitosan and the crosslinker interaction occurs in -NH group and the interaction between crosslinker and xanthan gum occurs in the carboxylic group.

Once these results suggest that the crosslinking effect occurred in all structures, the next step was to measure the swelling capacity of each one.

3.2.3 Swelling Tests

After FTIR-ATR analysis, the structures were submitted to swelling tests, in order to evaluate the water uptake capacity, at acidic and neutral medium. The pH solutions for these tests were set as 3.8 and 7 for the structures for vaginal application and 5 and 7 for the structures for oral application. This choice of pH is important once vaginal medium pH is acidic and also, when there is an infection of oral mucosa the pH decreases, turning the mouth an acidic medium.

a)

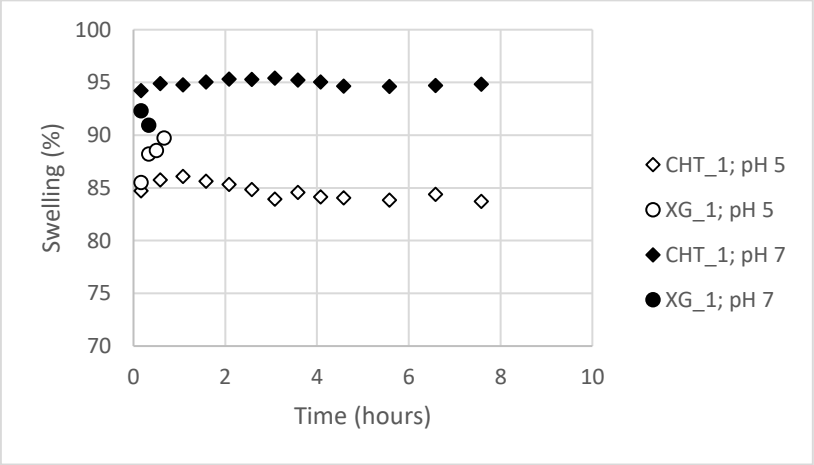

b)

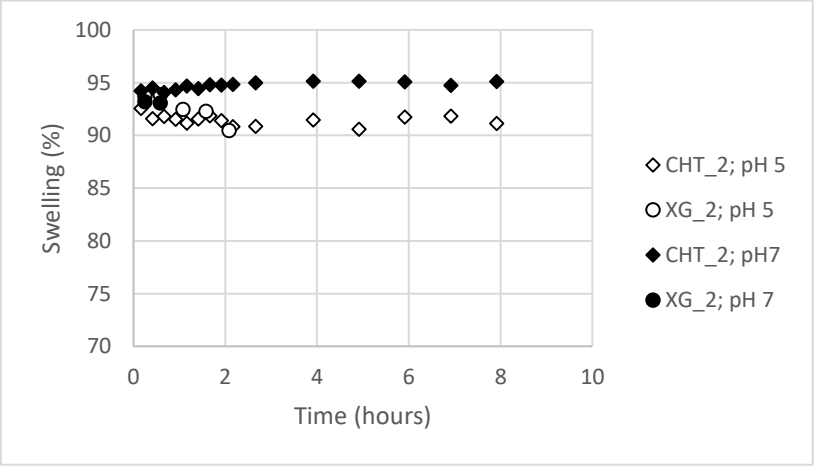

Figure 3.13 Swelling degree of: a) CHT_1 and XG_1 at pH 5 and 7; b) CHT_2 and XG_2 at pH 5 and 7.

a)

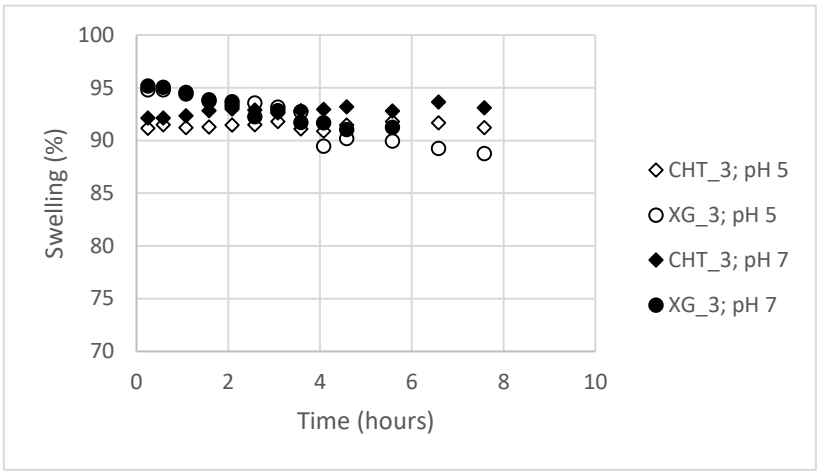

b)

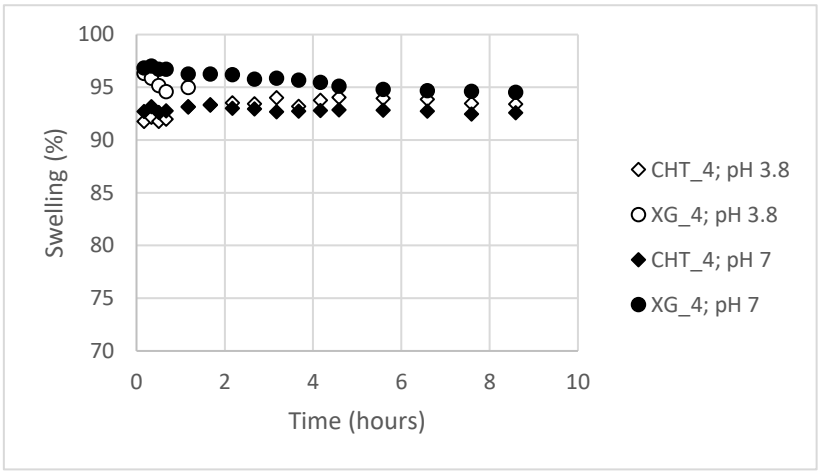

c)

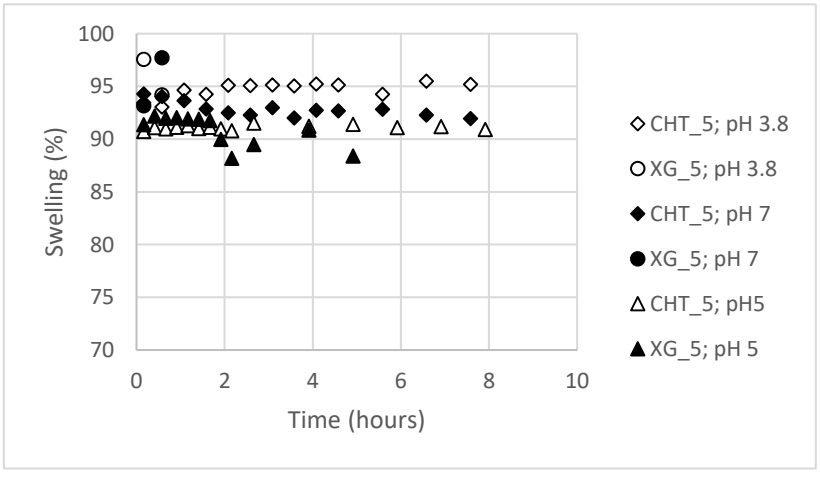

Figure 3.14 Swelling degree of: a) CHT_3 and XG_3 at pH 5 and 7; b) CHT_4 and XG_4 at pH 5 and 7; c) CHT_5 and XG_5 at pH 3.8, 5 and 7;

In **Figure 3.13** and **Figure 3.14**, it is possible to observe the swelling degree for the first ten runs studied. It is useful to notice that each graphic represents the swelling degree for two types of medium: acidic and neutral. Another point to consider in these plots is the fact that the processing conditions are the same, namely, polymer concentration, crosslinker concentration and freezing

temperature (CHT_1 and XG_1: 2,5% polymer, 1,3% crosslinker, -20ºC; CHT_2 and XG_2: 2,35% polymer, 1% crosslinker, -20ºC; CHT_3 and XG_3: 2,5% polymer, 1,3% crosslinker, -80ºC; CHT_4 and XG_4: 2,5% polymer, 1,7% crosslinker, -80 ºC; CHT_5 and XG_5: 2,35% polymer, 1% crosslinker, -80ºC).

In **Figure 3.13** a) it is possible to analyze the swelling capacity of CHT_1 and XG_1, and in **Figure 3.13** b), the swelling capacity of CHT_2 and XG_2. In both cases, the xanthan gum based structures disintegrated during the first hours of the tests while chitosan based structures remained stable. In **Figure 3.14** a), it is possible to analyze the swelling capacity of CHT_3 and XG_3, and both structures withstand for the first 8 hours, which represents a huge improvement from the first two scaffolds. In **Figure 3.14** b) it is represented the swelling capacity of CHT_4 and XG_4, and in this case, the xanthan gum structure only withstands for more than 3 hours at neutral pH. At last, in **Figure 3.14** c) it is possible to analyze the swelling capacity of CHT_5 and XG_5, and in this case, the xanthan gum based structure only withstands for more than 2 hours at pH 5.

Thus, it is worth noting that the structures composed by xanthan gum tend to disintegrate in the first hour, even when they are crosslinked, except for XG_5 that withstands for 5 hours at pH 5, XG_3 that also withstands for approximately 5 hours in both mediums and XG_4 that withstands for 24 hours in neutral medium. Regarding chitosan based scaffolds, all of them withstand for 24 hours. A possible explanation for these high values of swelling degree, as well as, for xanthan gum structures disintegrating faster, might be the low concentration of crosslinker in the casting solutions. Lower concentration of crosslinker (1% w/w) causes the mesh formed by the pores to be wider. Consequently, this allows the swelling capacity to be greater, reaching values above 90%. Another explanation might be the solubility of xanthan gum. It is known that xanthan gum, as a gum, has a very high solubility in all kind of medium, acidic, neutral or basic [119]. Thus, xanthan gum based scaffolds were expected to disintegrate more easily than chitosan based scaffolds.

a)

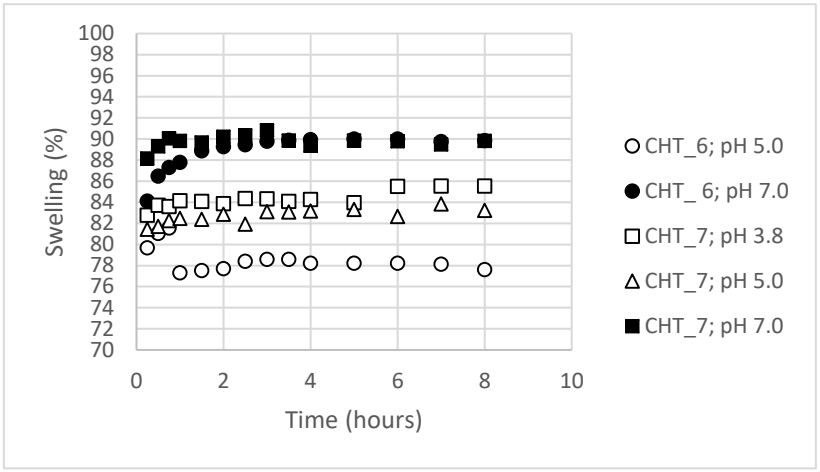

b)

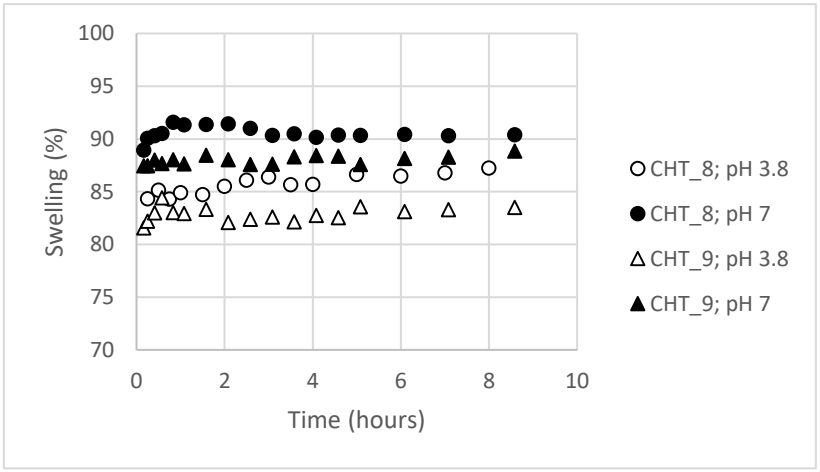

c)

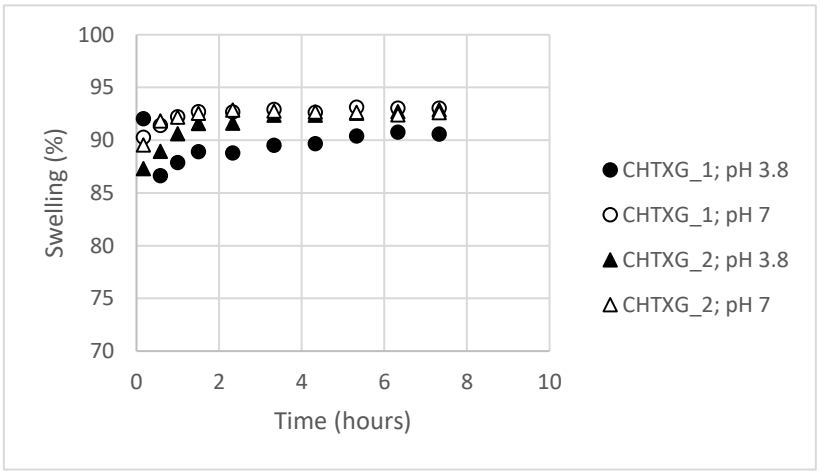

Figure 3.15 Swelling degree of: a) CHT_6 CHT_6 and CHT_7 at pH 5, CHT_7 at pH 3.8 and CHT_6 and CHT_7 at pH 7; b) CHT_8 and CHT_9 at pH 3.8 and CHT_8 and CHT_9 at pH 7; c) CHTXG_1 and CHTXG_2 at pH 3.8 and CHTXG_1 and CHTXG_2 at pH 7.

In **Figure 3.15**, it is possible to analyze the swelling capacity of the second set of scaffolds produced. The processing conditions of this set was chosen according to QbD Design Space, but

in this case, some of the conditions were chosen from the yellow zone of the plot (the yellow zone indicates a probability of failure between 5% and 10%).

Figure 3.15 a), shows the swelling capacities of CHT_6 and CHT_7 in acidic and neutral medium. None of these structures disintegrated during the tests and the maximum swelling degree achieved was about 90 %. In **Figure 3.15** b), it is represented the swelling capacities of CHT_8 and CHT_9 in acidic and neutral medium. In this case, also none of the structures disintegrated during the tests and the maximum swelling degree achieved was by CHT_8 at neutral pH with approximately 90%. In figure, **Figure 3.15** c), there are represented the swelling capacities of CHTXG_1 and CHTXG_2 in acidic and neutral pH. Herein, the structures remained entire until the end of the tests and the higher swelling degree achieved (for CHTXG_1 and CHTXG_2) was around 93%.

In general, the swelling capacity of these structures are higher than the expected, once they achieved more than 90%, and according to QbD studies it should be around 30%, even for the last six structures that suffer a slight decrease in the values of swelling degree. However, once there is no specific value for this capacity for the structures to be used in oral route of administration, these values can be within the objectives. Although the QbD studies set this conditions as suitable for achieving 30% of swelling degree, the obtained results are in accordance with the literature, once higher polymer and crosslinker concentrations lead to a lower swelling capacity [197].

During this thesis, there were a set of structures that were selected to slightly different swelling tests. These structures were CHT_2, CHT_4, CHT_5, XG_5, CHT_6, CHT_7, CHT_8, CHT_9, CHTXG_1 and CHTXG_2. These structures were selected once they presented mechanical properties and swelling degrees within the objectives. The difference between this test and the previous one is the volume of the buffer solution that decrease from 100 mL to 2 or 5 mL (depending on the application – 2 mL for tampon and 5 mL for candy).

a)

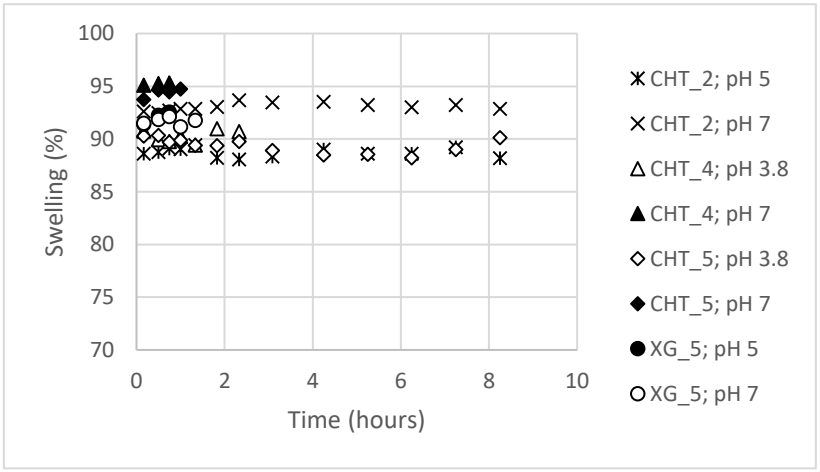

b)

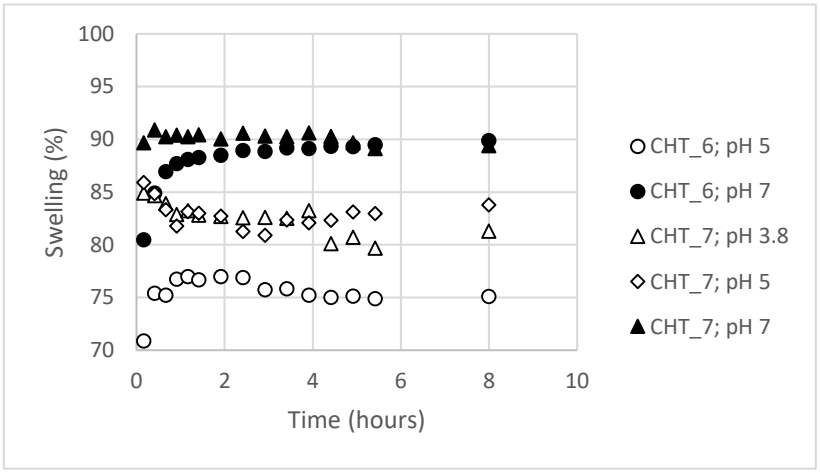

c)

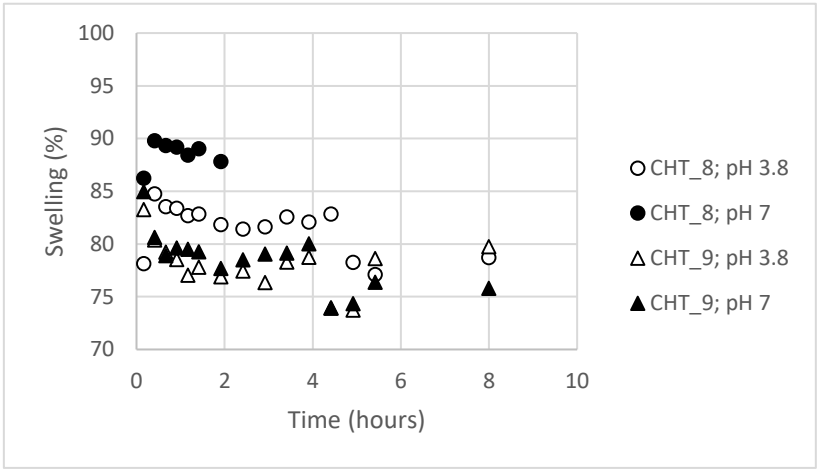

Figure 3.16 Swelling degree of: a) CHT_2 at pH 5 and 7, CHT_4 at pH3.8 and 7, CHT_5 at pH 3.8 and 7 and XG_5 at pH 5 and 7; b) CHT_6 at pH 5 and 7 and CHT_7 at pH 3.8, 5 and 7; c) CHT_8 at pH 3.8 and 7 and CHT_9 at pH 3.8 and 7

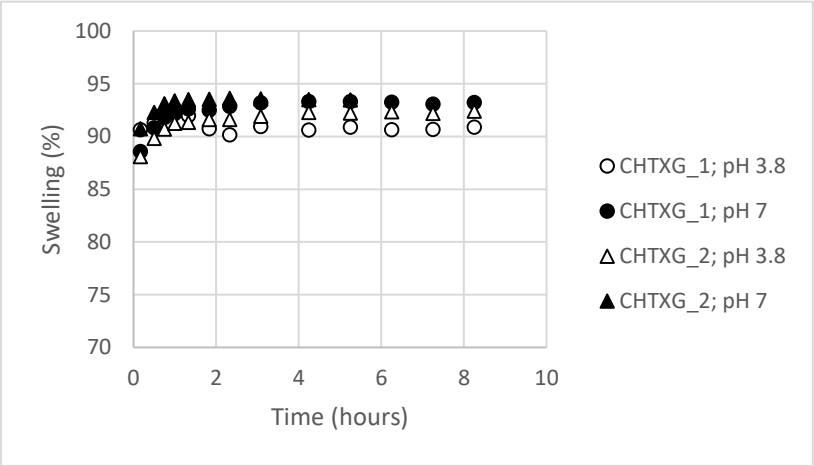

Figure 3.17 Swelling degree of CHTXG_1 at pH 3.8 and 7 and CHTXG_2 at pH 3.8 and 7.

In **Figure 3.16** and **Figure 3.17**, there are represented the swelling capacities of the chosen structures, in a confined volume. For the structures tested at pH 3.8, the buffer solution volume was 2 mL and for the structures tested at pH 5, the volume was 5 mL. This volumes were chosen according to the amout of salive and vaginal fluid produced in 24 hours [198], [199]. The lack of points in this plots do not represent the desintegration of the structure but it means that all the volume of buffer solution was absorved by the scaffold.

In **Figure 3.16** a), it is possible to observe that CHT_4, CHT_5 at neutral pH and XG_5 at both pH absorved all the volume of swelling medium in the first two hours. Regarding the structures represented in **Figure 3.16** b), CHT_6 and CHT_7, none of them absorved all the medium before eight hours. In **Figure 3.16** c), where are represented the swelling capacities of CHT_8 and CHT_9 it is possible to observe that only CHT_8 at neutral pH absorved all the volume of swelling medium. At last, in **Figure 3.17**, the structures represented, CHTXG_1 and CHTXG_2, did not absorved all of the buffer solution. The total medium absorption by some of the structures might be related to the concentration of polymer and crosslinker in casting solutions. For example, CHT_4 (2,5% polymer and 1,7% crosslinker), CHT_5 (2,35% polymer and 1% crosslinker) and XG_5 (2,35% polymer and 1% crosslinker), are structures that absorved all medium and have lower concentration of polymer and crosslinker compared with CHT_6 (3% polymer and 2% crosslinker) or CHT_9 (3% polymer and 1,5% crosslinker), which are structures that did not absorved all medium. Once again, density might be related with the total medium absorption. For example, CHT_8 have density of 0,127 g/cm^3, which is one of the highest densities obtained, and this structure did not absorved all the medium, while CHT_4 has 0,061 g/cm^3 and it absorved all medium.

In these tests, the swelling capacities were expected to be lower than in the tests taken in 100 mL. However, this was not verified for all structures. The structure that presented the higher

difference in swelling degree was CHT_9 that presented 88% in the first tests (using 100 mL) and this value was reduced to 77% when using confined volume.

It is also important to notice that some points in the plots (for example in **Figure 3.16** c)), regarding CHT_9 at neutral pH and after 4 hours of the beginning of the test) have lower value than the one before, which might suggest weight loss of the structures. This indicates that small portions of the scaffold desintegrated from the initial structures, which is not supposed to happen, once the structures should remain entire during the full test. Besides that, the result suggest a swelling capacity above 77% which is expected to be high enough to release the drug. However, the drug release profile will be further discussed.

In order to make a wise and informed choice of which structures should proceed for further investigation, it is important to take into account other studies, like porosity and density measurements and also mechanical analysis.

3.2.4 Porosity and Density Measurements

The aim of this section was to estimate the porosity and the density of the scaffolds. Porosity is a characteristic that is directly related with the presence of open pores and which might influence the permeability and surface area of the porous structures that consequently will have impact in drug release profile of the structures. Therefore, this kind of characteristic is essential in providing controlled drug delivery, once it is through the pores that the impregnated drugs in the scaffolds will pass and be released [200].

Table 3.3 Density and Porosity of the scaffolds.

Application	Structure	Density (g/cm^3)	Porosity (%)
Candy	CHT_1	0,032	50
	XG_1	0,058	50
	CHT_2	0,062	70
	XG_2	0,065	40
	CHT_3	0,059	80
	XG_3	0,034	40
Tampon	CHT_4	0,061	60
	XG_4	0,039	50
Candy and Tampon	CHT_5	0,066	65
	XG_5	0,056	50
	CHT_7	0,035	25
Tampon	CHT_6	0,102	42
	CHT_8	0,174	50
	CHT_9	0,127	58
	CHTXG_1	0,056	42
	CHTXG_2	0,072	50

In **Table 3.3**, it is possible to observed the values of density and porosity for each scaffold.

The porosity values are always higher in the case of chitosan based scaffolds, comparing with the xanthan gum based structures, except for CHT_6 and CHT_7. Thus, the higher porosity belongs to CHT_3 with 80% and the lower belongs to CHT_7 with 25%. In the case of density, the structures with higher density are CHT_6, CHT_8 and CHT_9 and the lower is CHT_1.

Usually, the structures with higher swelling capacity present higher porosity. Despite the proximity of swelling capacity values for these structures, CHT_3, the structure with higher porosity, do not present the greater swelling capacity. Thus, this information is not in agreement with the literature [201]. This might be due do the poor interconnectivity between pores. The structures that present high porosity but the pores are not connected to each other tend to have a lower swelling capacity compared with the structures with high interconnectivity [202]. Also, this might be related with the nature of the polymers. The polymers used in this thesis are natural polymers and due to that, it is not possible to control and change the physical characteristics of this polymers. In the other hand, density is related to mechanical strength, and usually structures with higher density present higher mechanical strength. So, it is expected that CHT_6, CHT_8 and CHT_9 present higher compressive moduli and CHT_1 the lowest.

To make it possible to compare the density with the mechanical strength, and to conclude if the results are in accordance with the tendencies, next subchapter will show the results for mechanical analysis.

3.2.5 Mechanical Analysis

The mechanical analysis was performed to determine the compressive modulus. For each compressive test, the stress-strain curve was plotted and the slope was calculated giving the compressive modulus for the specific scaffold.

Table 3.4 Compressive modulus of the scaffolds.

Structure	Compressive Modulus (kPa)
CHT_1	0,54
XG_1	0,41
CHT_2	2,64
XG_2	0,91
CHT_3	0,94
XG_3	1,73
CHT_4	0,37
XG_4	0,79
CHT_5	1,09
XG_5	1,42
CHT_6	5,14
CHT_7	6,80
CHT_8	3,31
CHT_9	0,76
CHTXG_1	4,11
CHTXG_2	3,14

The results do not show a tendency of which polymer origins structures with greater stiffness. The structures that present higher compression modulus are CHT_6 (5,14 kPa), CHT_7 (6,80 kPa) and CHTXG_1 (4,11 kPa). In contrast, the structures with lower compression modulus are CHT_4 and XG_1.

The values of compressive modulus of the first ten structures studied (the ones obtained from the conditions presented by the green zone of the QbD) are far from the objective set for any of the structures (5 kPa to candy and higher than 4.7 kPa for the tampon), and this difference might be explained by the low concentrations of crosslinker present in these structures, which varied from 1% to 1.7%, and by the low concentration of polymer in casting solutions (that varied from 2.35%

to 2.5%). Thus, the results are not in accordance with the literature [203]. Both chitosan and xanthan gum are natural polymers with high molecular weight, for chitosan it can vary between 10 and 100 000 kDa [204] and for xanthan gum between 1 000 and 20 000 kDa [120], and due to that, they lead to a very viscous solutions, even with low concentrations of polymer (2,5%, for example). Therefore, it was expected that the density of the structures was high enough so they presented higher compressive modulus, as, for example, CHT_6 and CHT_8.

For the last structures, CHT_6 (5,14 kPa), CHT_7 (6,80 kPa), CHT_8 (3,31 kPa), CHTXG_1 (4,11 kPa) and CHTXG_2 (3,14 kPa), the ones processed by the selected conditions of the yellow zone of QbD Design Space plots, the results were closer to the objective, however, only CHT_6, CHT_7 fit in the objective for mechanical analysis (> 4,7 kPa), and CHTXG_1 was very close from the objective. So, it is reasonable to conclude that working on the yellow zone improved a lot the mechanical characteristics of the structures.

As said in the previous subchapter, density is related with mechanical strength, and usually structures with higher density present higher mechanical strength. It was expected that CHT_6, CHT_8 and CHT_9 presented higher compression modulus, once they have the greater densities, however this only happened for CHT_6. Regarding the structure with lower density, CHT_1, it is not the structure with lower compression modulus, however, it represents the third structure with lower compression modulus.

3.2.6 Scanning electron microscopy (SEM)

In SEM analysis, the main objective was to evaluate the pore size of each structure. However, this kind of analysis, gives an idea about the morphology of the scaffolds and consequently the connection between the pores (interconnectivity). The interconnectivity between pores can be seen in the cross section images when it is possible to see a pore through another.

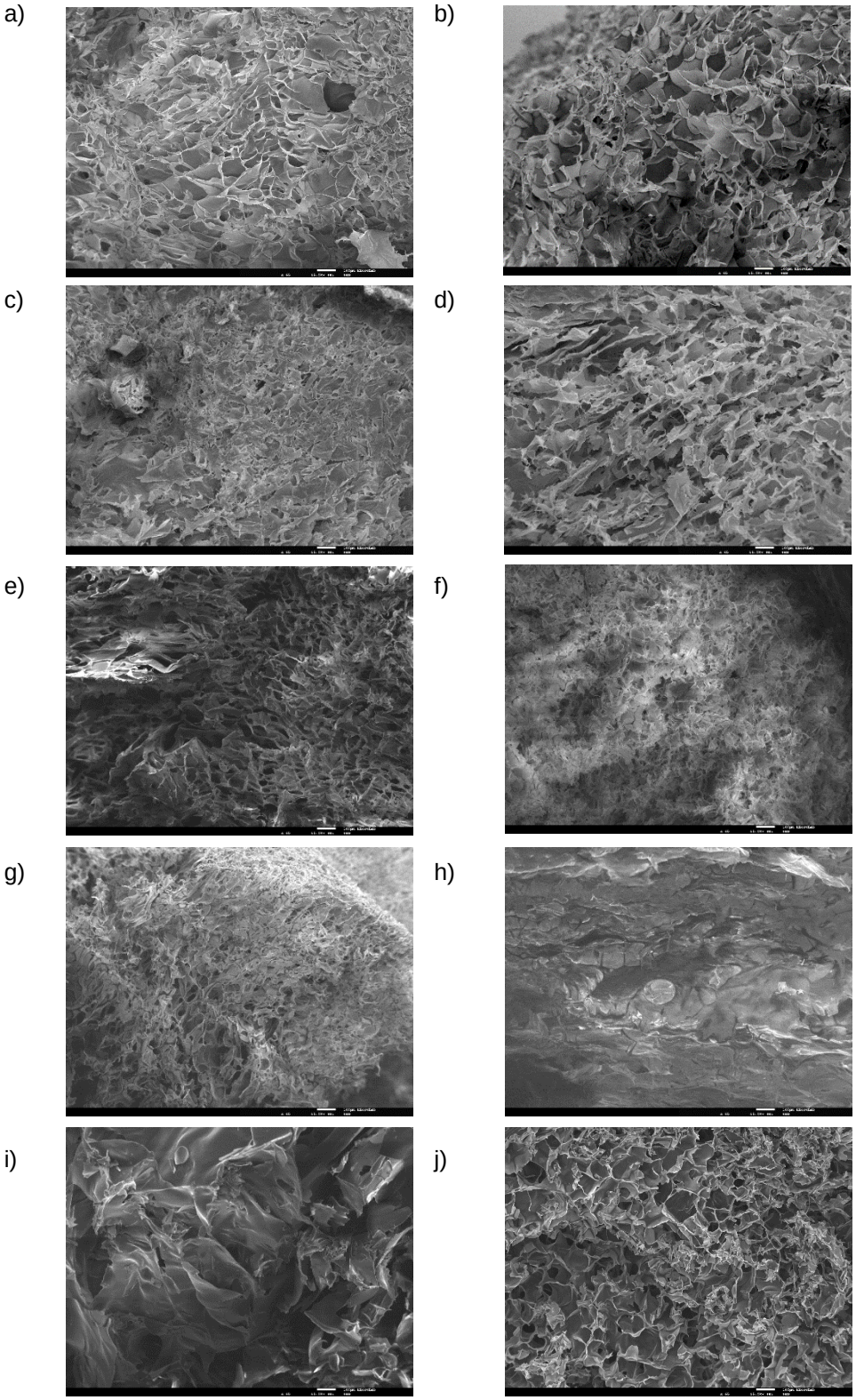

Figure 3.18 SEM images of surface and cross section of the structures : a)surface of CHT_1; b) cross section of CHT_1; c) surface of XG_1; d) corss section of XG_1; e) cross section of CHT_2; f) Cross section of XG_2; g) cross section of CHT_5; h) cross section of XG_5; i) cross section of CHT_3; j) cross section of CHT_4. All the micrographs have a magnification of 65 and the scale bar in white indicates 100 µm.

In **Figure 3.18** is represented the SEM images for some of the studied structures. Analyzingthe SEM image for the surface of CHT_1 and cross section of the same scaffold (**Figure 3.18** a) and b), it is possible to notice a difference between the pores of the two regions, being the pores in the surface smaller than the ones in the cross section. This happens in all structures, independently of the polymer nature. The 5mL tubes where the scaffolds are lyophilized are not porous, so the water ice crystals sublimated during this process is released through the nucleus of the sample and through the top of the flask and not through the side. So, the porous formed in the outer surface of the scaffolds are smaller comparing to the interior of the matrix.

Figure 3.18 b) and d) are an example of the cross section of two structures with the same concentration of polymer and crosslinker and the same freezing temperature, being the only difference the nature of the polymer, chitosan for the first one and xanthan gum for the second one. It is possible to see that chitosan based scaffolds have rounder and homogeneous pores than xanthan gum based scaffolds, which present porous more heterogeneous and with irregular shape. This is recurrent in all studied structures and it is in accordance with the literature [205].

The difference between the structure represented in **Figure 3.18** b) and e) is the concentration of the polymer (chitosan) in the casting solution. For CHT_1 (figure b)) and for XG_1 (figure d)) the polymer concentration is 2,5% and in figure e), CHT_2) and figure f) XG_2 the polymer concentration is 2,35%. It was expected that the pore size was smaller in CHT_1 and XG_1, once the polymer concentration is higher [206]. However, this is not verified, because the medium pore size for CHT_1 is 101 µm and for CHT_2 is 61 µm, and for XG_1 and XG_2 is 78 µm and 49 µm, respectively. Comparing **Figure 3.18** e) and g), the only difference is in the freezing temperature. For the first, image e), representing CHT_2, the freezing temperature was -20ºC, while in figure g), CHT_5, the freezing temperature was -80ºC. According to the literature, the structures with lower freezing temperature should present smaller pores [206], [207], however, for CHT_2 the pore size was 61 µm and for CHT_5 it was 64 µm, which is not in accordance with the literature. For XG_2 (figure f)) and XG_5 (figure h)), the results also are not according to the literature, once the medium pore size is the same for both structures, 49 µm. At last, comparing **Figure 3.18** i) and j), the difference between these structures is the concentration of the crosslinker in the casting solution. For CHT_3 (figure i)) the crosslinker solution is 1,3% and for CHT_4 (figure j)) the concentration is 1,7%. According to the literature, structures with higher crosslinker concentration tend to have smaller pores [207]. In this case, CHT_3 present a medium pore size of 93 µm and CHT_4 a medium pore size of 79 µm, which was expected. XG_3 and XG_4 (data not shown) are in the same situation. For the first, XG_3 the crosslinker concentration is 1,3% and for the second, XG_4 is 1,7%. The medium pore size for XG_3 is 85 µm and for XG_4 is 75 µm, which are also in accordance with the literature.

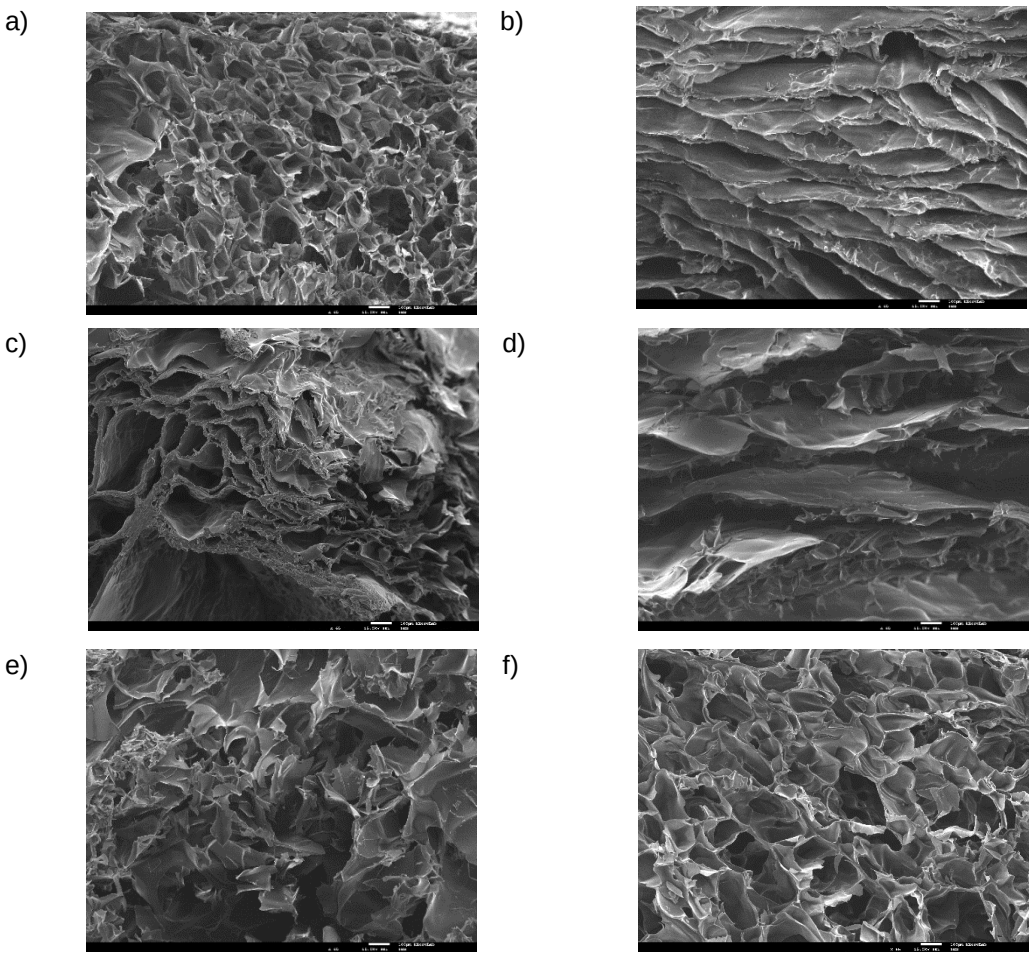

Figure 3.19 SEM images of the cross section of: a) CHT_6; b) CHT_7; c) CHT_8; d) CHT_9; e) CHTXG_1; f) CHTXG_2. All the micrographs have a magnification of 65 and the scale bar in white indicates 100 µm.

In **Figure 3.19** there are represented the SEM images of the cross section of the second set of the produced structures. **Figure 3.19** a) represents the cross section of CHT_6. For this set of structures, this was the only one that was frozen at -20ºC, and due to that, it will be compared with CHT_1 (2,5% polymer, 1,3% crosslinker), **Figure 3.18** b), and CHT_2 (2,35% polymer, 1% crosslinker), **Figure 3.18** e). Thus, comparing CHT_6 to those two structures, both polymer and crosslinker concentrations were higher for CHT_6 (3% polymer, 2% crosslinker). Due to that, it is expected that the pore size is lower than the pore size of CHT_1(101 µm) and CHT_2 (61 µm), which only happens for the first comparison, since the medium pore size of CHT_6 is 71 µm. Regarding CHT_8 (figure c)), the polymer concentration is 2%, the crosslinker concentration is 2,5% and the freezing temperature is -80ºC. This structure was the only that suffer a decrease in polymer concentration comparing with the first set of structures. Comparing this structure, CHT_8, with CHT_3 (2,5% polymer, 1,3% crosslinker, -80ºC), **Figure 3.18** i), CHT_4 (2,5% polymer, 1,7% crosslinker, -80ºC), **Figure 3.18** j) and CHT_5 (2,35% polymer, 1% crosslinker, -80ºC), **Figure 3.18** g), the difference is that the polymer concentration is lower, the crosslinker concentration is higher and the freezing temperature is the same. The medium pore size for CHT_3 is 93 µm, for CHT_4

is 79 µm, for CHT_5 is 64 µm and for CHT_8 is 122 µm, which lead to conclude that the decrease of polymer concentration had a higher impact than the increase of crosslinker concentration, once the value of medium pore size showed to be higher for CHT_6.

Comparing CHT_7 (figure b)) and CHT_9 (figure d)), the polymer concentration is 3% for both structures, the freezing temperature is also the same for both structures (-80ºC) but the crosslinker concentration is slightly lower in CHT_9 (1,5% crosslinker) than in CHT_7 (2% crosslinker). As it was referred before, it was expected that the structure with lower crosslinker concentration presented higher value of pore size [207]. In this case, this is not observed, once the medium pore size of both structures is the same, 119 µm. Regarding the structures composed by CHT and XG, CHTXG_1 and CHTXG_2, the crosslinker concentration for both structures is 2% and the freezing temperature is -80ºC. However, for CHTXG_1 the concentration of CHT is 2% and XG is 1%, and for CHTXG_2 is 1,5% for both polymers. The medium pore size of CHTXG_1 is 110 µm and for CHTXG_2 is 100 µm, which are a little bit higher that the ones reported in the literature (68-72 µm) [207].

It should be noticed that the pore size measurement estimated were only performed in a small portion of the samples. Thus, the fact that the crosslinker added to the casting solutions might not be homogeneously dissolved, there may be sample zones with more quantity of crosslinker than others, and those zones might present smaller pores, comparing to the other. Also, the variation on polymer and crosslinker concentrations between structures might not be sufficient or significant to observe alteration with higher impact in the pore size of each structure.

Another characteristic which is possible to observe in SEM images is the interconnectivity between pores. This is important, because in impregnated scaffolds the connectivity between pores facilitates the drug release. The structures which SEM clearly revealed some interconnectivity were XG_1, **Figure 3.18** d), CHT_2, **Figure 3.18** e), XG_2, **Figure 3.18** f), CHT_5, **Figure 3.18** g) and XG_5, **Figure 3.18** h).

In general, it is possible to affirm that working on the yellow zone of QbD Design Space improved the morphological characteristics of the structures, especially for candy structures, once the value of pore size increased round 40%.

Taking into account the results of swelling tests, mechanical analysis and morphology of the structures, CHT_6, CHT_7 and CHTXG_1 were the structures selected for drug impregnation. These structures presented high swelling capacities, 75-91% in acidic medium and 89-93% in neutral medium, high compressive modulus, 5.14 kPa, 6.8 kPa and 4.11 kPa and pore sizes of 72 µm, 118 µm and 110 µm, respectively, which are within the objectives of this work.

3.2.7 Drug Release

After drug impregnation, the structures (CHT_6, CHT_7 and CHTXG_1) were submitted to drug release studies, with the aim of determine the amount of drug released by each structure.

3.2.7.1 Release Studies

The pharmokinetics release profile was investigated under different physiological conditions, for candy structures two different pH were tested, 5,0 and 7,0, and for tampon structures, pH 3,8. as well as their responsiveness to pH stimuli, to evaluate the performance of the scaffolds as drug delivery systems.

a)

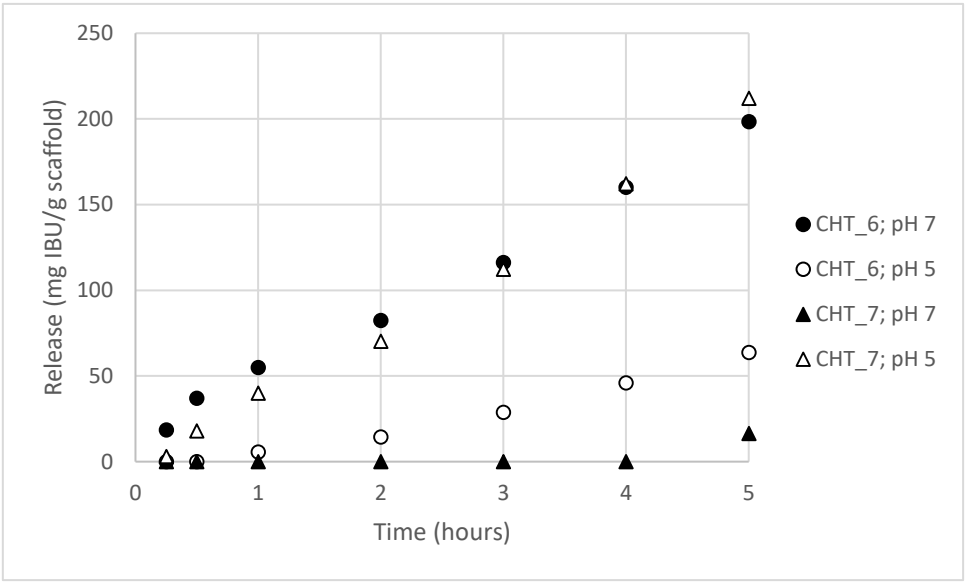

b)

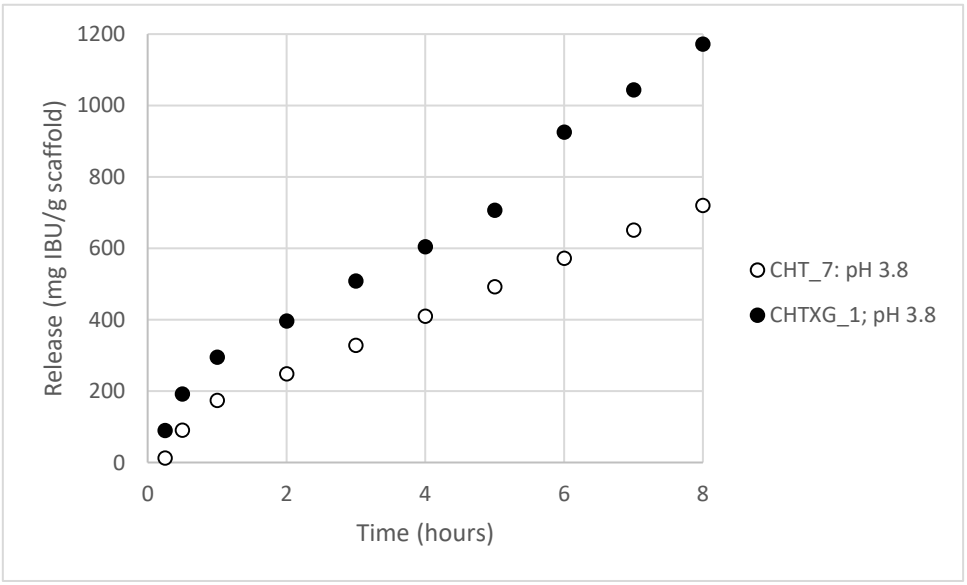

Figure 3.20 Release profiles for: a) CHT_6 at pH 7 (●), CHT_6 at pH 5 (○), CHT_7 at pH 7 (▲) and CHT_7 at pH 5 (Δ), obtained in 8 h; b) CHT_7 at pH 3.8 (○) and CHTXG_1 at pH 3.8 (●), obtained in 8 hours.

In **Figure 3.20**, it is represented the release profiles of ibuprofen for the impregnated structures, CHT_6, CHT_7 and CHTXG_1. CHT_6 and CHT_7 were impregnated as candy structure for pH 5.0 and 7.0 and as tampon structure for pH 3.8 and CHTXG_1 was impregnated only as tampon structure.

In detail, **Figure 3.20** a) represents the release profiles for the structures impregnated as candy structures. Due to that, the release profile studied was at two different pH's (5,0 and 7,0). At neutral pH, CHT_6 released 198,4 mg IBU/g scaffolds, while CHT_7 released 16,5 mg IBU/g scaffold. At acidic pH, CHT_6 released 63,6 mg IBU/g scaffold while CHT_7 released 211,9 mg IBU/g scaffold.

In CHT_6, is clear that the drug release is slower at acidic pH, as it was expected [208]. This is due to the fact that at this pH value, CHT is protonated and Ibu is deprotonated which result in an interaction between the polymer and the drug and, consequently, the drug release is delayed. At neutral pH, CHT is uncharged, which means that it does not contribute with repulsive or attractive forces, while Ibu remains deprotonated, which make the attractive forces weaker. This leads to a faster drug release. However, this tendency is not observed in CHT_7. This fact might be due to the low homogeneity of the drug in the structure. All the results were obtained through two different samples, and each sample was about half of a structure, however, the samples selected from this structure might be the half of the structure with lower quantity of drug impregnated, and it did not release enough drug. Another reason for this discrepancy might be the fact that CHT_7 has higher medium pore size (118 µm) than CHT_6 (71 µm), and this can reduce the effect of the pH in drug release and the structural effect prevails.

Figure 3.20 b) represents the release profiles for the structures impregnated as tampon structures. The release studies were performed at pH 3.8, during 8 hours. CHT_7 released 720,1 mg IBU/g scaffold and CHTXG_1 released 1200 mg IBU/g scaffold. The difference between the values for drug release in this two structures are expected, however, it was also expected that CHTXG_1 release less quantity and slower than CHT_7 [124], which did not happen. It is important to notice that, at this pH, 3,8, both CHT (as mentioned before) and XG are protonated [209], and IBU is deprotonated (also mentioned before), which creates an interaction between the polymers and the drug and consequently, delays the drug release. However, this discrepancy might be justified by the presence of XG in this structure. The swelling tests revealed a strong tendency for XG structures to disintegrate in acidic or neutral pH's. Also, the release of IBU might create an additional stress in the structure which promote the disintegration of the structure.

Regarding the drug release studies, the objectives set in the beginning of this thesis were different for the two structures in study. In the case of candy structures, they should release 50 mg IBU/g scaffold, in 5 hours and in a pH range from 5 to 7. However, it is known that when there is an infection in oral mucosa, the pH decreases and the mouth turns into an acidic medium. Thus,

it is essential and more important that the drug release occurs in acidic pH (5). Analyzing the results for these structures, both structures achieved the objective, however for CHT_7, the objective was achieved after 2 hours, releasing 70 mg IBU/g scaffold., CHT_6 released 63,6 mg IBU/g scaffold in 5 hours. Regarding tampon structures, the objective is a drug release of 800 mg IBU/g scaffold, in 8 hours, at pH 3,8. For these structures only CHTXG_1 achieved the objective, once it released 100% of the drug impregnated, however, the suspect of the possible disintegration of the structure is not a positive aspect for this structure. Regarding CHT_7, it did not achieve the objective, however, it was very close to it, releasing 720,1 mg IBU/g scaffold.

In the previous studies, performed in GEO company, the structures that achieved the quantity of drug release nearest to the target value were the mixture of xanthan gum and polygeo, with 2% of polymer concentration, 2% crosslinker and a freezing temperature of -20ºC, which released 80 mg drug/g scaffold, in the case of candy structure. Regarding tampon, it was the mixture of chitosan with xanthan gum, with 2% of polymer concentration, without any crosslinker (native structure) and a freezing temperature of -80 ºC, which released 104,8 mg drug/g scaffold. Thus, it is possible to conclude that QbD provided the conditions to improve the results, comparing with the ones obtained before, especially in the case of the tampon structures. Moreover, in the previous studies, there was a need to perform 30-70 shots, whereas in this work, only sixteen structures were produced and characterized. Once again, it is demonstrated the importance of QbD in reducing the numer of experiments needed to achieve the objectives.

3.2.7.2 Modeling of Drug Release

After drug release tests, it was important to find a model/equation that could describe the profile of drug release for each structure. This mathematical modulation is important once it helps to have a better knowledge of the treatment efficiency and may lead to a better design of the release structures. Moreover it is also important due to the fact that the physical medium where the release occurs is very complex and heterogeneous [210].

The mathematical models applied were Higuchi model and Korsmeyer-Peppas model (Power Law). For the first, Higuchi model, the assumptions are [211]: (i) the drug concentration in time zero is much higher than drug solubility, (ii) the diffusion only occurs in one-dimension (surface effect is negligible), (iii) the drug particles are much smaller than the thickness of the system, (iv) the swelling and the dissolution of the matrices are negligible, (v) drug diffusion is constant and (iv) the sink conditions are perfect and always attained in the release environment. The assumptions of Power law are [211]: (i) General equation is applicable in small values of time or short times (till 8h), (ii) the portion of release curve used to calculate exponent n is only where $M_t/M_\infty<0,6$, (iii) the release occurs at one dimension and (iv) the relation length/thickness ≥10.

Table 3.5 Modelation values for Higuchi model and Power law.

Structure	Application	pH	Higuchi		Power Law		
			k	r^2	k	n	r^2
CHT_6	Candy	5,0	0,36	0,89	0,13	1,31	0,99
		7,0	0,47	0,96	0,15	0,70	0,98
CHT_7	Candy	5,0	0,53	0,95	0,24	1,37	0,94
		7,0	0,05	0,34	N.A	N.A	N.A
	Tampon	3,8	0,33	0,99	0,15	1,07	0,89
CHTXG_1	Tampon	3,8	0,48	0,96	0,15	0,66	0,97

N.A: The power law was not applicable to the release curve.

Table 3.5 represents the modeling values for both models used, Higuchi and Power law. The plots of these modulations are showed in Appendix I. and II. Higuchi model is a good model to describe and study the dissolution through a planar heterogeneous matrix, where the drug concentration is lower than its solubility and the release of the drug occurs through the pores of the structure. In Higuchi model, k represents the Higuchi dissolution constant and it is calculated through a linear relationship between the cumulative percentage of drug release and the square root of the time (in hours).

Regarding Power law, it is used to study the release through different systems. Equation (7) represents the relationship between the fraction of drug release at time t (in hours) and the release rate constant (k), taking into account the value of the release exponent, n.

$$\frac{M_t}{M_\infty} = k.t^n \qquad (7)$$

The release exponent, n, is used to characterize different release profiles in cylindrical matrices. Taking this into account, when n<0,45, it indicates a diffusion-controlled drug release, when 0,45<n<0,89, it indicates both diffusion and swelling-controlled release and, when n>0,89, it indicates swelling-controlled release [212]. Thus, none of the structures presented a diffusion-controlled drug release, however, CHT_6 at neutral pH and CHTXG_1 presented both diffusion and swelling controlled release and CHT_6 at acidic pH and CHT_7 (at both acidic pH) presented swelling-controlled release. Regarding CHT_7 at neutral pH, it was impossible to apply Power law once it only starts to release between the fourth and the fifth hours (which means, in the last hour of the test).

The mathematical modeling provided a good idea of how the drug release mechanism occurs. The results of this modulation are the expected [213]. First, for swelling-controlled release, it happens in acidic pH. Thus, once IBU solubility in acidic medium is very low, it was expected that in this case the release was caused by the structure swelling. On the other hand, for CHT_6 at neutral pH release was diffusion and swelling-controlled, which also make sense, once Ibu is

soluble in neutral medium and CHT_6 presented 90% swelling. For CHTXG_1, which test occurred in acidic medium, both diffusion and swelling-controlled release were observed; however, it is important to take into account that, it is suspected that this structure disintegrated during the drug release test.

4. Conclusion

The main objective of this project was the application of Quality by Design approach in the optimization of the processing method of two pH sensitive, with controlled morphological and mechanical properties scaffolds for oral and vaginal routes of administration.

The application of QbD approach provided great conditions to design 3D porous structures for oral and vaginal routes of administration improving the characteristics of the structures until now obtained, and also reducing the number of experimental shots performed to achieve the objectives. In total, only sixteen structures were produced and characterized while for previous studies for each application were performed 30-70 shots tests. During QbD application, the polymer and crosslinker concentrations and the freezing temperature were the conditions studied and optimized, and the conditions chosen to produce those sixteen structures were given by QbD Design Space, as the suitable to achieve the objectives. Thus, it is possible to conclude and reinforce that QbD is an important and essential tool to optimize work conditions and complex processes.

Regarding candy structures, the ones that reached the target values for swelling tests, mechanical analysis and SEM were CHT_6 (75% swelling (at pH 5,0), 5,14 kPa, 71 µm) and CHT_7 (83% swelling, 6,80 kPa, 118 µm). Considering tampon structures, the ones that achieved the target values for swelling tests, mechanical analysis and SEM were CHT_7 (81% swelling (at pH 3,8), 6,80 kPa, 118 µm) and CHTXG_1 (91%, 4,11 kPa, 110 µm).

The release profiles showed to be dependent of the diffusional and swelling effects of the structure, considering the IBU as the model drug. The best matches in drug release were CHT_6 and CHT_7 for candy structures, that release 63,6 mg IBU/g scaffold and 211,9 mg IBU/g scaffold, respectively. Regarding tampon structures the best match for drug release was CHTXG_1 that released 1200 mg IBU/g scaffold, however, CHT_7 was also very close to the objective, releasing 720,1 mg IBU/g scaffold.

As future work, other aspects should be considered, especially regarding QbD studies, such as (i) incorporating more process conditions than only concentration of polymer and crosslinker and freezing temperature (ii) find a QbD model that can incorporate qualitative variables and still give trustable results and (iii) the method used for polymers processing, that may better tune the porous network of the scaffolds. Thus, during this thesis, three of the four objectives purposed were achieved in both structures, namely, the swelling capacity, the mechanical strength and the drug release.

References

[1] L. P. Samaranayake, W. Keung Leung, and L. Jin, “Oral mucosal fungal infections,” *Periodontol ogy2000*, vol. 49, pp. 39–59, 2009.

[2] U. Invasive, “How Common are Fungal Diseases ?,” *Oral, oesophageal and vulvovaginal candidiasis (thrush)*, 2011. [Online]. Available: https://www.fungalinfectiontrust.org/how-common-are-fungal-diseases. [Accessed: 16-Mar-2017].

[3] A. Dovnik, A. Golle, D. Novak, D. Arko, and I. Takač, “Treatment of vulvovaginal candidiasis: A review of the literature,” *Acta Dermatovenerologica Alpina, Pannonica Adriat.*, vol. 24, no. 1, pp. 5–7, 2015.

[4] A. V KRISHNA SV and C. A, “A review on vaginal drug delivery systems,” *Int. J. Biol. , Pharm. Allied Sci.*, vol. 1, no. 2, pp. 152–167, 2012.

[5] A. H. Shojaei, “Buccal Mucosa As A Route For Systemic Drug Delivery : A Review Epithelium Lamina Propria,” *J. Pharm. Pharm. Sci.*, vol. 1, no. 1, pp. 15–30, 1998.

[6] G. Sandri, S. Rossi, F. Ferrari, M. C. Bonferoni, C. Muzzarelli, and C. Caramella, “Assessment of chitosan derivatives as buccal and vaginal penetration enhancers,” *Eur. J. Pharm. Sci.*, vol. 21, no. 2–3, pp. 351–359, 2004.

[7] D. Laboratories, “What is Quality by Design (QbD) - And why should you care?,” *DPT Thought Leadership*, no. 11, San Antonio, Texas, pp. 1–5, 2013.

[8] T. Kourti and B. Davis, “The Business Benefits of Quality by Design (QbD),” *Pharmaceutical Engineering*, vol. 32, no. 4, pp. 1–10, 2012.

[9] M. Shivhare and G. Mccreath, “Practical Considerations for DoE Implementation in Quality By Design,” *Bio Process International*, pp. 1–7, 2010.

[10] Ich, “ICH Topic Q2 (R1) Validation of Analytical Procedures : Text and Methodology,” in *International Conference on Harmonization*, 2005, vol. 4, pp. 1–17.

[11] L. X. Yu *et al.*, “Understanding pharmaceutical quality by design.,” *AAPS J.*, vol. 16, no. 4, pp. 771–83, 2014.

[12] N. Izat, F. Yerlikaya, and Y. Capan, “A glance on the history of pharmaceutical quality by design,” *OA Drug Desing Deliv.*, vol. 2, no. 1, pp. 1–8, 2014.

[13] S. Miksinski, “Regulatory Assessment of Applications Containing QbD Elements - Reviewer Experience,” 2012. [Online]. Available: https://www.fda.gov/downloads/AboutFDA/CentersOffices/OfficeofMedicalProductsandTobacco/CDER/UCM341173.pdf. [Accessed: 23-Feb-2017].

[14] U.S. Department of Health and Human Services and F. and D. Administration, “Q8(R2) Pharmaceutical Development,” 2009.

[15] M. Summers and K. J. Fountain, “A Quality by Design (QbD) Based Method Development for the Determination of Impurities in a Peroxide Degraded Sample of Ziprasidone,” Milford, MA, 2011.

[16] P. G. Alden, W. Potts, and D. Yurach, “A Qbd With Design of Experiments Approach To the Development of a Chromatographic Method for the Separation of Impurities in Vancomycin,” Milford, MA, 2009.

[17] F. G. Vogt and A. S. Kord, “Development of quality by design analytical methods,” *J. Pharm. Sci.*, vol. 100, no. 3, pp. 797–812, 2011.

[18] S. S. S. Kakodkar, S. Bhilegaonkar, A. M. Godbole, and P. Gajare, “Pharmaceutical Quality-by-Design (QbD): Basic Principles,” *Hum. Journals*, vol. 1, no. 1, pp. 1–19, 2015.

[19] J. Maguire and D. Peng, “How to Identify Critical Quality Attributes and Critical Process Parameters,” *FDA/PQRI 2nd Conference*, 2015. [Online]. Available: http://pqri.org/wp-content/uploads/2015/10/01-How-to-identify-CQA-CPP-CMA-Final.pdf. [Accessed: 10-Feb-2017].

[20] N. V. G. Vemuri Pavan Kumar, “A Review on quality by design approach (QBD) for Pharmaceuticals,” *Int. J. Drug Dev. Res.*, vol. 7, no. 1, pp. 52–60, 2015.

[21] GE Healthcare, *Design of Experiments in Protein Production and Purification*. 2014.

[22] B. Debrus *et al.*, “Application of new methodologies based on design of experiments, independent component analysis and design space for robust optimization in liquid chromatography,” *Anal. Chim. Acta*, vol. 691, no. 1–2, pp. 33–42, 2011.

[23] W. Dewé, R. D. Marini, P. Chiap, P. Hubert, J. Crommen, and B. Boulanger, “Development of response models for optimising HPLC methods,” *Chemom. Intell. Lab. Syst.*, vol. 74, pp. 263–268, 2004.

[24] A. Baldinger, L. Clerdent, J. Rantanen, M. Yang, and H. Grohganz, “Quality by design approach in the optimization of the spray-drying process,” *Pharm. Dev. Technol.*, vol. 17, no. 4, pp. 389–397, 2012.
[25] E. Pallagi, R. Ambrus, P. Szabó-Révész, and I. Csóka, “Adaptation of the quality by design concept in early pharmaceutical development of an intranasal nanosized formulation,” *Int. J. Pharm.*, vol. 491, no. 1–2, pp. 384–392, 2015.
[26] C.-I. W. Group, “Pharmaceutical Development Case Study: ‘ACE Tablets,’” 2008.
[27] Bosch Company, “Statistical Design Space Development for Pharma – from Design of Experiment to Granules ‘ Master of Solids ’ Certification Seminar Statistical Design Space Development for Pharma ‘ Master of Solids ’ Certification Seminar,” 2015.
[28] M. Alsumidaie, “How Bristol-Myers Squibb is doing Risk-Based Monitoring,” *Applied Clinical Trials*, 2014. [Online]. Available: http://www.appliedclinicaltrialsonline.com/how-bristol-myers-squibb-doing-risk-based-monitoring. [Accessed: 10-Mar-2017].
[29] S. Milmo, “Quality by Design—Bridging the Gap between Concept and Implementation,” *PharmaTech.com*, 2014. [Online]. Available: http://www.pharmtech.com/quality-design-bridging-gap-between-concept-and-implementation. [Accessed: 10-Mar-2017].
[30] G. Stephenson and E. Lilly, “Application of Quality by Design In Drug Product Process Development II Implementing Quality by Design in Pharmaceutical Salt Selection,” *AIChE Academy*, 2011. [Online]. Available: https://www.aiche.org/conferences/aiche-annual-meeting/2011/proceeding/paper/implementing-quality-design-pharmaceutical-salt-selection. [Accessed: 10-Mar-2017].
[31] E. C. Esber, “Quality by Design for Biologics : An Industry Perspective,” 2007.
[32] D. E. Smith, “Quality by Design (QbD) for the Continuous Manufacturing of Solid Oral Dosage Forms,” 2014.
[33] A. S. Rathore, “Roadmap for implementation of quality by design (QbD) for biotechnology products,” *Trends Biotechnol.*, vol. 27, no. 9, pp. 546–553, 2009.
[34] MKS Umetrics, “User Guide to Modde,” 2014.
[35] “Multiple Linear Regression.” [Online]. Available: http://www.stat.yale.edu/Courses/1997-98/101/linmult.htm. [Accessed: 21-May-2017].
[36] E. S. DE TECNOLOGIA and U. DO ALGARVE, “Regressão Linear Múltipla,” no. 2, 2008.
[37] A. C. Rencher and G. B. Schaalje, *Linear models in statistics*, 2nd ed. John Wiley & Sons, INC., 2008.
[38] M. Lacey, “Multiple Linear Regression,” vol. 2, pp. 1–18, 1997.
[39] J. Osborne and E. Waters, “Four assumptions of multiple regression that researchers should always test,” *Pract. Assessment, Res. Eval.*, vol. 8, no. 2, p. 1, 2002.
[40] H. Abdi, “Partial least squares regression and projection on latent structure regression,” *Wiley Interdiscip. Rev. Comput.*, vol. 2, pp. 97–106, 2010.
[41] R. Ruby-Figueroa, “Partial Least Square Regression (PLSR),” *Encycl. Meas. Stat.*, pp. 1–3, 2007.
[42] R. D. Tobias, “An introduction to partial least squares regression,” *SAS Conf. Proc. SAS Users Gr. Int. 20 (SUGI 20)*, pp. 2–5, 1995.
[43] S. S. M. Wold and L. Eriksson, “PLS-Regression: A Basic Tool of Chemometrics,” *Chemom. Intell. Lab. Syst.*, vol. 58, no. 2, pp. 109–130, 2001.
[44] C. K. Bayne and R. Kramer, “Chemometric Techniques for Quantitative Analysis,” *Technometrics*, vol. 41, no. 2. p. 173, 1999.
[45] M. Haenlein and A. M. Kaplan, “A Beginner’s Guide to Partial Least Squares Analysis,” *Underst. Stat.*, vol. 3, no. 4, pp. 283–297, 2004.
[46] W. C. Gonsalves, A. C. Chi, and B. W. Neville, “Common Oral Lesions : Part I . Superficial Mucosal Lesions,” *Am. Acad. Fam. Physicians*, 2007.
[47] W. C. Gonsalves, A. C. Chi, and B. W. Neville, “Common Oral Lesions : Part II . Masses and Neoplasia,” *Am. Acad. Fam. Physicians*, 2007.
[48] J. a Maertens, “History of the development of azole derivatives.,” *Clin. Microbiol. Infect.*, vol. 10, no. 1, pp. 1–10, 2004.
[49] J. A. Barnett, F. Borg, C. Robin, and R. Benham, “A history of research on yeasts 12 : medical yeasts part 1 , Candida albicans Keywords : history of yeast research ; Candida albicans ; pathogenic yeasts ; Dimor-,” *Wiley Intersci.*, no. 25, pp. 385–417, 2008.
[50] F. Ayoade, “Herpes Simplex,” *Medscape*, 2011. [Online]. Available: http://emedicine.medscape.com/article/218580-overview#a4. [Accessed: 21-Feb-2017].
[51] K. Shinkai, M. Rosenbach, I. Ahronowitz, J. Harp, U. W. Bruce, and T. G. Berger,

"Therapeutic strategies in dermatology." [Online]. Available: https://www.derm101.com/therapeutic/aphthous-stomatitis/. [Accessed: 21-Feb-2017].
[52] L. Blanton, B. Keith, and W. Brzezinski, "Southern Tick-Associated Rash Illness: Erythema Migrans Is Not Always Lyme Disease," *South Med J.*, vol. 101, no. 7, 2008.
[53] M. Z. Handler, "Hairy Tongue," *Medscape*, 2016. [Online]. Available: http://emedicine.medscape.com/article/1075886-overview#a4. [Accessed: 21-Feb-2017].
[54] N. Burkhart, "Oral Lichen Planus," *American Academy of Oral Medicine*, 2013. [Online]. Available: http://www.aaom.com/oral-lichen-planus. [Accessed: 21-Feb-2017].
[55] N. Lavanya, P. Jayanthi, U. K. Rao, and K. Ranganathan, "Oral lichen planus: An update on pathogenesis and treatment," *J. Oral Maxillofac. Pathol.*, vol. 15, no. 2, pp. 127–132, 2011.
[56] H. Jadwiga *et al.*, "Mandibular and Palatal Tori, Bone Mineral Density, and Salivary Cortisol in Community-Dwelling Elderly Men and Women," *journals Gerontol.*, vol. 56, no. 11, 2001.
[57] T. Kenny, "Oral Thrush (Yeast Infection)," *Patient PlatformLimited*, 2017. [Online]. Available: http://patient.info/health/oral-thrush-yeast-infection%0A. [Accessed: 10-Mar-2017].
[58] "Herpes Simplex: Diagnosis and Treatment," *American Academy of Dermatology*, 2017. [Online]. Available: https://www.aad.org/public/diseases/contagious-skin-diseases/herpes-simplex#treatment. [Accessed: 10-Mar-2017].
[59] Micromedex, "Acyclovir (Oral Route, Intravenous Route)," *Truven Health Analytics Inc.*, 2017. [Online]. Available: http://www.mayoclinic.org/drugs-supplements/acyclovir-oral-route-intravenous-route/proper-use/drg-20068393. [Accessed: 10-Mar-2017].
[60] "Famciclovir (Rx)," *Medscape*, 2017. [Online]. Available: http://reference.medscape.com/drug/famvir-famciclovir-342611. [Accessed: 10-Mar-2017].
[61] Micromedex, "Valacyclovir (Oral Route)," *Truven Health Analytics Inc.*, 2017. [Online]. Available: http://www.mayoclinic.org/drugs-supplements/valacyclovir-oral-route/proper-use/drg-20066635. [Accessed: 10-Mar-2017].
[62] I. Belenguer-Guallar, Y. Jiménez-Soriano, and A. Claramunt-Lozano, "Treatment of recurrent aphthous stomatitis. A literature review," *J. Clin. Exp. Dent.*, vol. 6, no. 2, pp. 168–174, 2014.
[63] D. Assimakopoulos, G. Patrikakos, C. Fotika, and M. Elisaf, "Benign migratory glossitis or geographic tongue: An enigmatic oral lesion," *Am. J. Med.*, vol. 113, no. 9, pp. 751–755, 2002.
[64] G. E. Gurvits and A. Tan, "Black hairy tongue syndrome," *World J. Gastroenterol.*, vol. 20, no. 31, pp. 10845–10850, 2014.
[65] Mayo Clinic Staff, "Oral lichen planus," *Mayo Clinic*, 2016. [Online]. Available: http://www.mayoclinic.org/diseases-conditions/oral-lichen-planus/diagnosis-treatment/treatment/txc-20196809. [Accessed: 14-Mar-2017].
[66] L. L. H. Chen, D. J. Chetty, and Y. W. Chien, "A mechanistic analysis to characterize oramucosal permeation properties," *Int. J. Pharm.*, vol. 184, no. 1, pp. 63–72, 1999.
[67] S. M. Pond and T. N. Tozer, "First-Pass Elimination Basic Concepts and Clinical Consequences," *Clin. Pharmacokinet.*, no. 1, pp. 1–25, 1984.
[68] K. R. Shah and T. A. Mehta, "Medicated chewing gum-a mobile oral drug delivery system," *Int. J. PharmTech Res.*, vol. 6, no. 1, pp. 35–48, 2014.
[69] M. A. Russell, M. Raw, and M. J. Jarvis, "Clinical use of nicotine chewing-gum.," *Br. Med. J.*, vol. 280, no. 6231, pp. 1599–1602, 1980.
[70] D. Development and I. Pharmacy, "Miconazole chewing gum as a drug delivery system: test of release promoting additives," *Drug Dev. Ind. Pharm.*, vol. 17, no. 3, pp. 411–420, 1991.
[71] L. Maggi, L. Segale, S. Conti, E. Ochoa Machiste, A. Salini, and U. Conte, "Preparation and evaluation of release characteristics of 3TabGum, a novel chewing device," *Eur. J. Pharm. Sci.*, vol. 24, no. 5, pp. 487–493, 2005.
[72] A. Aslani and F. Jalilian, "Design, formulation and evaluation of caffeine chewing gum," *Adv. Biomed. Res.*, vol. 2, no. 3, p. 72, 2012.
[73] T. Stanley and B. Haque, "Methods and compositions for noninvasive administration of sedatives, analgesics and anesthetics," 4 671 953, 1987.
[74] R. Archarya, "Calcium polycarbophil controlled release composition and method," 5 102 666, 1992.

[75] A. R. Batuca, “Development of 3D porous structures for buccal drug delivery,” FCT-UNL, 2016.
[76] “Vaginal Thrush (Yeast Infection, Vulvovaginal Candidiasis, VVT, VVC),” *Virtual Medical Center*, 2006. [Online]. Available: https://www.myvmc.com/diseases/vaginal-thrush-yeast-infection-vulvovaginal-candidiasis-vvt-vvc/. [Accessed: 10-Mar-2017].
[77] D. Spence, “Candidiasis (vulvovaginal),” 2009.
[78] S. D. Rathod, J. D. Klausner, K. Krupp, A. L. Reingold, and P. Madhivanan, “Epidemiologic features of vulvovaginal candidiasis among reproductive-age women in India,” *Infect. Dis. Obstet. Gynecol.*, pp. 1–8, 2012.
[79] A. Cassone and J. D. Sobel, “Experimental models of vaginal candidiasis and their relevance to human candidiasis,” *Infect. Immun.*, vol. 84, no. 5, pp. 1255–1261, 2016.
[80] R. Negroni, “Historical aspects of dermatomycoses,” *Clin. Dermatol.*, vol. 28, no. 2, pp. 125–132, 2010.
[81] J. A. Vazquez, “Invasive oesophageal candidiasis: Current and developing treatment options,” *Drugs*, vol. 63, no. 10, pp. 971–989, 2003.
[82] M. C. Stöppler, “Vaginal Infections (Vaginitis),” *e Medicine Health*, 2015. [Online]. Available: http://www.emedicinehealth.com/vaginal_infections/article_em.htm. [Accessed: 09-Mar-2017].
[83] P. Nyirjesy and J. D. Sobel, “Vulvovaginal candidiasis,” *Obstet. Gynecol. Clin. North Am.*, vol. 30, no. 4, pp. 671–684, 2006.
[84] A. B. Khan and C. Saha, “A Review on Vaginal Drug Delivery System,” *J. Pharm. Sci.*, vol. 4, no. 4, pp. 142–147, 2014.
[85] N. Dobaria, “Vaginal Drug Delivery Systems: A Review,” *East Cent. African J. Pharm. Sci.*, vol. 10, pp. 3–13, 2007.
[86] D. Lopes, “Development of 3D porous structures for drug delivery in vulvovaginal candidiasis treatments,” FCT-UNL, 2016.
[87] G. a Digenis, D. Nosek, F. Mohammadi, N. B. Darwazeh, H. S. Anwar, and P. M. Zavos, “Novel vaginal controlled-delivery systems incorporating coprecipitates of nonoxynol-9.,” *Pharm. Dev. Technol.*, vol. 4, no. 3, pp. 421–30, 1999.
[88] A. O. Andrade, M. E. Parente, and G. Ares, “Screening of mucoadhesive vaginal gel formulations,” *Brazilian J. Pharm. Sci.*, vol. 50, no. 4, pp. 931–942, 2014.
[89] S. E. Moulton and G. G. Wallace, “3-dimensional (3D) fabricated polymer based drug delivery systems,” *J Control Release*, vol. 193, pp. 27–34, 2014.
[90] O. Shimoni *et al.*, “Macromolecule Functionalization of Disul fi de-Bonded Polymer Hydrogel Capsules and Cancer Cell Targeting,” *Am. Chem. Soc.*, vol. 6, no. 2, pp. 1463–1472, 2012.
[91] Q. L. Loh and C. Choong, “Three-dimensional scaffolds for tissue engineering applications: role of porosity and pore size.,” *Tissue Eng. Reviwes*, vol. 19, no. 6, pp. 485–502, 2013.
[92] T. Garg, O. Singh, S. Arora, and M. R.S.R, “Scaffold: A Novel Carrier for Cell and Drug Delivery,” *Crit. Rev. Ther. Drug Carr. Syst.*, vol. 29, no. 1, pp. 1–63, 2012.
[93] V. Pande, A. Kharde, P. Bhawar, and V. Abhale, “Scaffolds : Porous Scaffold for Modulated Drug Delivery,” *Austin Ther.*, vol. 3, no. 1, 2016.
[94] J. K. Oh, R. Drumright, D. J. Siegwart, and K. Matyjaszewski, “The development of microgels/nanogels for drug delivery applications,” *Prog. Polym. Sci.*, vol. 33, no. 4, pp. 448–477, 2008.
[95] H. J. Chung and T. G. Park, “Surface engineered and drug releasing pre-fabricated scaffolds for tissue engineering,” *Adv. Drug Deliv. Rev.*, vol. 59, no. 4–5, pp. 249–262, 2007.
[96] G. Vilar, J. Tulla-Puche, and F. Albericio, “Polymers and drug delivery systems.,” *Curr. Drug Deliv.*, vol. 9, no. 4, pp. 367–394, 2012.
[97] K. Shalumon and J. Chen, “Scaffold-based Drug Delivery for Cartilage Tissue Regeneration,” *Curr. Pharm. Des.*, vol. 21, no. 15, 2015.
[98] C. T. Vogelson, “Advances in drug delivery systems,” *ACS Publications*, 2001. [Online]. Available: http://pubs.acs.org/subscribe/archive/mdd/v04/i04/html/MDD04FeatureVogelson.html. [Accessed: 22-Feb-2017].
[99] S. P. Chaudhari and P. S. Patil, “Pharmaceutical Excipients : A review,” *Int. J. Adv. Pharmacy, Biol. Chem.*, vol. 1, no. 1, pp. 21–34, 2012.
[100] A. Katdare and M. V. Chaubal, *Excipient Development for Pharmaceutical,*

Biotechnology, and Drug Delivery Systems. 2006.
[101] K. J. Gandhi, S. V. Deshmane, and K. R. Biyani, “Polymers in pharmaceutical drug delivery system: A review,” *Int. J. Pharm. Sci. Rev. Res.*, vol. 14, no. 2, pp. 57–66, 2012.
[102] D. Jones, *Pharmaceutical Applications of Polymers for Drug Delivery*. 2004.
[103] F. Universita, “Calculation of the Dimensions of Drug − Polymer Devices Based on,” *J. Pharm. Sci.*, vol. 87, no. 7, pp. 827–832, 1998.
[104] R. K. Verma, B. Mishra, and S. Garg, “Osmotically Controlled Oral Drug Delivery* INTRODUCTION AND HISTORICAL BACKGROUND,” *Drug Dev. Ind. Pharm.*, vol. 26, no. 7, pp. 695–708, 2000.
[105] K. R. Kamath and K. Park, “Biodegradable hydrogels in drug delivery,” *Adv. Drug Deliv. Rev.*, vol. 11, no. 1–2, pp. 59–84, 1993.
[106] M. Hrubý, S. K. Filippov, and P. Štěpánek, “Smart polymers in drug delivery systems on crossroads: Which way deserves following?,” *Eur. Polym. J.*, vol. 65, pp. 82–97, 2015.
[107] N. A. Liechty, W. B., Kryscio, D.R., Slaughter, B. V. and Peppas, “Polymers for drug delivery systems,” *Annu. Rev. Chem. Biomol. Eng.*, vol. 1, pp. 149–173, 2010.
[108] P. Colombo, R. Bettini, P. Santi, and N. A. Peppas, “Swellable matrices for controlled drug delivery: Gel-layer behaviour, mechanisms and optimal performance,” *Pharm. Sci. Technol. Today*, vol. 3, no. 6, pp. 198–204, 2000.
[109] J. F. Coelho *et al.*, “Drug delivery systems: Advanced technologies potentially applicable in personalized treatments,” *EPMA J.*, vol. 1, pp. 164–209, 2010.
[110] M. Shaik, M. Korsapati, and D. Panati, “Polymers in Controlled Drug Delivery Systems,” *Int. J. Pharma Sci.*, vol. 2, no. 4, pp. 112–116, 2012.
[111] M. Rinaudo, “Chitin and chitosan: Properties and applications,” *Prog. Polym. Sci.*, vol. 31, no. 7, pp. 603–632, 2006.
[112] Y. Luo and Q. Wang, “Recent development of chitosan-based polyelectrolyte complexes with natural polysaccharides for drug delivery,” *Int. J. Biol. Macromol.*, vol. 64, pp. 353–367, 2014.
[113] T. Kean and M. Thanou, “Biodegradation, biodistribution and toxicity of chitosan,” *Adv. Drug Deliv. Rev.*, vol. 62, no. 1, pp. 3–11, 2009.
[114] M. Thanou, J. C. Verhoef, and H. E. Junginger, “Oral drug absorption enhancement by chitosan and its derivatives,” *Adv. Drug Deliv. Rev.*, vol. 52, no. 2, pp. 117–126, 2001.
[115] A. Anitha *et al.*, “Chitin and chitosan in selected biomedical applications,” *Prog. Polym. Sci.*, vol. 39, no. 9, pp. 1644–1667, 2014.
[116] J. E. Lee *et al.*, “Effects of the controlled-released TGF-b1 from chitosan microspheres on chondrocytes cultured in a collagen/chitosan/glycosaminoglycan scaffold,” *Biomaterials*, vol. 25, no. 18, pp. 4163–4173, 2004.
[117] Y.-C. Ho, F.-M. Huang, and Y.-C. Chang, “Cytotoxicity of formaldehyde on human osteoblastic cells is related to intracellular glutathione levels.,” *J. Biomed. Mater. Res. B. Appl. Biomater.*, vol. 83, no. 2, pp. 340–344, 2007.
[118] U. Adhikari, N. P. Rijal, S. Khanal, D. Pai, J. Sankar, and N. Bhattarai, “Magnesium incorporated chitosan based scaffolds for tissue engineering applications,” *Bioact. Mater.*, vol. 1, no. 2, pp. 132–139, 2016.
[119] F. García-Ochoa, V. E. Santos, J. A. Casas, and E. Gómez, “Xanthan gum: Production, recovery, and properties,” *Biotechnol. Adv.*, vol. 18, no. 7, pp. 549–579, 2000.
[120] D. F. S. Petri, “Xanthan gum: A versatile biopolymer for biomedical and technological applications,” *J. Appl. Polym. Sci.*, vol. 132, no. 23, 2015.
[121] A. Becker, F. Katzen, A. Pühler, and L. Ielpi, “Xanthan gum biosynthesis and application: A biochemical/genetic perspective,” *Appl. Microbiol. Biotechnol.*, vol. 50, no. 2, pp. 145–152, 1998.
[122] M. M. Talukdar and R. Kinget, “Swelling and Drug-Release Behavior of Xanthan Gum Matrix Tablets,” *Int. J. Pharm.*, vol. 120, pp. 63–72, 1995.
[123] O. J. D’Cruz, P. Samuel, B. Waurzyniak, and F. M. Uckun, “In vivo evaluation of a gel formulation of stampidine, a novel nonspermicidal broad-spectrum anti-HIV microbicide,” *Am. J. Drug Deliv.*, vol. 1, no. 4, pp. 275–285, 2003.
[124] T. Phaechamud and G. C. Ritthidej, “Sustained-release from layered matrix system comprising chitosan and xanthan gum.,” *Drug Dev. Ind. Pharm.*, vol. 33, no. 6, pp. 595–605, 2007.
[125] “Xanthan Gum for another encapsulation option,” *Open WetWare*, 2009. [Online]. Available: http://www.openwetware.org/wiki/IGEM:IMPERIAL/2009/Encapsulation/Phase2/Xanthan

_Gum. [Accessed: 03-Mar-2017].
[126] M. J. Caulfield, X. Hao, G. G. Qiao, and D. H. Solomon, “Degradation on polyacrylamides. Part I. Linear polyacrylamide,” *Polymer (Guildf).*, vol. 44, no. 5, pp. 1331–1337, 2003.
[127] M. J. Caulfield, X. Hao, G. G. Qiao, and D. H. Solomon, “Degradation on polyacrylamides. Part II. Polyacrylamide gels,” *Polymer (Guildf).*, vol. 44, no. 14, pp. 3817–3826, 2003.
[128] P. Guo, Y. Yuan, and F. Chi, “Biomimetic alginate/polyacrylamide porous scaffold supports human mesenchymal stem cell proliferation and chondrogenesis,” *Mater. Sci. Eng. C*, vol. 42, pp. 622–628, 2014.
[129] L. H. Christensen, V. . Breiting, A. Aasted, A. Jorgensen, and I. Kebuladze, “Long-term effects of polyacrylamide hydrogel on human breast tissue,” *Plast. Reconstr. Surg.*, vol. 111, no. 6, pp. 1883–1890, 2003.
[130] K. S. Soppirnath and T. M. Aminabhavi, “Water transport and drug release study from cross-linked polyacrylamide grafted guar gum hydrogel microspheres for the controlled release application,” *Eur. J. Pharm. Biopharm.*, vol. 53, no. 1, pp. 87–98, 2002.
[131] L. Liu and H. Sheardown, “Glucose permeable poly (dimethyl siloxane) poly (N-isopropyl acrylamide) interpenetrating networks as ophthalmic biomaterials,” *Biomaterials*, vol. 26, no. 3, pp. 233–244, 2005.
[132] M. Pulat, A. S. Kahraman, N. Tan, and M. Gümüşderelioğlu, “Sequential antibiotic and growth factor releasing chitosan-PAAm semi-IPN hydrogel as a novel wound dressing.,” *J. Biomater. Sci. Polym. Ed.*, vol. 24, no. 7, pp. 807–819, 2013.
[133] a Thakur, S. Monga, and R. K. Wanchoo, “Sorption and Drug Release Studies from Semi-interpenetrating Polymer Networks of Chitosan and Xanthan Gum,” *Chem. Biochem. Eng. Q.*, vol. 28, no. 1, pp. 105–115, 2014.
[134] J. Zhang and N. A. Peppas, “Synthesis and Characterization of pH- and Temperature-Sensitive Poly(methacrylic acid)/Poly(N-isopropylacrylamide) Interpenetrating Polymeric Networks,” *Macromolecules*, vol. 33, pp. 102–107, 2000.
[135] X. Zhang, D. Wu, and C. C. Chu, “Synthesis and characterization of partially biodegradable, temperature and pH sensitive Dex-MA/PNIPAAm hydrogels,” *Biomaterials*, vol. 25, no. 19, pp. 4719–4730, 2004.
[136] N. K. Singh and D. S. Lee, “In situ gelling pH- and temperature-sensitive biodegradable block copolymer hydrogels for drug delivery,” *J. Control. Release*, vol. 193, pp. 214–227, 2014.
[137] M. A. De Moraes and M. M. Beppu, “Biocomposite membranes of sodium alginate and silk fibroin fibers for biomedical applications,” *J. Appl. Polym. Sci.*, vol. 130, no. 5, pp. 3451–3457, 2013.
[138] W. R. Gombotz and S. Wee, “Protein release from alginate matrixes,” *Adv. Drug Deliv. Rev.*, vol. 31, no. 3, pp. 267–285, 1998.
[139] U. Remminghorst and B. H. A. Rehm, “Bacterial alginates: From biosynthesis to applications,” *Biotechnol. Lett.*, vol. 28, no. 21, pp. 1701–1712, 2006.
[140] S. Wang, H. Yang, Z. Tang, G. Long, and W. Huang, “Wound dressing model of human umbilical cord mesenchymal stem cells-alginates complex promotes skin wound healing by paracrine signaling,” *Stem Cells Int.*, 2016.
[141] J. P. Cattalini *et al.*, “Nanocomposite scaffolds with tunable mechanical and degradation capabilities: co-delivery of bioactive agents for bone tissue engineering,” *Biomed. Mater.*, vol. 11, no. 6, 2016.
[142] C. Y. Chen, C. J. Ke, K. C. Yen, H. C. Hsieh, J. S. Sun, and F. H. Lin, “3D porous calcium-alginate scaffolds cell culture system improved human osteoblast cell clusters for cell therapy,” *Theranostics*, vol. 5, no. 6, pp. 643–655, 2015.
[143] A. Manuscript, “Alginate : properties and biomedical applications,” vol. 37, no. 1, pp. 106–126, 2012.
[144] G. Sharma, S. Jain, A. K. Tiwary, and G. Kaur, “Once daily bioadhesive vaginal clotrimazole tablets: design and evaluation,” *Acta Pharm*, vol. 56, no. 3, pp. 337–345, 2006.
[145] Y. Xu, C. Zhan, L. Fan, L. Wang, and H. Zheng, “Preparation of dual crosslinked alginate-chitosan blend gel beads and in vitro controlled release in oral site-specific drug delivery system,” *Int. J. Pharm.*, vol. 336, no. 2, pp. 329–337, 2007.
[146] G. S. Lee, J. H. Park, U. S. Shin, and H. W. Kim, “Direct deposited porous scaffolds of calcium phosphate cement with alginate for drug delivery and bone tissue engineering,”

Acta Biomater., vol. 7, no. 8, pp. 3178–3186, 2011.
[147] "Sodium Alginate-Industrial Grade," *IRO Group Inc.*, 2013. [Online]. Available: http://www.irochemical.com/product/Alginates/Sodium-Alginate-I.htm. [Accessed: 03-Mar-2017].
[148] C. Xiao, H. Liu, Y. Lu, and L. Zhang, "Blend Films From Sodium Alginate and Gelatin Solutions.," *J. Macromol. Sci. Pure Appl. Chem.*, vol. 38, no. 3, pp. 317–328, 2007.
[149] A. J. Kuijpers, G. H. M. Engbers, J. Krijgsveld, S. A. J. Zaat, and J. Feijen, "Cross-linking and characterisation of gelatin matrices for biomedical applications," *J. Biomater. Sci. , Polym. Ed.*, no. February 2013, pp. 37–41, 2012.
[150] X. Liu and P. X. Ma, "Phase separation, pore structure, and properties of nanofibrous gelatin scaffolds," *Biomaterials*, vol. 30, no. 25, pp. 4094–4103, 2009.
[151] H. W. Kang, Y. Tabata, and Y. Ikada, "Fabrication of porous gelatin scaffolds for tissue engineering.," *Biomaterials*, vol. 20, no. 14, pp. 1339–1344, 1999.
[152] X. Wu *et al.*, "Preparation of aligned porous gelatin scaffolds by unidirectional freeze-drying method," *Acta Biomater.*, vol. 6, no. 3, pp. 1167–1177, 2010.
[153] "Gelatine : a protein," *jelly.e-monosite*. [Online]. Available: http://jelly.e-monsite.com/pages/in-english/scientific-part/gelatine-a-protein.html. [Accessed: 03-Mar-2017].
[154] a. Martins, R. L. Reis, and N. M. Neves, "Electrospinning: processing technique for tissue engineering scaffolding," *Int. Mater. Rev.*, vol. 53, no. 5, pp. 257–274, 2008.
[155] H. N. Chia and B. M. Wu, "Recent advances in 3D printing of biomaterials," *J. Biol. Eng.*, vol. 9, 2015.
[156] Q. Yang, L. Chen, X. Shen, and Z. Tan, "Preparation of Polycaprolactone Tissue Engineering Scaffolds by Improved Solvent Casting/Particulate Leaching Method," *J. Macromol. Sci. Part B Phys.*, vol. 45, no. 6, pp. 1171–1181, 2006.
[157] J. A. Vélez-Riaño and C. E. Echeverri-Cuartas, "PLLA scaffold fabrication using salt leaching/gas foaming method," *Adv. Drug Deliv. Rev.*, 2013.
[158] M. Houmard, Q. Fu, E. Saiz, and A. P. Tomsia, "Sol-gel method to fabricate CaP scaffolds by robocasting for tissue engineering," *Ed Acad. Press Ser. Biomed. Eng.*, vol. 23, no. 4, pp. 921–930, 2012.
[159] Y. S. Nam and T. G. Park, "Porous biodegradable polymeric scaffolds prepared by thermally induced phase separation," *J. Biomed. Mater. Res.*, vol. 47, no. 1, pp. 8–17, 1999.
[160] V. M. Correlo *et al.*, "Melt Processing of Chitosan-Based Fibers and Fiber-Mesh Scaffolds for the Engineering of Connective Tissues," *Macromol. Biosci.*, vol. 10, no. 12, pp. 1495–1504, 2010.
[161] O. A. Abdelaal and S. M. Darwish, "Fabrication of Tissue Engineering Scaffolds Using Rapid Prototyping Techniques," *World Acad. Sci. Eng. Technol. Int. Sci. Index*, vol. 59, no. 11, pp. 1325–1333, 2011.
[162] R. Owen, C. Sherborne, T. Paterson, N. H. Green, G. C. Reilly, and F. Claeyssens, "Emulsion templated scaffolds with tunable mechanical properties for bone tissue engineering," *J. Mech. Behav. Biomed. Mater.*, vol. 54, pp. 159–172, 2016.
[163] D. Aibibu, M. Hild, M. Woltje, and C. Cherif, "Textile cell-free scaffolds for in situ tissue engineering applications," *J. Mater. Sci. Mater. Med.*, vol. 27, no. 3, pp. 1–20, 2016.
[164] D. W. Hutmacher, "Scaffolds in tissue engineering bone and cartilage.," *Biomaterials*, vol. 21, no. 24, pp. 2529–2543, 2000.
[165] S. F. Badylak, D. O. Freytes, and T. W. Gilbert, "Extracellular matrix as a biological scaffold material: Structure and function," *Acta Biomater.*, vol. 5, no. 1, pp. 1–13, 2009.
[166] W. Abdelwahed, G. Degobert, S. Stainmesse, and H. Fessi, "Freeze-drying of nanoparticles: Formulation, process and storage considerations," *Adv. Drug Deliv. Rev.*, vol. 58, no. 15, pp. 1688–1713, 2006.
[167] H. W. Kang, Y. Tabata, and Y. Ikada, "Fabrication of porous gelatin scaffolds for tissue engineering.," *Biomaterials*, vol. 20, no. 14. pp. 1339–1344, 1999.
[168] F. Franks, "Freeze-drying of bioproducts: Putting principles into practice," *Eur. J. Pharm. Biopharm.*, vol. 45, no. 3, pp. 221–229, 1998.
[169] X. Tang and M. J. Pikal, "Design of Freeze-Drying Processes for Pharmaceuticals: Practical Advice," *Pharm. Res.*, vol. 21, no. 2, pp. 191–200, 2004.
[170] L. Rey, *Freeze Drying / Lyophilization of Pharmaceutical and Biological Products*. Informa, 2010.
[171] J. F. Carpenter and L. M. . Crowc, "Stabilization of phosphofructokinase with sugars

during freeze-drying: characterization of enhanced protection in the presence of divalent cations," vol. 923, pp. 109–115, 1987.
[172] T. Arakawa, S. J. Prestrelski, W. C. Kenney, and J. F. Carpenter, "Factors affecting short-term and long term stabilities of proteins," *Adv. Drug Deliv. Rev.*, vol. 10, pp. 1–28, 1993.
[173] M. C. Lai and E. M. Topp, "Solid-State Chemical Stability of Proteins and Peptides," vol. 88, no. 5, 1999.
[174] I. Roy and M. N. Gupta, "Freeze-drying of proteins: some emerging concerns.," *Biotechnol. Appl. Biochem.*, vol. 39, no. 2, pp. 165–77, 2004.
[175] L. Qian and H. Zhang, "Controlled freezing and freeze drying: A versatile route for porous and micro-/nano-structured materials," *J. Chem. Technol. Biotechnol.*, vol. 86, no. 2, pp. 172–184, 2010.
[176] N. Sultana, *Biodegradable Polymer-Based Scaffolds for Bone Tissue Engineering*. 2013.
[177] N. Sultana and M. Wang, "Fabrication of HA/PHBV composite scaffolds through the emulsion freezing/freeze-drying process and characterisation of the scaffolds," *J. Mater. Sci. Mater. Med.*, vol. 19, no. 7, pp. 2555–2561, 2008.
[178] T. Garg, A. Chanana, and R. Joshi, "Preparation of Chitosan Scaffolds for Tissue Engineering using Freeze drying Technology," *IOSR J. Pharm.*, vol. 2, no. 1, pp. 72–73, 2012.
[179] A. Abdal-hay, K. A. Khalil, A. S. Hamdy, and F. F. Al-Jassir, "Fabrication of highly porous biodegradable biomimetic nanocomposite as advanced bone tissue scaffold," *Arab. J. Chem.*, vol. 10, no. 2, pp. 240–252, 2016.
[180] T. Casimiro *et al.*, "Porous chitosan-drug formulations by scCO2-assisted atomization."
[181] S. G. Kazarian, "Polymer Processing with Supercritical Fluids," *Polym. Sci.*, vol. 42, no. 2, pp. 78–101, 2000.
[182] M. Temtem *et al.*, "Supercritical CO2 generating chitosan devices with controlled morphology. Potential application for drug delivery and mesenchymal stem cell culture," *J. Supercrit. Fluids*, vol. 48, no. 3, pp. 269–277, 2009.
[183] A. I. Cooper, "Polymer synthesis and processing using supercritical carbon dioxide," *J. Mater. Chem.*, vol. 10, no. 2, pp. 207–234, 2000.
[184] H. Tai *et al.*, "Control of pore size and structure of tissue engineering scaffolds produced by supercritical fluid processing - Discussion with reviewers," *Eur. Cell. Mater.*, vol. 14, no. February, pp. 76–77, 2007.
[185] I. Kikic and F. Vecchione, "Supercritical impregnation of polymers," *Curr. Opin. Solid State Mater. Sci.*, vol. 7, no. 4–5, pp. 399–405, 2003.
[186] H. Tai *et al.*, "Control of pore size and structure of tissue engineering scaffolds produced by supercritical fluid processing," *Eur. Cell. Mater.*, vol. 14, pp. 76–77, 2007.
[187] R. Sengupta *et al.*, "Fabrication of Polylactic Acid/Polyethylene Glycol (PLA/PEG) Porous Scaffold by Supercritical CO2 Foaming and Particle Leaching," *Engineering*, vol. 47, pp. 21–25, 2015.
[188] P. He, S. S. Davis, and L. Illum, "In vitro evaluation of the mucoadhesive properties of chitosan microspheres," *Int. J. Pharm.*, vol. 166, pp. 75–68, 1998.
[189] T. Barroso, R. Viveiros, T. Casimiro, and A. Aguiar-ricardo, "The Journal of Supercritical Fluids Development of dual-responsive chitosan – collagen scaffolds for pulsatile release of bioactive molecules," *J. Supercrit. Fluids*, vol. 94, pp. 102–112, 2014.
[190] S. Senel, M. J. Kremer, S. Kaş, P. W. Wertz, A. A. Hincal, and C. A. Squier, "Enhancing effect of chitosan on peptide drug delivery across buccal mucosa.," *Biomaterials*, vol. 21, no. 20, pp. 2067–71, 2000.
[191] T. R. Bhardwaj, M. Kanwar, and R. Lal, "Natural Gums and Modified Natural Gums as Sustained-Release Carriers," vol. 26, no. 10, pp. 1025–1038, 2000.
[192] R. E. K. Inget, "Rheological Characterization of Xanthan Gum and Hydroxypropylmethyl Cellulose with Respect to Controlled-Release Drug Delivery," vol. 85, no. 5, pp. 537–540, 1996.
[193] T. Barroso, A. C. A. Roque, and A. Aguiar-ricardo, "Bioinspired and sustainable chitosan-based monoliths for antibody capture and release," *RSC Adv.*, no. 2, pp. 11285–11294, 2012.
[194] G. Kumar, A. Wadood, M. Datta, and D. Ramchand, "Interpenetrating polymeric network hydrogel for stomach-specific drug delivery of clarithromycin: Preparation and evaluations," *Asian J. Pharm.*, vol. 4, no. 4, 2010.
[195] T. Giri, A. Thakur, A. Alexander, H. Badwaik, and D. Tripathi, "Modified chitosan

hydrogels as drug delivery and tissue engineering systems:present status and applications," *Acta Pharm. Sin. B*, vol. 2, no. 5, pp. 439–449, 2012.
[196] S. Kumari, "Preparation and Characterization of Interpenetrating Hydrogel for Colon Drug Delivery," National Institute of Technology - India, 2014.
[197] A. Pourjavadi, H. Ghasemzadeh, and R. Soleyman, "Synthesis , Characterization , and Swelling Behavior of Alginate- g -Poly (sodium acrylate)/ Kaolin Superabsorbent Hydrogel Composites," *Wiley Intersci.*, vol. 105, pp. 2631–2639, 2007.
[198] U. Brasil, "Você sabe quanta saliva produz o corpo humano?," 2011. [Online]. Available: http://noticias.universia.com.br/destaque/noticia/2011/04/12/810685/voce-sabe-quanta-saliva-produz-corpo-humano.html. [Accessed: 11-Jul-2017].
[199] S. C. Fox, *Pharmaceutics*. Remington Educations, 2014.
[200] G. Ahuja and K. Pathak, "Porous Carriers for Controlled/Modulated Drug Delivery," *Indian J. Pharm. Sci.*, vol. 71, no. 6, pp. 599–607, 2007.
[201] Z. Li, H. R. Ramay, K. D. Hauch, D. Xiao, and M. Zhang, "Chitosan – alginate hybrid scaffolds for bone tissue engineering," *Biomaterials*, vol. 26, pp. 3919–3928, 2005.
[202] H. Park, K. Park, and D. Kim, "Preparation and swelling behavior of chitosan-based superporous hydrogels for gastric retention application," *Wiley Intersci.*, pp. 144–150, 2005.
[203] N. Sultana, M. I. Hassan, and M. M. Lim, *Composite Synthetic Scaffolds for Tissue Engineering and Regenerative Medicine*. Springer, 2015.
[204] E. Szymanka and K. Winnicka, "Stability of Chitosan—A Challenge for Pharmaceutical and Biomedical Applications," *Mar. Drugs*, vol. 13, pp. 1819–1846, 2015.
[205] V. Blasques, R. Bentini, L. Henrique, L. R. S. Barbosa, D. Freitas, and S. Petri, "Synthesis and characterization of xanthan – hydroxyapatite nanocomposites for cellular uptake," *Mater. Sci. Eng. C*, vol. 37, pp. 195–203, 2014.
[206] S. L. Levengood and M. Zhang, "Chitosan-based scaffolds for bone tissue engineering," *J Mater Chem B Mater Biol Med.*, vol. 2, no. 21, pp. 3161–3184, 2014.
[207] H. Liu, K. Nakagawa, D. Chaudhary, Y. Asakuma, and M. O. Tadé, "Freeze-dried macroporous foam prepared from chitosan/xanthangum/montmorillonite nanocomposites," *Chem. Eng. Res. Des.*, vol. 89, no. 11, pp. 2356–2364, 2011.
[208] P. P. Win, Y. Shin-ya, K. J. Hong, and T. Kajiuchi, "Formulation and characterization of pH sensitive drug carrier based on phosphorylated chitosan (PCS)," *Carbohydr. Polym.*, vol. 53, no. 3, pp. 305–310, 2003.
[209] C.-E. Brunchi, M. Bercea, S. Morariu, and M. Dascalu, "Some properties of xanthan gum in aqueous solutions : effect of temperature and pH," *J. Polym. Res.*, vol. 23, no. 123, pp. 1–8, 2016.
[210] S. Maharjan, "Assignment on Mathematical models used in drug release studies," Kathmandu University, 214AD.
[211] H. K. Shaikh, R. V Kshirsagar, and S. G. Patil, "Mathematical models for drug release characterization: A review," *World J. Pharm. Pharm. Sci.*, vol. 4, no. 4, pp. 324–338, 2015.
[212] J. Siepmann and N. A. Peppas, "Modeling of drug release from delivery systems based on hydroxypropyl methylcellulose (HPMC)," *Adv. Drug Deliv. Rev.*, vol. 48, pp. 139–157, 2001.
[213] M. H. Shoaib, J. Tazeen, H. A. Merchant, and R. I. Yousuf, "Evaluation of drug release kinetics from Ibuprofen matrix tablets using HPMC," *Pak. J. Pharm. Sci.*, vol. 19, no. 2, pp. 119–124, 2006.
[214] X. Li *et al.*, "Chitin, chitosan, and glycated chitosan regulate immune responses: The novel adjuvants for cancer vaccine," *Clin. Dev. Immunol.*, pp. 1–9, 2013.

Appendix

I. Drug Release Profiles modulated through Higuchi Model

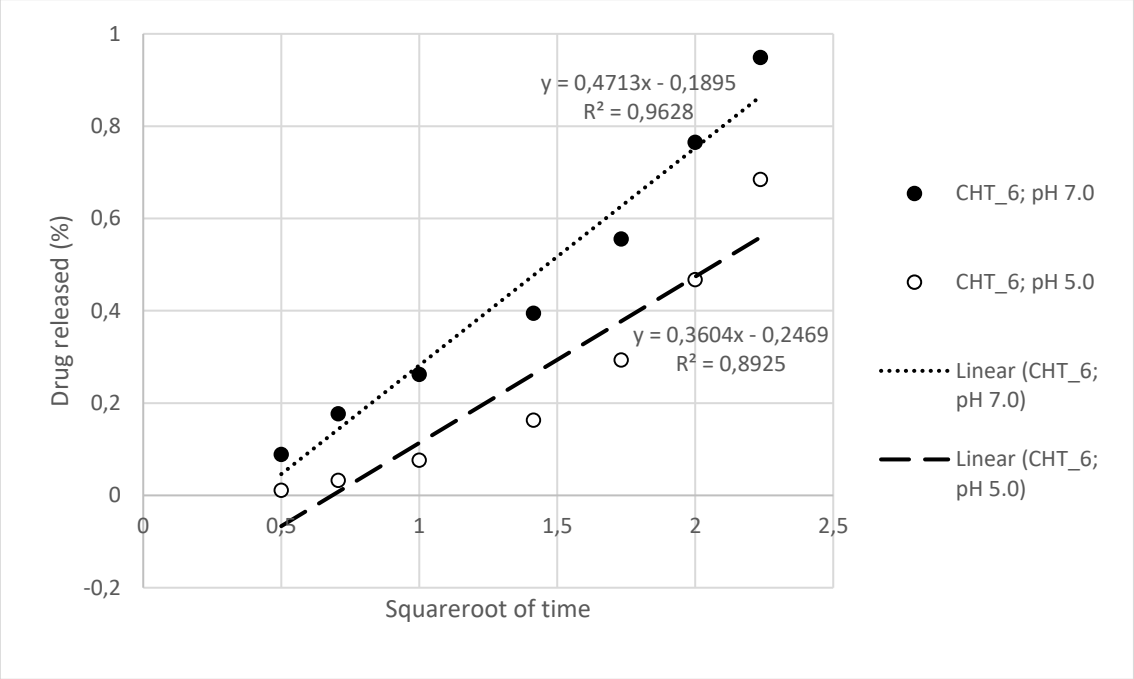

Figure I.1 Drug release profiles of CHT_6 at pH 7.0 and CHT_6 at pH 5.0, modulated through Higuchi Model.

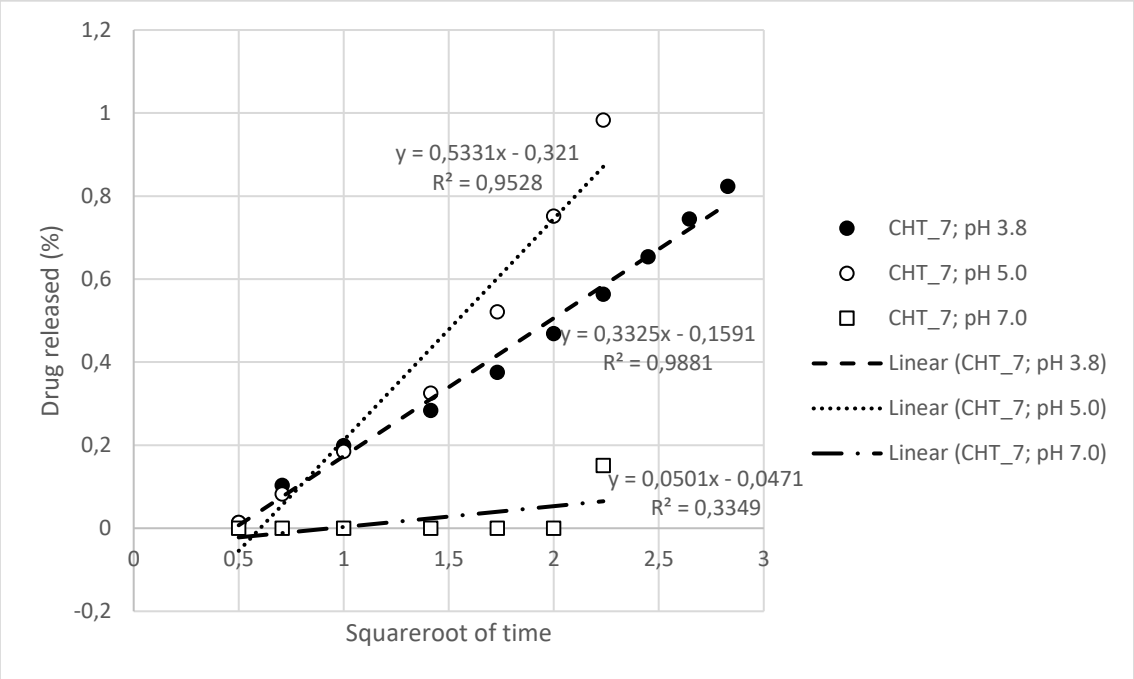

Figure I.2 Drug release profiles of CHT_7 at pH 3.8, CHT_7 at pH 5.0 and CHT_7 at pH 3.8, modulated through Higuchi Model.

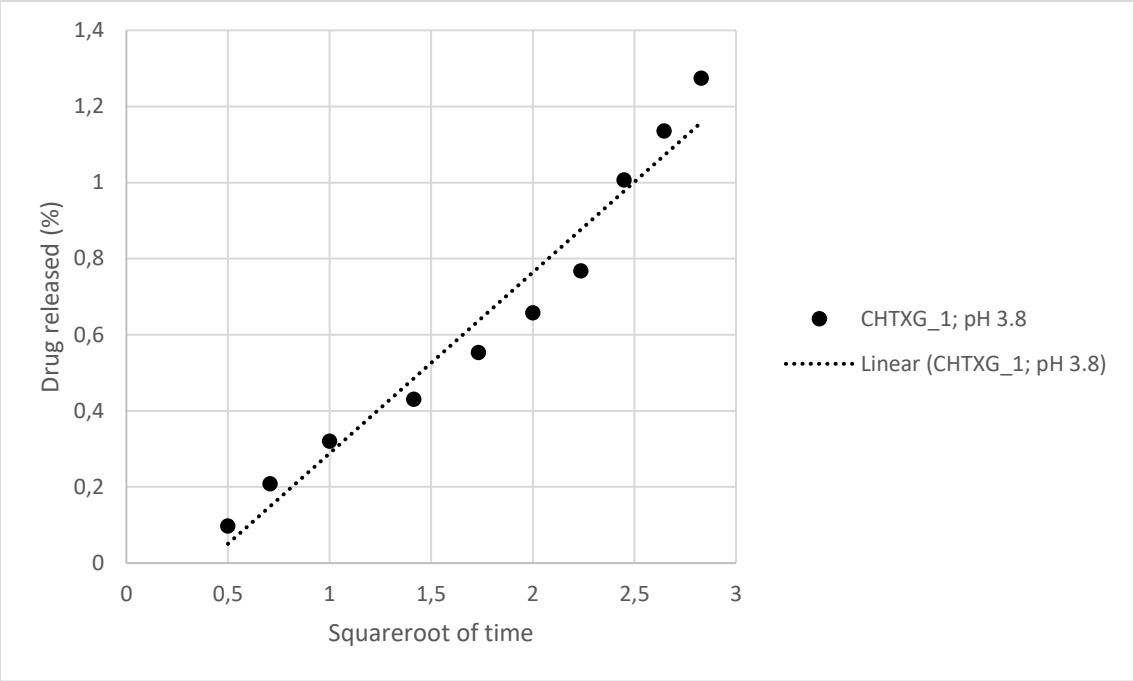

Figure I.3 Drug release profiles of CHTXG_1 at pH 3.8, modulated through Higuchi Model.

II. Drug Release Profiles modulated through Power Law

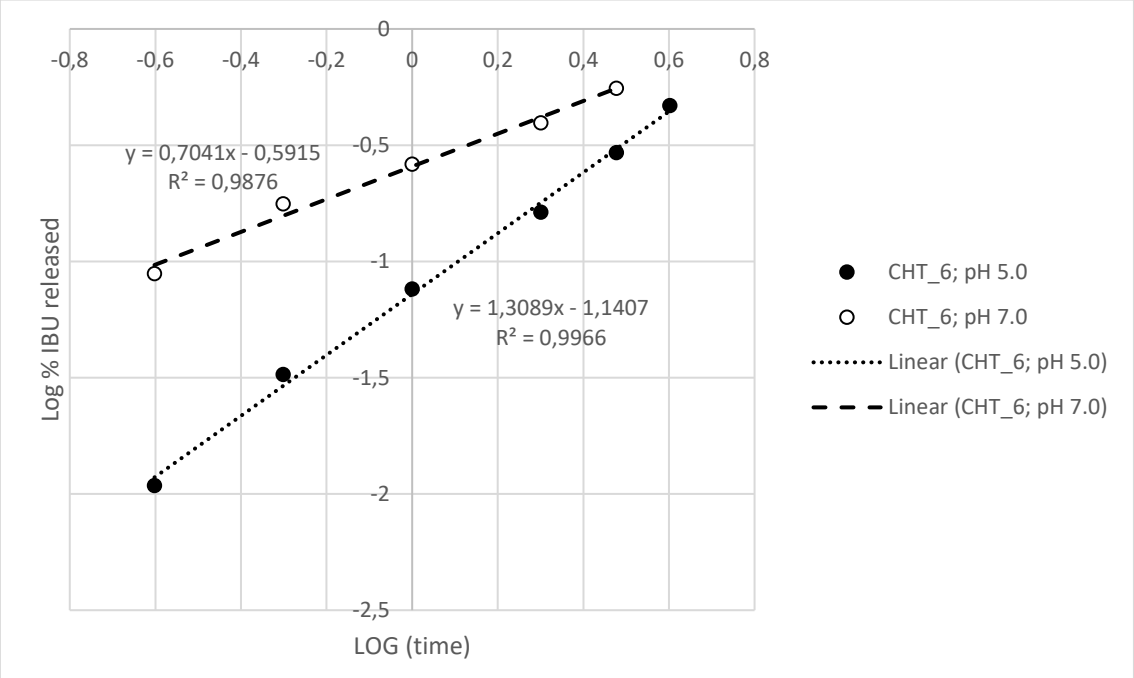

Figure II.4 Drug release profiles of CHT_6 at pH 5.0 and CHT_6 at pH 7.0, modulated through Power Law.

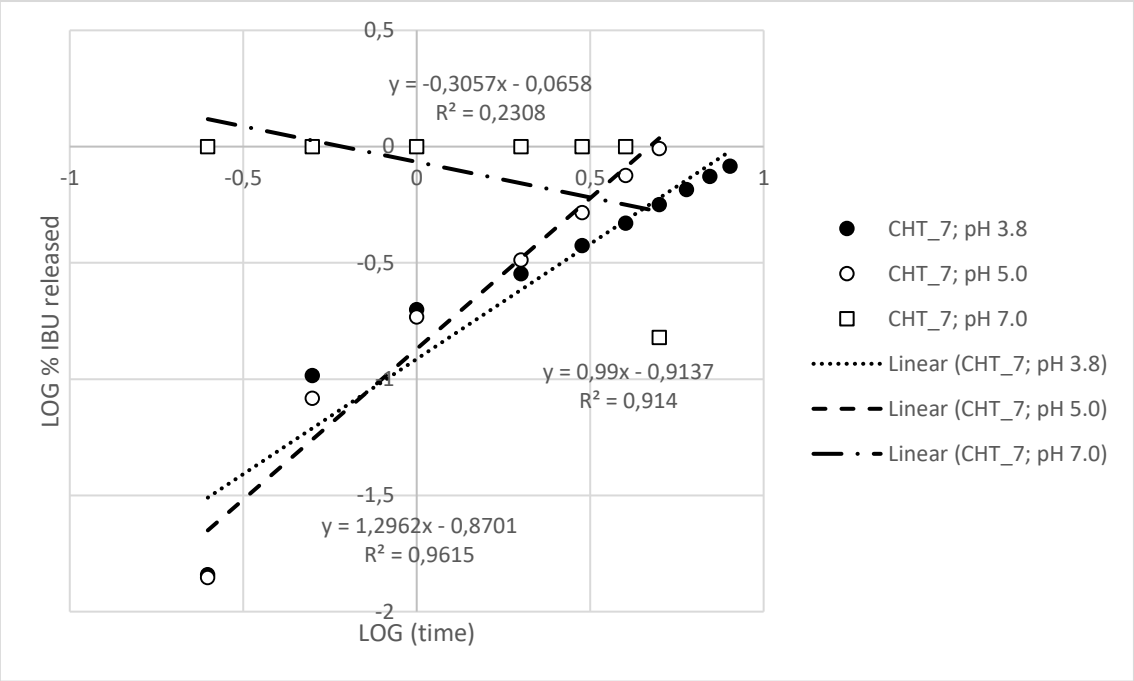

Figure II.5 Drug release profiles of CHT_7 at pH 3.8, CHT_7 at pH 5.0 and CHT_7 at pH 3.8, modulated through Power Law.

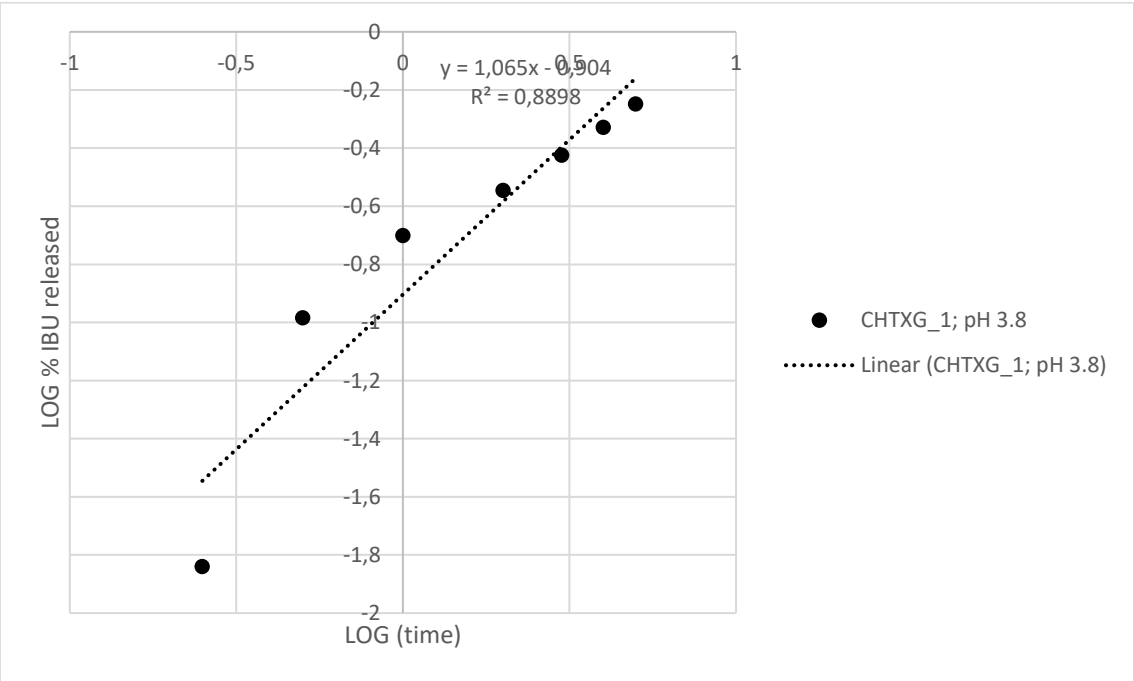

Figure II.6 Drug release profiles of CHTXG_1 at pH 3.8, modulated through Power Law.